PROCEEDINGS

OF THE

5TH ACOT RESEARCH SEMINAR

TRIBOLOGY RESEARCH FOR CANADIAN INDUSTRY

at

Pulp and Paper Research Institute of Canada
570 St. John's Boulevard
Pointe Claire
Quebec, H9R 3J9

National Research
Council Canada

Conseil national
de recherches Canada

ASSOCIATE COMMITTEE ON TRIBOLOGY

Proceedings of the

5th ACOT Research Seminar

TRIBOLOGY RESEARCH FOR CANADIAN INDUSTRY

held

November 9 - 10, 1989

at

Pulp and Paper Research Institute of Canada
570 St. John's Boulevard
Pointe Claire
Quebec, H9R 3J9

Editors

R. L. Kushwaha
Agricultural Engineering Department, University of Saskatchewan
Saskatoon, Saskatchewan, S7N 0W0

K. R. Brockwell
Tribology and Mechanics Laboratory, National Research Council
3650 Wesbrook Mall, Vancouver, B.C. V6S 2L2

90-07132/

FOREWORD

The members of the Associate Committee on Tribology (ACOT) welcome you to the 5th ACOT Research Seminar entitled **Tribology Research for Canadian Industry**.

The Committee was pleased to see such an enthusiastic response to call for abstracts. The diversity of submissions represents a wide range of new ideas and innovative technologies aimed at solving the age old problems of friction, wear and lubrication.

We are very pleased to have Professor John A. Schey from the Mechanical Engineering Department at the University of Waterloo (Waterloo, Ontario) presenting the keynote address. He will speak on **Tribology Research for the Metalworking Industry**, focusing on how recent research is directed towards finding solutions to real industrial problems.

The technical programme consists of 23 research papers written by 46 national and international authors. The research papers fall into three major categories; friction (10 papers), lubrication (4 papers) and wear (9 papers). The contributing researchers represent university laboratories (12 papers), government labs (7) and industrial research (4 papers), although it should be noted that several of the papers involve authors with more than one affiliation.

In keeping with our focus on friction, lubrication and wear problems encountered by industry, all of the papers connect their research to an industrial problem or application. A written abstract of each paper is included in this seminar proceedings. In addition, the journal **Tribology International** has agreed to publish an issue dedicated to this Research Seminar. Five authors have indicated their intent to submit their papers to the journal.

The members of the ACOT would like to thank the Pulp and Paper Research Institute of Canada (PAPRICAN) for the time and effort they have devoted in the organization and hosting of this seminar. The enthusiastic response from Canadian and International researchers with diverse affiliations clearly indicate the importance of tribology as an area of international industrial research.

K.R. Brockwell
Organizing Committee

R.L. Kushwaha
Seminar Coordinator

TABLE OF CONTENTS

Foreword i

Table of Contents ii

Keynote Address

Tribology Research for the Metalworking Industry. 1
Professor John A. Schey, Mechanical Engineering Department, University of Waterloo, Waterloo, Ontario.

Friction I

Friction and sliding wear behaviour of 2014 Al-SiC particle reinforced composite. 5
A.T. Alpas, Engineering Materials, University of Windsor, and J.D. Embury, Materials Science and Engineering, McMaster University.

Rebuilding railroad frogs by overlay welding 7
Isobel Bravo, William Mackay, John Cameron and R.W. Smith, Metallurgical Engineering, Queens University, Kingston, Ontario.

The influence of normal load roughness and speed on micro-sliding friction of UHMWPE, PA 66, POM against steel. 8
S.M.H. Benabdalla and J.P. Chalifoux, Mechanical Engineering, Ecole Polytechnique de Montreal, Quebec.

Correlation between a laboratory impact-abrasion test and in-situ marked-ball test. 16
Michel Fiset, Universite Laval; Gilles Huard and Jacques Masounave, IMRI, National Research Council Canada, Quebec.

Investigations with plasma sprayed coating of agricultural tools 20
R.L. Kushwaha, Agricultural Engineering, University of Saskatchewan, Saskatoon, Sask.; and C. Roy, Mechanical Engineering, University of Sherbrooke, Sherbrooke, Quebec.

Friction II

Une etude de l'usure du nylon et de l'acetal frottant contre l'acier. 25
M. Amarouch and H. Yelle. Groupe de Recherche sur les Materiaux Plastiques et Composites (GRPC), Ecole Polytechnique de Montreal, Quebec.

Scientific numeric databases - Tools for tribology. 29
Gordon Wood, NRC/CISTI, Ottawa.

Modelling of rolled joints. 34
R. Metcalfe and J.M. Pietralik, Atomic Energy of Canada Ltd. Chalk River, Ontario.

Qualification testing of wear materials for mining and extraction applications at Syncrude's oil sands plant. 40
Rees Llewellyn, Syncrude Canada Research Ltd. Edmonton, Alberta.

An investigation of the state of friction and oil film in oscilating bearings under dynamic loading. 42
O.S. Dinc, Mechanical Engineering, Rensselaer Polytechnic Institute, Troy, NY, and M. Gediktas, Mechanical Engineering, Gumussuyu, Istanbul, Turkey.

Lubrication

Development of a method for prediction of viscosity of liquid lubricants 49
Birbal Singh and V.R. Puttagunta, Mechanical Engineering, Lakehead University, Thunder Bay, Ontario.

Experimental determination of the steady state and dynamic performance characteristics of a journal bearing. 53
K. Brockwell*, W. Dmochowski** and D. Kleinbub*
*Tribology and Mechanics Lab, National Research Council of Canada,
** Institute of Fluid Flow Machinery, Polish Academy of Sciences.

Elasto-hydrodynamic lubrication and monitoring 58
Albert Koehler, Tribotec Int. Ltd.

Tribology of large spherical roller bearings used in paper machines. 60
Stephen D. Fysh, Edward M. Oravec, Oakville Research Centre, Shell Canada Ltd. and John B. Medley, University of Waterloo, Waterloo, Ontario.

Wear I

Metallographic examination of failed jet engine compressor blades. 64
Pak L. Ko, J. Kalousek and M. Robertson, Tribology and Mechanics Lab., National Research Council of Canada, Vancouver, B.C.

Wear studies using acoustic emission techniques. 69
R.J. Boness, S.L. McBride and M. Sobczyk, Mechanical Engineering, Royal Military College of Canada, Kingston, Ontario.

Development of a prototype abrasive wear tester for tillage tool materials. 75
He-Jin Yu and S.D. Bhole, Faculty of Engineering, University of Regina. Regina, Sask.

The friction and wear of polymeric and ceramic based materials in a high vacuum tribosystem. 79
H.M. Hawthorne, Tribology and Mechanics lab., National Research Council of Canada, Vancouver, B.C.

A reciprocating wear test for evaluating boundary lubrication. 82
J.S. Sheasby, T.A. Caughlin, University of Western Ontario, London, Ontario; and A.G. Blahey, K.F. Laycock, Esso Petroleum Canada, Sarnia, Ontario.

Wear II

Effect of the abrasive nature on the impact and impact-abrasion wear rate of a martensitic cast iron. 88
Michel Fiset, Universite Laval; Gilles Huard and Jacques Masounave, IMRI, National Research Council Canada, Quebec.

The influence of corrosion on the low-stress abrasion resistance of refiner plate stainless steels and cast irons. 92
C.B. Thompson, PAPRICAN, Pointe Claire, Quebec.

Development of CANMETCOAT digger teeth for oil sands bucket wheel reclaimer service. 98
Keith Davies, Metals Technology Lab., CANMET, Ottawa, and Glenn Doonanco and Rees Llewellyn, Syncrude Canada Ltd., Edmonton, Alberta.

Tribotesting of materials for aeroengine flexible element seals. 100
H.M. Hawthorne, Tribology and Mechanics lab., National Research Council of Canada, Vancouver, B.C.

Author Index 104

KEYNOTE ADDRESS

Tribology Research for the Metalworking Industry

Keynote Address

John A. Schey
Department of Mechanical Engineering
University of Waterloo
Waterloo, Ontario, N2L 3G1

There is general agreement that solutions to most problems in tribology require a systems approach. Because of the very large number of variables involved, in most cases one is forced to simplify the problem to make it more tractable. In doing so, the relevance of the solution may be jeopardized, unless there is sufficient understanding of the problem to assure that none of the important factors have been sacrificed. The dilemma is particularly acute when the results are to be applied in industry.

A typical example of this situation is found in metalworking tribology. It is perhaps understandable that, in most instances, intensive development efforts concentrate on materials and processes; tribology is given only passing thought, at least until problems are encountered in the development or, more likely, production stage. Only then may there be a realization that the solution of these problems might require more than a straightforward application of existing knowledge and may indeed call for intense efforts at the quite fundamental level. To the delight of the metalworking tribologist, such situations occasionally arise.

In the 1960s, developments in the aerospace industry required solutions for the hot and cold working of advanced steels, aluminum alloys, titanium alloys, and superalloys, in general, relatively hard and non-reactive (or highly reactive) materials. Luckily, there was a simultaneous, huge development effort to find solutions to the tribology problems of space travel, and some of the results could be applied to industrial processes too.

Today there is another resurgence of interest, but this time it is due to problems associated with terrestrial travel. Over the last decade, the automobile has undergone a remarkable transformation. Not only have microprocessors become essential to its operation, but body construction too has moved from the old established bare automotive steel to steel sheet coated with a wide range of zinc and zinc alloys. Suddenly, all the basic and applied knowledge relating to the tribology of bare steel has become of doubtful value.

Examples from recent work will be used to illustrate how research can be directed towards finding solutions of the real problems faced by industry. While practical solutions are within reach, much work needs to be done at the fundamental level too, and the following are but a few of the critical aspects.

1. Adhesion between die and workpiece materials determines the consequences of local lubricant breakdown and as such is of extreme importance both from the friction and wear points of view. Ideally, one should be able to predict adhesion from fundamental quantities. Indeed, great promise is

shown by an approach based on calculating the energy of adhesion from the surface energy of the contacting solid metals. Unfortunately, it cannot be applied yet to tool steels of complex composition and structure or to ceramic coatings. Hence, adhesion between real die-workpiece material combinations can still be judged only from experimental observations.

2. Process geometry, lubricant rheology, and sliding speed are among the most important factors affecting the thickness of a film developed at entry to the deformation zone, and theory adequately describes these effects. Survival of the entrained film is, however, determined to a large extent by the microgeometry during deformation. Incorporation of these factors into a generalized theory of lubrication is still in the future, and there is barely a beginning in understanding the effects of such factors as the structure of crystalline coatings found in electro-plated zinc.

3. Characterization of the microtopography of the surface by some appropriate measure or mathematical function is still a subject of intense inquiry. There is still no generally accepted criterion for a sheet surface that resists galling (metal transfer and scoring).

4. Tribochemical reactions in the deformation zone are vital for the development of boundary and EP layers. Despite advances in surface analytical techniques, neither the composition nor the shear characteristics of reaction layers are adequately known. This is particularly true of systems in which one or both contacting surfaces are coated.

5. Wear processes are notorious for their complexity and, not surprisingly, the study of wear is in its infancy for systems incorporating coated surfaces. Most conclusions are based on industrial observations where neither process conditions nor lubricants are simple or well defined. In consequence, hardly any relations of general validity are known yet.

FRICTION I

Friction and Sliding Wear Behaviour of 2014 Al-SiC Particle Reinforced Composite

by

A.T. Alpas
Department of Engineering Materials
University of Windsor
Windsor, Ontario
Canada N9B 3P4

and

J.D. Embury
Department of Materials Science and Engineering
McMaster University
Hamilton, Ontario
Canada L8S 4L7

Abstract

In recent years, increased demand for lightweight materials with high specific strengths has led to rapid developments in the technology of metal matrix composites. Among these, aluminum alloys reinforced by whiskers or particles of SiC are particularly attractive because they can be produced using conventional metallurgical processing techniques and have the advantage of being machinable. For a number of applications the tribological properties of these materials are useful but to date there have been few studies of the micromechanisms of friction and wear in particle reinforced composites. The objective of the present work was to investigate the effect of SiC particles on the sliding wear characteristics of aluminum alloys.

The material used in this investigation was a commercial alloy with 2014 Al alloy matrix reinforced with 20% SiC particles. The average particle size and the aspect ratio were 14μm and 1.2 respectively. Sliding wear tests were performed on solution treated samples using a block-on-ring type wear rig. The slider was a hardened SAE 52100 bearing steel ring. A normal weight of 8N and a sliding velocity of 0.12 ms^{-1} were used for most of the tests. The wear rate was calculated from the weight loss of the specimens. To measure coefficient of friction a pin-on-disc type equipment was used. Tangential sliding forces were measured using a strain gauge bridge. After the wear tests, wear tracks and the collected loose debris were examined by a scanning electron microscope. Energy dispersive X-ray analysis were performed to determine local changes in chemical compositions that took place during wear process. SEM observations were also made to determine the structure of material below the wear surfaces.

The friction coefficient showed a dependence on the sliding distance described by an initial incubation period of low friction coefficient (0.35) followed by a regime of high friction (0.6). The wear rate of the composite (4×10^{-3} gm/m) was found to be 4 times lower than the matrix material tested under the similar conditions. Wear rates and wear coefficients were also compared with those of the conventional Al alloys and it was concluded that

Al (2014)-SiCp is a more wear resistant material than conventional Al alloys.

Wear surfaces were characterized by an extensive plastic deformation. EDX analyses showed that substantial amount of iron were transferred from the slide to the surface of composite during sliding contact. Within a subsurface region about 40μm deep the microstructure was composed of deformed and distorted Al grains elongated in the sliding direction. Subsurface examination led to the following conclusions: i) the wear proceeded by a damage accumulation and delamination process; ii) subsurface damage initiated by void nucleation and decohesion at particle matrix interfaces and propagated along the interfaces; iii) the size and distribution of SiC particles controlled the void nucleation and crack propagation processes; iv) the abrasive action of SiC particles caused material transfer from the slider to the specimen surface.

The shear strain distribution below the worn surfaces was measured and a quantitative wear model was developed. The model will be presented during the seminar.

REBUILDING RAILROAD FROGS BY OVERLAY WELDING

Isobel Bravo, William Mackay, John Cameron and R.W. Smith

Queen's University, Kingston, Ontario, Canada

In 1882, Sir Robert Hadfield patented a steel containing 1.2wt% carbon and 12.5wt% manganese and possessing such exceptional toughness and impact wear resistance that a century later, the basic alloy, occasionally with minor additions, is still used for in-track railroad components and rock-crushing equipment.

A continuing research programme at Queen's University has been concerned with modifying the composition of Hadfield's steel in order to improve the abrasion-resistance of the standard alloy without seriously reducing the alloy's toughness. As part of this study, and noting that any railroad frog is usually rebuilt a number of times by overlay welding when in service, a number of compositions have been examined for the rebuilding electrodes.

These electrodes were prepared by casting in silica-tube and then used to overlay a Hadfields steel base using a submerged arc welding practice. A number of compositions were used for the base steel.

Small specimens, 10 x 10 x 30mm, were cut from the overlay-welded section such that the major axis of the specimen was normal to the overlay. These were then subjected to rolling-impact deformation in the Queen's TIMPACT machine, a rail-wheel interaction simulation. This device subjects a specimen to repeated impacts under a hydraulically applied load, delivered via a rolling contact, and attempts to simulate the conditions experienced by the various regions of a railroad frog when in service. The progressive dimensional changes of the specimens are then correlated with the microstructure of the specimen.

Our experiments suggest that significant improvements could result from the use of novel compositions for the electrodes used when rebuilding railroad frogs. This work will be discussed.

THE INFLUENCE OF NORMAL LOAD ROUGHNESS AND SPEED ON MICRO-SLIDING FRICTION OF UHMW-POLYETHYLENE, NYLON, ACETAL AGAINST STEEL

S.M.H. Benabdallah, J.-P. Chalifoux

Department of Mechanical Engineering
École Polytechnique de Montréal
Montreal, CANADA

INTRODUCTION

The objective of the work reported in this paper was to evaluate the static and quasi-dynamic coefficients of friction of different engineering thermoplastics in contact with steel. The variables studied are the normal load, the surface roughness of the thermoplastic specimens and the sliding speed.

Using a newly designed apparatus (Benabdallah, 1987), the critical location where gross slip occurs could be defined reasonably well over a wide range of tangential loading rates.

Three popular engineering thermoplastics were tested, namely a Ultra High-Molecular-Weight Polyethylene (UHMWPE, Hercules 1900 supplied by Solidur Plastics), Polyoxymethylene (POM, Delrin 500, Du Pont) and Polyamide 66 (PA 66, zytel 101, Du Pont). The plastic specimens have a rectangular shape of 1 cm x 2 cm x 1 cm (see Fig. 1a) giving 2 cm^2 of apparent area. The specimens were machined from extruded plate. The directions of extrusion, sliding and machining are shown in Fig. 1a.

During the experiments, the plastic specimens was pressed against the steel slider as shown in Fig. 1b with a normal load varying from 8 N to 160 N. The slider is machined from mild steel and grinded to a surface roughness of 0.16 µm CLA, measured in the direction of sliding. The surface roughness achieved on the plastic specimens are in the order of 0.8 µm, 3 µm, 18 µm and 35 µm CLA, measured in the direction of sliding.

The sliding speed, although small, varied by a factor of over 10 from about 15 µm/s to 180 µm/s. All the tests were conducted in air at 50 % R.H., 23°C and without lubrication.

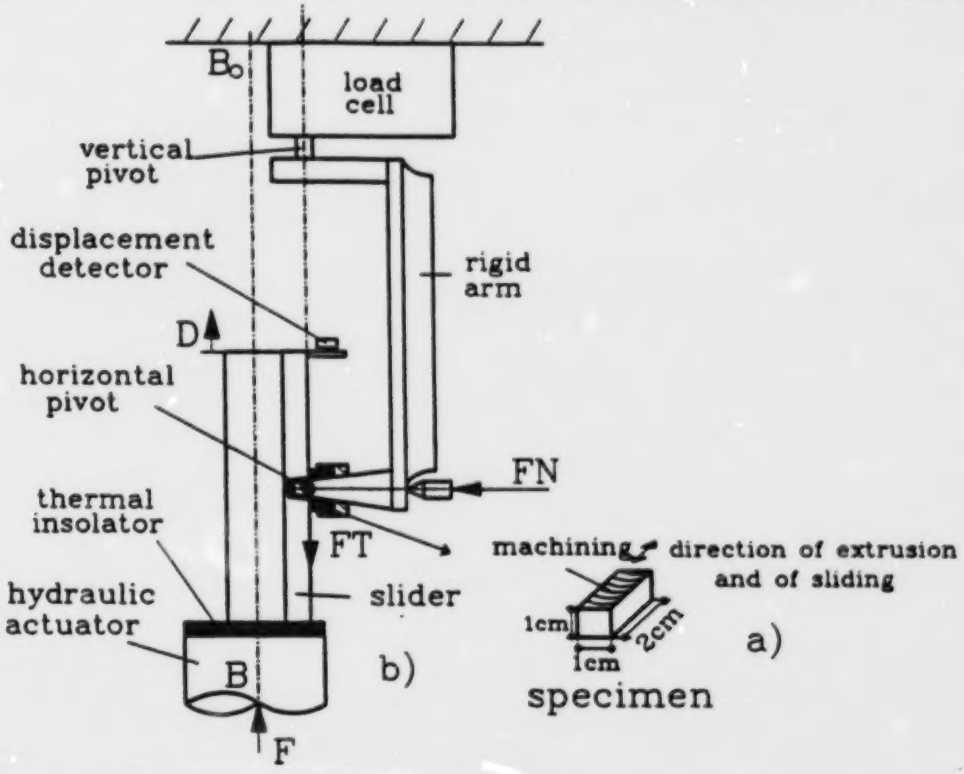

Fig. 1: Schematic of apparatus of the measurement of coefficients of friction

EXPERIMENTAL PROCEDURE

To reproduce the principle of the tilting plane, a gradually increasing force F (Fig. 1b) is applied to the steel slider by the hydraulic actuator until it starts to move. The process and the data acquisition is under the control of a microcomputer. Figure 2 shows a flow chart of the computer procedure. The chart is divided in three blocs: A- initialization of the variables and input of the constant for the test; B- control of the test and data acquisition; C- calculation and display of the results.

Bloc A: the input constants for the test at step 1 are the rate f at which the tangential force F will be increased and the maximum duration time K of the test. Values of the rate f varied from 0.22 to 15 N/s. The value of K is dictated by the data acquisition rate (1 KHz) and the maximum storage capacity of the computer (640 KBytes). The increasing rate f shall then be set such that relative sliding occurs within the time K.

Step 2 is to set all the storage memories to zero. Step 3 is to apply the normal load F_n. At step 4, the operator hit a key to start the test at time t = 0.

Bloc B: the computer first measures and stores F, F_n, friction force F_T, displacement D and time t at step 5. Then, it checks if relative sliding has started (D > 0) in step 6. If not, the increase in force F continues. At the first detection of a relative movement, which corresponds to a sudden decrease in friction force F_T, t is recorded as t_{cr} (t critical), F as F_{max} and the increment ΔF is set to zero, the whole in step 7. From that time, then, and for about 50 ms, the force F is kept equal to F_{max} to allow the hydraulic actuator-slider assembly to accelerate and pick up speed (step 8). After that time, F is set equal to F_T (step 9) and the whole assembly moves at constant speed.

Bloc C: the measurements of the parameters (forces, displacements and time) continue until at the end of time K (step 10). The hydraulic actuator is then stopped (step 11) and μ_s and μ_{qd} are calculated from stored data (step 12) according to the equations

$$\mu_s = \frac{F_{max}}{F_n} \qquad \text{at } t = t_{cr} \tag{1}$$

and

$$\mu_{qd} = \frac{F_T}{F_n} \qquad \text{at } t_{cr} < t < K \tag{2}$$

where μ_s = static coefficient of friction
μ_{qd} = coefficient of quasi-dynamic conditions.

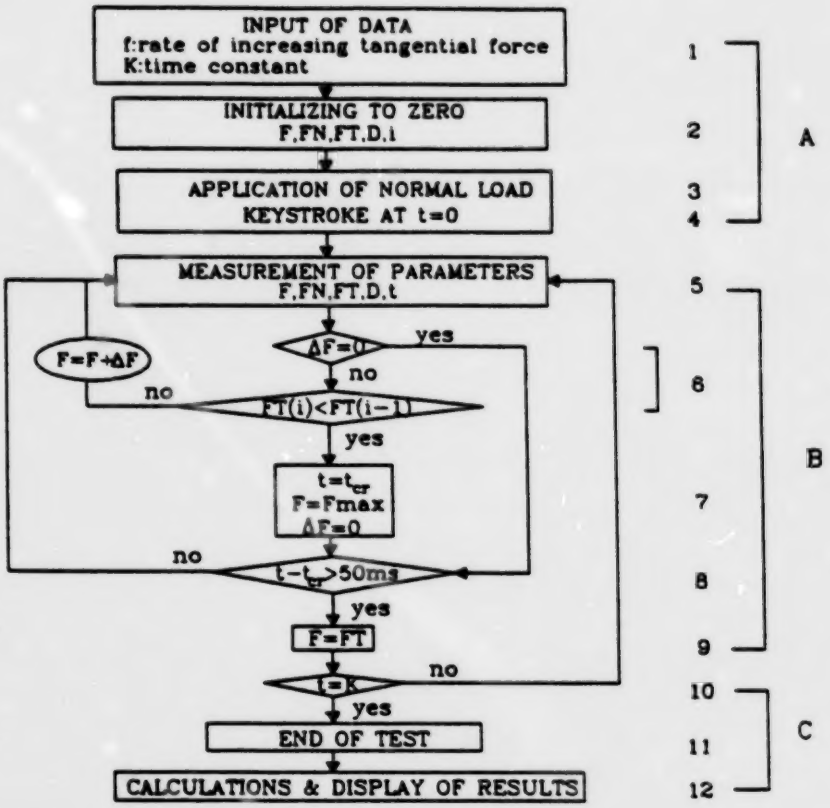

Fig. 2: Flow chart of software to measure static and quasi-dynamic friction coefficients

RESULTS

Figure 3 is a plot of the values of F_t and D recorded during a typical test. This figure shows clearly that F_t increases linearly until t_{cr} is reached. At t_{cr}, the relative

displacement D starts to increase while F_T decreases and reaches a new stable value. The amount of this decrease depends on the property of the plastic to transfer or not a film to the slider (Tabor, 1961).

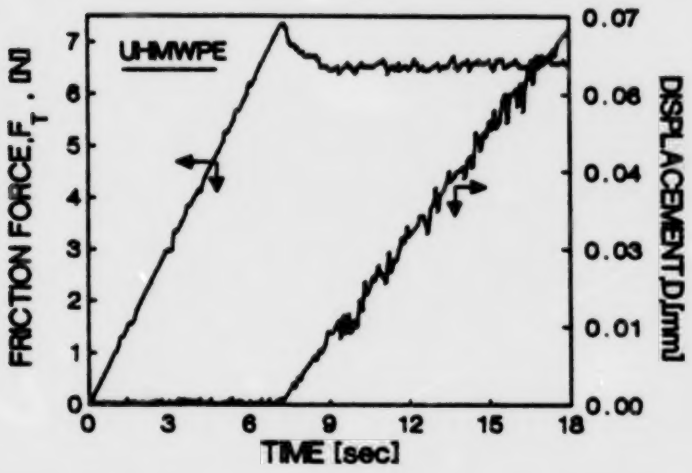

Fig. 3: Relative displacement and friction force as function of time: F_n = 50 N, CLA = 0.7 µm

The data points in Fig. 4 represent the values of the static coefficient of friction μ_s calculated by equation (1) as function of the normal load for UHMWPE (taken as example). The solid lines represent the best fit using a power law. μ_s decreases as the normal load increases, which permits to believe that adhesion is the main component of friction in this case (Savkoor, 1974).

It was found that a relation of the form $\mu_s = \alpha F_n^n$ fits well the experimental data. Table 1 lists the values of exponent n and α for the three thermoplastic materials at the four surface roughness studied. The proportionality constant has

a value which depends on the roughness of the plastic specimen.

Table 1: Experimental values of n and α in $\mu_s = \alpha F_N^n$

PLASTIC	n	α
UHMWPE	-0.184	0.22 - 0.32
POM	-0.069	0.28 - 0.32
PA 66	-0.037	0.39 - 0.42

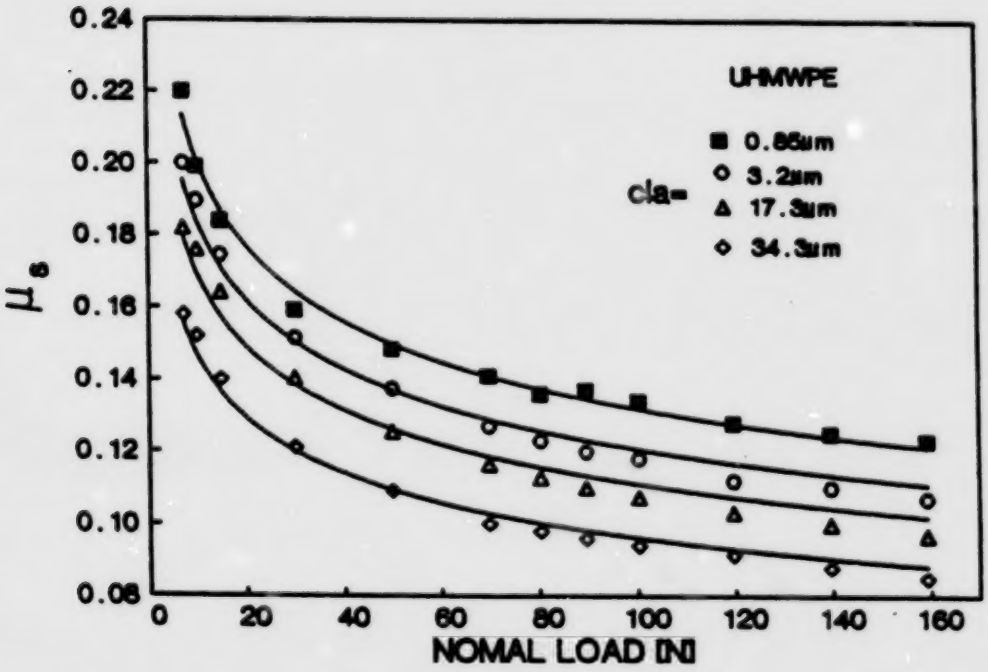

Fig. 4: Static coefficient of friction versus normal load

Figure 5 represents the variation of quasi-dynamic coefficient of friction μ_{qd} as function of the product of the normal load by the relative sliding speed established from the corresponding portion of displacement diagram (Fig. 3). Those results indicate a rapid decrease of μ_{qd} then a constant value is reached as $F_N v$ increases. This is well represented by the solid lines obtained by fitting the data to an exponential function $\mu_{qd} = k_1 + k_2 \exp(F_N v)$ where k_1 and k_2 are constants using a least-square fit.

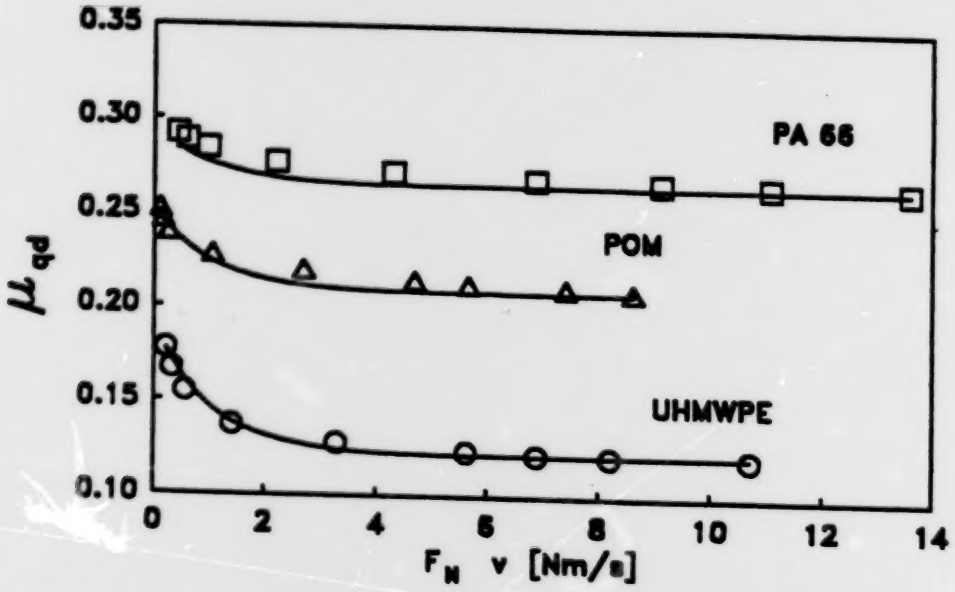

Fig. 5: Quasi-dynamic coefficient of friction as function of normal load and relative sliding speed: CLA = 0.7 µm

CONCLUSION

That procedure is useful to determine easily and accurately the coefficient of static friction in a variety of useful conditions.

The experimental measurements have confirmed that the static coefficient of friction decreases when the normal load and the roughness increase in the range of values tested.

The experimental procedure allowing a constant speed when relative movement starts shows that any increase in the normal load would increase the speed at which slip occurs.

REFERENCES

Benabdallah, S.M. (1987) Study of sliding friction between thermoplastics and metal under plane on plane contact. Ph.D. Thesis. École Polytechnique de Montréal.

Savkoor, A.R. (1974) Adhesion and deformation friction of polymer on hard solids. In Advances in Polymer Friction and Wear. Plenum Press. New York, 69-121.

Tabor, D., Wynne Williams, D.E. (1961) The effect of orientation on the friction of polytetrafluoroethylene. Wear, 4, 391-400.

ACKNOWLEDGEMENTS

The authors want to thank the National Research Council of Canada for their financial support.

Correlation between a laboratory impact-abrasion test and an *in-situ* marked-ball test

Michel Fiset
Université Laval
Ste-Foy, Québec

Gilles Huard and Jacques Masounave
Industrial Materials Research Institute
National Research Council Canada
Boucherville, Québec

INTRODUCTION

The elaboration of new materials for grinding balls usuallly requires high costs, an important part of which is attributed to the wear investigation, especially when these tests are performed in actual industrial ore grinders. Large expenses could be avoided by the use of a laboratory test for a first ranking of the material wear resistance. But questions often arise about the validity of the test since the wear mechanisms encountered in grinders are hardly reproduced in laboratory tests. A simple impact-abrasion test was established and carried out on six experimental grinding ball cast irons. The results were compared with others coming from a marked-ball extensive investigation conducted on the same materials and a good linear correlarion was obtained between them.

TEST METHOD

Impact-abrasion tests were carried out with an abrasion pin-test apparatus using standard abrasive belts available on the market. The operation parameters were first set-up using a martensitic high chromium white cast iron (3.05%C, 17.00%Cr, 0.50%Mn, 0.50%Si - 31.9 vol% carbide - 67 HRC). Cylindrical specimens (6 mm in diameter) were then taken out from a variety of six different grinding balls by electro-erosion. A flat end was machined perpendicular to the specimen length, so that the nominal contact area remains constant along the entire test.

Each sample was submitted to a series of 540 impact-abrasion cycles. In each cycle, the specimen was first lifted up, then dropped on the fixed abrasive paper (SiC, 40 grit, 425 μm) with an impact load of 550 MPa, which is comparable to what is encountered in actual grinders [1]. The rotating specimen was subsequently maintained on the abrasive paper during approximately one second, independently of the rotation speed, under a constant static load of approximately 100 N. It was finally lifted up for a new cycle and during its ascendent motion, the paper was displaced so that the sample will drop on fresh abrasive. Wear measurements were done at intervals of 90, 180, 360 and 540 impact-abrasion cycles for the chromium cast iron, but only after the whole series of 540 in the case of the experimental materials. Three rotation speeds of the specimen were looked at: 0 (impact wear), 20 and 60 rpm.

Prior and after each measurement, the specimen was cleaned and weighed with a precision of 0.1 mg. Mass losses were used as wear rate values, which is fully acceptable in view of the similar density of these materials.

RESULTS AND DISCUSSION

Figure 1 exhibits the results obtained on the martensitic high-chromium white cast iron. In some cases, it shows a relatively short running-in period which may be neglected, particularly if a rotation is applied to the sample. During the steady-state, linear relations hold between the wear loss and the number of cycles. Impact-abrasion tests indicate that the abrasion wear is almost completely achieved after one third of a specimen rotation (at 20 rpm during one second). A full rotation (60 rpm) only leads to a slight increase of mass loss.

The wear rates at steady state should be expressed by the slope of the linear regressions shown in Figure 1, rather than by the mass loss after a given number of cycles. Both types of calculation were however executed for this cast iron and showed that the difference between them could be neglected if the test duration was long enough. In view of this, and in order to accelerate the experimental procedure, it was decided to use mass losses after 540-cycle tests to compare the laboratory results on grinding balls with the *in situ* wear measurements.

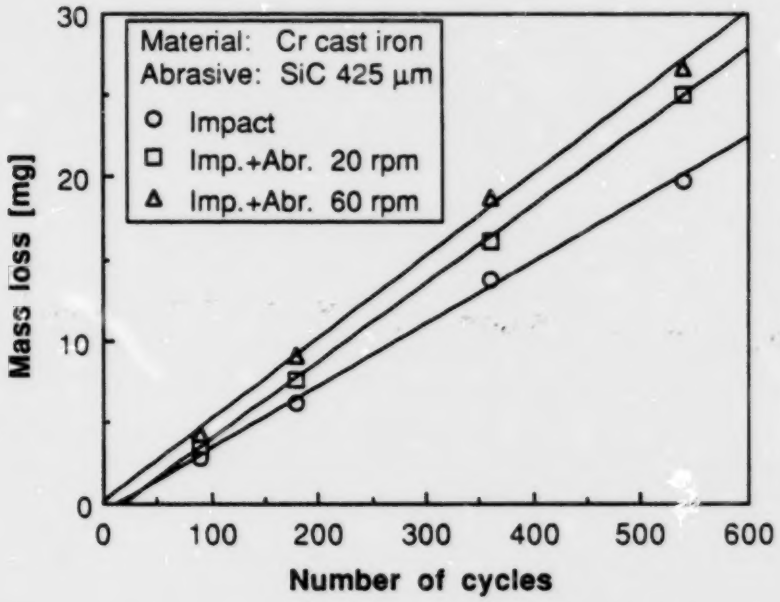

Figure 1. Wear loss of the martensitic cast iron.

Figures 2 and 3 show the correlation between laboratory and field measurements for the six investigated materials. Field measurements come from marked-ball tests carried out by Dumont together with Magotteaux Canada Company. The method and results have been extensively described elsewhere [2]. The marked-ball tests were conducted on 4 cm diameter balls in a 4187 kW grinder of 5 m inside diameter filled with a mixture of hematite and coal at 37% of its maximum charge and rotating at 73% of its critical speed. Figure 2 correlates laboratory wear losses to those measured on balls removed from the grinder after four different periods of time. It is seen that in each case a linear correlation holds between these two parameters. The slope slightly increases with the duration of the marked-ball test while the increase of the intercept value is more pronounced. The straight lines shown in Figure 2 are actually portions of curves which should intercept the origin. The fact that these curves are not linear over the entire range may be attributed to the longer time needed to reach the steady-state over the whole ball surface in the grinder, compared to what happens in the laboratory test in which the impact always occurs on the same surface area. At the beginning of the marked-ball test, abrasion does not

not necessarily occur on a hardened portion of the ball surface and the mass loss should be higher. This will be so as far as the whole surface has not attained its steady-state.

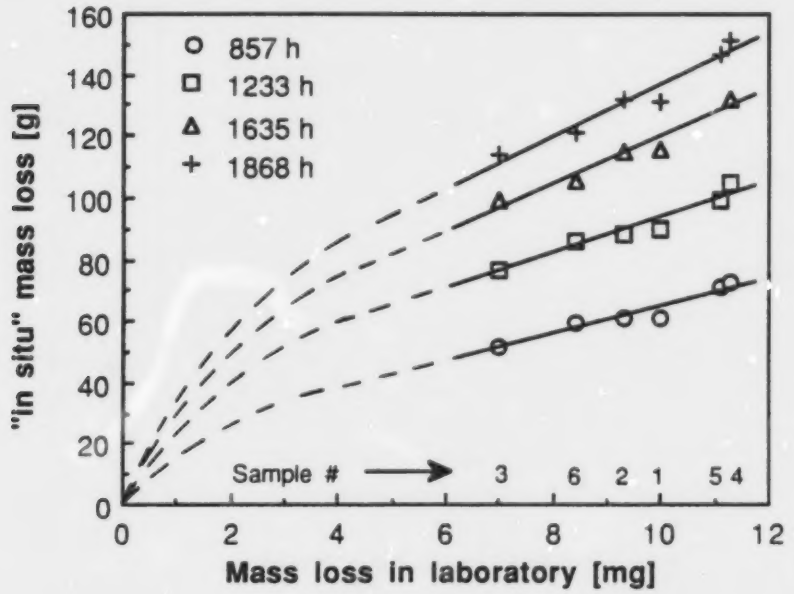

Figure 2. Correlation between wear loss obtained with the marked-ball test and those coming from the laboratory impact-abrasion pin test.

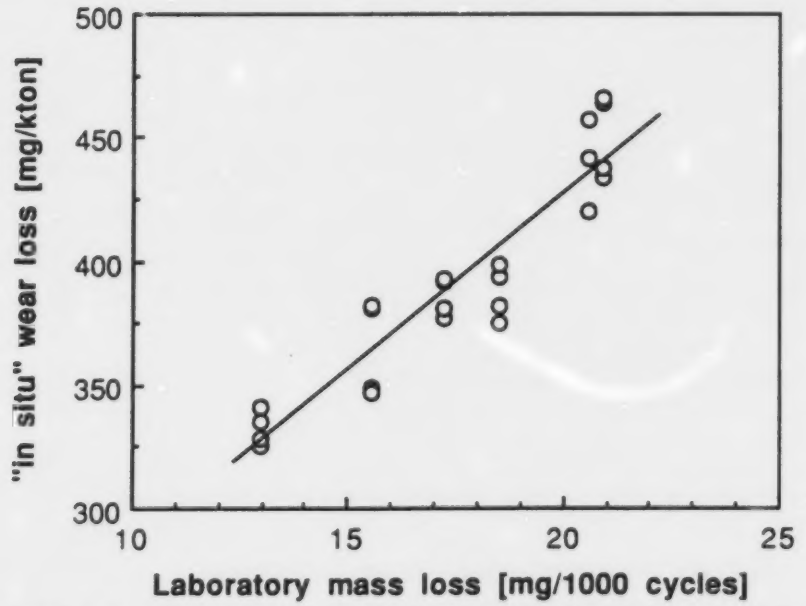

Figure 3. Correlation between "*in-situ*" wear loss per kiloton of crushed ore and the wear loss measured in the laboratory.

Figure 3 shows the wear in the grinder expressed in ball mass loss per kiloton of crushed ore as related to the pin wear loss obtained in laboratory. The relation is similar to those in Fig. 2.

CONCLUSIONS

The results of the present study show that a simple laboratory direct impact-abrasion pin test can rank the wear resistance of materials selected to be used for industrial ore grinding balls. This test basicallly consists in the repetition of impact-abrasion cycles, each of them including a drop of the tested specimen onto unworn abrasive paper (SiC, 40 grit, 425 µm) with a nominal impact load comparable to those encountered in real grinders (550 MPa), followed by the removal of the impacted layer of the specimen through abrasion mechanisms. Using this method, a linear correlation was established between results of 540-cycle laboratory tests and marked-ball tests carried out on six different experimental grinding ball white cast irons. It is therefore expected that such a test could be used in industry to obtain a first ranking of the wear resistance of experimental grinding ball materials.

ACKNOWLEDGEMENTS

The authors wish to thank M. Léon Leclercq from Magotteaux Canada for having supplied the cast iron balls and Sylvain Turenne from IMRI for his comments on the paper.

REFERENCES

1. D.J. Dunn and R.G. Martin, Measurement of Impact Forces in Ball Mills, Mining Engineering, April 1978, 384-388.

2. R. Dumont, Elaboration et calibration d'un modèle d'usure pour les corps broyants, Master Thesis, Univesité Laval, Québec, May 1988.

INVESTIGATIONS WITH PLASMA-SPRAYED COATING OF AGRICULTURAL TOOLS

by

R.L. Kushwaha and C. Roy
Agricultural Engineering Department, Department Genie Mecanique
University of Saskatchewan, Universite de Sherbrooke
Saskatoon, Sask., Sherbrooke, Quebec

INTRODUCTION

A major portion of the energy and wear losses in agriculture can be attributed to the movement of tools in soil. The quantity of soil moved each year by these tools is enormous, even though the depth seldom exceeds 100 mm, as the area involved is large. The process by which agricultural tools wear evidently include impact, abrasion and chemical action.

A strategy for tribology in Canada published by the National Research Council (1986) states that total annual losses in agricultural sector due to friction amount to about 320 million dollars and due to wear about 940 million dollars. The potential savings due to reduction in friction and wear through improved tribology would amount to nearly 337 million dollars.

Researchers have tried for years to reduce the cost of tillage operations by reducing soil-metal friction. Most of the studies have been done on moldboard plows. Attempts have been made to use Teflon coatings, liquid emulsions or air, and electro osmosis. However, these techniques have not been successful at the farm level.

With current advances in hot plasma technology, tillage tool surfaces can be coated with amorphous alloys to reduce wear and friction. Therefore, the objectives of this study were to investigate soil forces on a metallic glass coated cultivator sweep and to compare these with the forces on a regular sweep.

LITERATURE SURVEY

All tillage operations involve a sliding action of soil over surface of the tool. The major component of friction on a tillage tool is usually soil-metal friction. The soil properties along with the shape of the tillage tool determine the soil forces on the tool. As a tool passes through the soil, the soil-metal friction causes the edge to become blunt, which results in higher soil forces.

Schafer et al. (1975) used a liquid polymer to lubricate the soil-metal interface in order to reduce friction. However, a practical device for field use was not developed. Moore and McLees (1980) studied the effect of speed on wear of steel and copper over a speed range of 1-18 km/h and found that there was an increase of 90 percent in volume wear for steel but no significant effect was found for copper. Fox and Bockhop (1965) reported that using Teflon or Teflon with glass filler reduced the draft by 6 to 38 percent depending upon clay content and

moisture content of soil. However, these materials would wear eight to ten times more rapidly than steel thus not being practical. The National Institute of Agricultural Engineers, U.K., has successfully tested ceramic substituted cutting edges and found them to last three times longer than steel (Williams, 1986).

The materials used in tillage equipment require strength and toughness to resist distortion and impacts, and hardness to resist wear. In general, steels have adequate strength and toughness, but relatively poor wear resistance. A surface coating could be used to increase the hardness of the material and yet retain the softer core to help absorb impacts (Foley, 1984). Metallic glass coating offers just these characteristics (Roy et Bacha 1986, 1988, 1989).

EXPERIMENTAL EQUIPMENT AND PROCEDURES

The top leading edge (cutting surface) of three sweeps of 203 mm (8 inch) size each were coated, using nickel based alloy powder (AMDRY-915) by plasma spraying. The coated and regular sweeps are shown in Fig. 1.

The sweeps were tested in the indoor soil bin facility of the Department of Agricultural Engineering, University of Saskatchewan. The soil forces were measured with a multi-directional transducer equipped with six load cells (model SSM-500 from Interface Inc.); one to measure the force in the direction of travel, (draft), two to measure the vertical force and three load cells to measure the side force (Kushwaha et al. 1986).

Soil preparation in the soil bin was extremely important to simulate field conditions as well as for the comparisons of tests from different soil preparations. The soil preparation procedure included adding water with a spray boom since uniformity of soil moisture was very essential for even preparation of soil. A soil moisture content of 12 to 15% was used to represent a typical field condition. The soil was then tilled with a full width roto-tiller once or twice depending upon soil conditions and was levelled with respect to the carriage to maintain uniform working depth of the sweeps. Soil compaction level comparable to the field conditions were obtained by packing the soil at the sub-surface and surface using a sheep foot packer first and then a smooth packer. Leveling was also important during packing operation for uniform compaction of soil. In order to ensure equivalent compaction level of field, compaction level in the soil bin was measured at surface, 50 mm, and 100 mm depth at various positions with a cone penetrometer (model CN-970-51 #15143 from Soiltest, Inc.) before each test.

Four tests, two with coated sweeps and two with regular sweeps, were conducted per soil preparation. The coated and uncoated sweeps were switched alternately in all four positions to minimize the effect of soil variability. An average pitch angle of 5 degrees was used for all the tests. This was considered to be a typical pitch angle for the light duty sweeps being tested. A depth of 75 mm was used for all tests because this depth is comparable to a field operation with these sweeps.

The speed of 6 km/h was used for all of the tests. The HP 1000

computer in conjunction with the HP 2240 datalogger was used for data acquisition. A set of 60 readings of soil force data were automatically collected at 50 ms intervals during each test run. Forty runs were made in the soil bin, twenty with the coated sweep and twenty with the regular sweep. The program also calculated the mean draft, vertical and side forces that acted on the sweep in the test run.

RESULTS AND DISCUSSION

The mean values of cone index at various depths for all soil preparations indicated that the cone index was comparable to the values obtained in the stubble fields reported by Kushwaha et al. (1986).

Table 1 lists the mean values of draft and vertical force for both type of sweeps along with two variables T-test statistics. The statistical analysis showed that there was a significant difference at the 95% confidence level, in the draft force of the coated sweeps as compared to the regular sweep. A highly significant difference in the vertical force of the coated sweep at a 99% confidence level was also observed.

Figure 2 shows a graphical representation of the mean values of draft and vertical forces. The side forces were not analyzed due to the numerical closeness of the values. The error bars shown were calculated at a 95% confidence level. On an average, there was a 15 percent reduction in the draft and a 75 percent reduction in the vertical force of the coated sweep. This shows a significant potential in using ceramic coatings to reduce energy requirement of tillage tools.

The problem of poor coating/substrate bonding was encountered in the testing of the coated sweeps. The coating flaked off of the first test sweep on the very first pass in the soil bin. The cause of this failure probably was the fact that the equipment used to coat the sweep was setup for coating flat surfaces and not the curved surfaces of the sweep. Therefore, the coating thickness ranged from 400 μm to 30 μm at the tip.

Tests by Foley (1984) and Moore (1975) suggested that plasma coating process leaves a coating with a high porosity, that has low bond strengths to the underlying component. Hamel (1986) observed that the cause of the poor coating/substrate bond may be due to incomplete melting of the ceramic powder because of there short exposure to the heat, and rapid particle acceleration.

The hardness varied from 600 to 800 HV (Vickers Hardness). By comparison the hardness of an optimized coating is around 1200 HV. It is at this hardness value that the coating performs the best as a wear resistant material. This shows a significant potential in using metallic glass coating to reduce energy requirement of tillage tools.

CONCLUSIONS

The metallic glass coating was effective in reducing the soil forces on the sweeps tested. A 15 percent decrease in draft, and a 75 percent decrease in the vertical force was observed in comparison to a regular

sweep. The difference in side forces was minimal and therefore not considered in the comparison.

Although the metallic glass coating was effective in reducing soil forces, its durability in the field tests have to be evaluated. The few tests carried out with the coated sweeps enabled us to assess the quality and strength of the bond between the coating and the substrate. Further work is necessary to optimize the coating procedures and to characterize the interfacial bonding strength.

REFERENCES

Bacha, N. 1988. Relation entre l'etat amorphe d'un alliage et l'amelioration de la resistance a l'usure. Memoire de maitrise (M.E.Sc.), Universite de Sherbrooke, Quebec.

Bacha, N., C. Roy and J. Masounave. 1986. Relation entre l'etat amorphe d'un alliage et l'amelioration de la resistance a l'usure abrasive. Advances in Thermal Spraying - ITSC-86, p.435.

Canada, National Research Council, 1986. A Strategy for Tribology in Canada. (Report) Ottawa.

Foley, A. 1984. Abrasive wear of cultivation equipment by soil. Soil and Water. Vol. 12:12-14.

Fox, W.R. and C.W. Bockhop. 1965. Characteristics of a Teflon-covered simple tillage tool. Trans. of the ASAE 8:227-229.

Hamel, E.S. 1986. Ceramic coatings: More than just wear resistant. Materials Engineering 103:46-50.

Kushwaha, R.L., A.S. Vaishnav and G.C. Zoerb. 1986. Soil bin evaluation of disc coulters under no-till crop residue conditions. Trans. of the ASAE 29:40-44.

Moore, M.A. 1975. The abrasive wear resistance of surface coatings. J. agric. Eng. Res. 20: 167-179.

Moore. M.A. and V.A. McLees. 1980. Effect of speed on wear of steel and copper by bonded abrasive and soil. J. Agric. Eng. Res. 25:37-45.

Roy, C. and N. Bacha. 1989. Amorphous alloy for coating with exceptional wear resistance. 5th International Congress on Tribology-Eurotrib-89, Helsinki, June 12-15.

Schafer, R.L., W.B. Gills and C.A. Reaves. 1975. Lubrication of soil metal interface. Trans. of the ASAE 18:848-851.

Williams, M. 1986. Ceramic material for farm equipment. Implement & Tractor. Feb. 1986. pp. 20-22.

Table 1. Mean Values of Soil Forces (N) and Statistical Analysis

DRAFT	VERTICAL FORCE	SIDE FORCE	
675.9	241.1	12.1	Mean Regular
573.0	60.9	11.1	Mean coated
157.2	58.9	10.9	Standard deviation regular
61.1	29.5	9.4	Standard deviation Coated
37.7	14.7	3.2	Standard Error
2.73	12.24	0.31	t calculated
38	38	38	Degrees of Freedom
23.3%	24.4%	89.8%	Coefficient of Variation Regular
10.7%	48.5%	84.9%	Coefficient of Variation Coated

The value of t at a 95% confidence level was 2.025 and at 99% confidence level was 2.713 for 38 degrees of freedom.

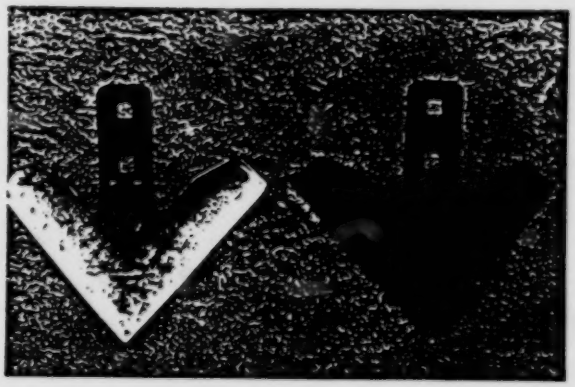

Figure 1. Coated and Regular 203 mm (8 in) sweeps.

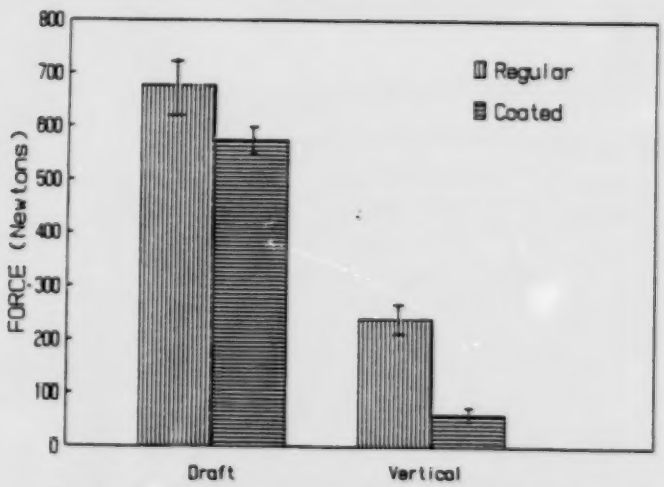

Figure 2. Soil forces on Regular and Coated Cultivator sweeps.

FRICTION II

UNE ÉTUDE DE L'USURE DU NYLON ET DE L'ACÉTAL FROTTANT CONTRE L'ACIER

M. Amarouch, H. Yelle
Groupe de Recherche sur les Matériaux
Plastiques et Composites (GRPC)
École Polytechnique de Montréal

ABSTRACT

A testing program has been conducted to evaluate the wear rate of nylon and acetal materials when sliding against steel in mild conditions of load (78 Kpa to 620 Kpa) and speed (0,1 m/s to 0,5 m/s). For the purpose of the program, a Tabor 505 Dual Abraser machine has been modified to simulate a pin-on-disc apparatus. This paper describes the experimental set-up as well as the testing conditions and procedures. Part of the raw results are presented. Complete results, along with a detailed analysis, shall be the subject of a future publication.

Keywords: wear, friction, nylon, acetal, plastic, polymer

1 - Introduction

Les dommages et les pertes dus à l'usure ont un effet néfaste sur l'économie nationale même si certains secteurs de celle-ci dépendent directement, pour fonctionner, du changement périodique des pièces usées. Ainsi, une étude dirigée par Énergie, mines et ressources du Canada [1], avec la collaboration du Conseil national de recherches du Canada (CNRC), rapporte une perte annuelle d'environ 5 milliards de dollars dans différents secteurs de l'industrie canadienne due au frottement et à l'usure, cette dernière représentant la majeure part, à savoir 3,9 milliards de dollars. Cette étude précise aussi que le quart de ces pertes peut être sauvé avec une bonne application des technologies existantes.

L'état de l'art du phénomène d'usure des matériaux n'est qu'à son stade embryonnaire surtout lorsqu'il s'agit de nouveaux matériaux comme les plastiques. L'usure et le frottement ne sont pas des propriétés intrinsèques des matériaux mais des caractéristiques du système frottant. Le moindre changement dans la charge, la vitesse ou l'environnement peut causer un changement considérable du taux d'usure d'une ou des deux surfaces en contact. Plusieurs études ont été faites pour déterminer l'influence de ces paramètres [2,4]. Dans ces études, pour obtenir beaucoup d'usure, les chercheurs imposaient souvent des conditions d'essai (charge, vitesse, fini de surface) assez sévères; peu d'entre eux, cependant, se sont intéressés au même phénomène mais dans des conditions moins sévères, conditions qu'on retrouve dans plusieurs applications qui causent aussi de l'usure et dont il est intéressant de connaître l'influence.

Notre intérêt a donc porté sur l'étude de l'usure du PA 101 (Nylon) et du POM (Acétal), POLYPENCO Ltée [5], lorsqu'ils frottent sur de l'acier, et ce pour une grille de charges et de vitesses variant de 78 KPa à 620 KPa et de 0,1 m/s à 0,5 m/s respectivement. Ces deux plastiques sont assez répandus dans la fabrication de pièces mécaniques frottantes. La combinaison plastique/métal présente des avantages liés aux problèmes thermiques et se retrouve dans beaucoup d'applications et de montages mécaniques [6]. Vu le caractère autolubrifiant des plastiques, on a choisi un frottement à sec. Ceci représente d'ailleurs la majorité des cas où les plastiques trouvent application.

2 - Machine d'essai

Pour notre étude, une machine TABOR 505 Dual Abraser, généralement utilisée pour l'évaluation de la résistance à l'abrasion des matériaux (figure 1), a été adaptée pour la rendre de type tige sur disque (pin-on-disc). Le montage permet de tester simultanément, à quatre vitesses différentes, huit échantillons pouvant supporter des charges différentes les unes des autres.

La modification apportée à la machine Tabor consiste à remplacer les disques et les meules originaux par:

- deux disques en acier qui contiennent des pistes d'usure (figure 2);
- un support en aluminium pouvant accueillir jusqu'à huit échantillons simultanément (figure 1);
- des poids de 250, 500 et 1000 g (figure 2) qui ont été usinés dans de l'acier et qui servent de charges qu'on applique individuellement sur les échantillons.

La machine telle que modifiée est montrée à la figure 1. La capsule représente la machine Tabor originale. Elle peut aussi être utilisée pour l'étude de paires de matériaux autres que plastique/acier. Notons qu'il est très facile de passer d'une version à l'autre de cette machine.

3 - Pistes d'usure et échantillons

Les disques de 19 mm d'épaisseur ont été usinés dans des barreaux d'acier fini à froid (AISI C-1020 -Drummond, McCall

& Co. [7]) de 152,4 mm de diamètre. Des pistes de 7 mm de large ont été par la suite aménagées sur ces disques en pratiquant des rainures circulaires de 9,5 mm de profondeur (figure 2). Ceci a été fait afin de minimiser le transfert de chaleur d'une piste à l'autre. Finalement, la surface des pistes a été rectifiée à la meule puis finie à la main à l'aide de papier abrasif (carbure de silicone - 400 mesh). Ceci a été fait pour enlever les marques unidirectionnelles de la rectification et obtenir ainsi un fini de surface presque uniforme d'environ 0,12 µm Ra dans toutes les directions.

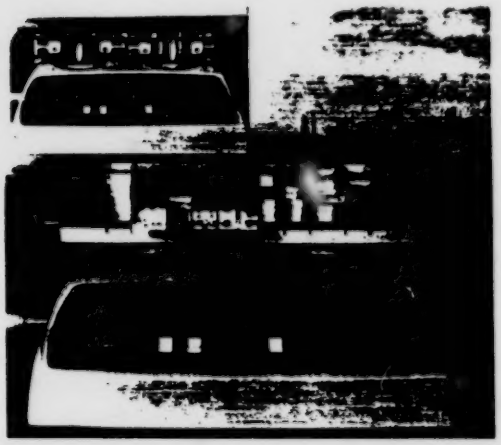

Figure 1
Version modifiée de la Tabor 505 Dual Abraser utilisée pour les essais.
En capsule, la version originale.

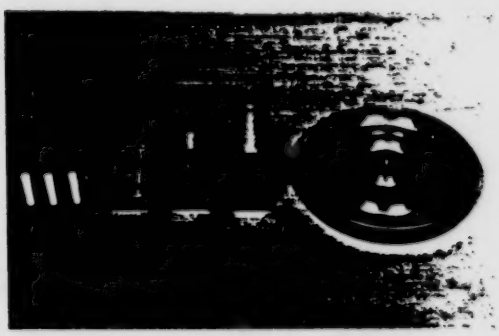

Figure 2
Exemples
(a) de la piste d'usure
(b) de poids de chargement
(c) d'échantillons utilisés lors des essais

Les échantillons sont des tiges de plastique extrudées de 6,35 mm de diamètre (1/4 po) et de 31,75 mm (1 1/4 po) de long (figure 2) . La première dimension a été choisie du fait que plusieurs matériaux sont fabriqués en tiges ayant ce diamètre. On évite ainsi l'usinage des pièces, chose qui peut modifier leurs propriétés mécaniques, sans oublier les pertes de temps et d'argent que cela occasionne. La hauteur de 31,75 mm a été choisie en fonction des dimensions du support d'aluminium afin d'éviter le flambage de la tige sous chargement et d'assurer du matériel en quantité suffisante pour des tests de durée raisonnable.

Les échantillons ont été fabriqués à partir de longues tiges de plastique qui ont été coupées à la scie en tigelles d'environ 32 mm. Leurs extrémités ont ensuite été usinées sur le tour puis surfacées à la main à l'aide de papier abrasif de 400 mesh aussi afin d'enlever les fragments d'usinage. Une fois finis, les échantillons de nylon et d'acétal pèsent environ 1,15 g et 1,40 g respectivement.

4 - Procédure expérimentale

Le schéma de la figure 3 illustre les différentes étapes de la procédure suivie lors des tests. Pour chaque plastique, après avoir complété les procédures A, B et C (figure 3), on choisit la charge à appliquer sur les huit échantillons qui seront testés simultanément (78 KPa à 620 KPa). Dépendamment de la piste sur laquelle ils seront placés, ces échantillons seront testés deux à deux à une vitesse de 0,1, 0,25, 0,35 ou 0,5 m/s. On procède par la suite aux étapes D, E, F, G et H puis on place les échantillons sur la machine (étape I). Après des durées cumulatives de glissement de 6 et 24 heures, on exécute les procédures J, K et H et on replace les échantillons sur la machine dans leur position azimuth initiale afin de respecter le sens des sillons d'usure (étape I). Lorsque l'expérience est terminée (48 h), on choisit d'autres conditions opératoires et on reprend à la procédure D.

L'usure des échantillons a été mesurée par pesée. Les pesées ont été faites à l'aide d'une balance d'analyse électronique (METTLER AE 240, précision d'affichage de 10^{-4}g). Les conditions ambiantes durant les essais étaient de 23°C ± 2°C et de 30 % ± 2 % d'humidité relative. Un échantillon témoin qui ne frottait pas était placé près de la machine durant tous les essais. Cet échantillon servait à détecter des variations éventuelles de poids dues principalement à l'absorption ou à la perte d'humidité, ou encore aux conditions de la pesée (la balance est sensible à la variation des conditions ambiantes).

Résultats

Les figures 4 et 5 présentent une partie des résultats bruts obtenus lors des essais d'usure sous forme de masse perdue en fonction du temps de glissement pour différentes conditions de vitesse et de charge, et ce pour le nylon et l'acétal. Chaque point apparaissant sur les courbes de ces figures est la moyenne arithmétique de deux essais. On remarque que la perte de masse, après 48 heures de glissement et sous une charge de 620 KPa, peut aller jusqu'à 20 mg

(figure 4-d), soit une diminution de presque 2 pour cent de la masse initiale de l'échantillon. Ceci est assez considérable et justifie bien l'intérêt de ces travaux et l'importance quant à la considération du paramètre "usure" même si les conditions opératoires sont relativement peu sévères.

La totalité des résultats ainsi qu'une analyse détaillée de ces derniers fera l'objet d'une présentation ultérieure.

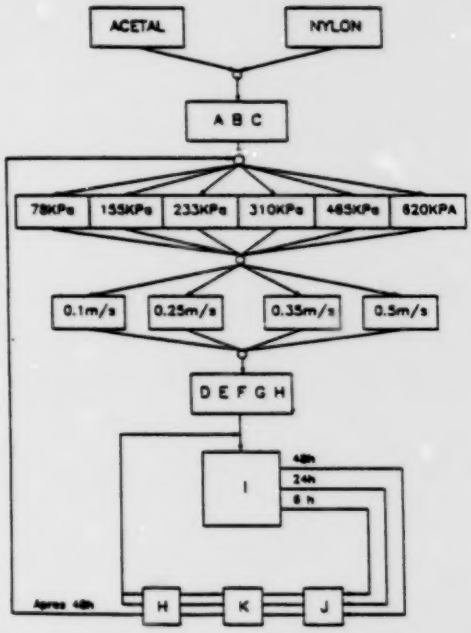

Légende

A - Nettoyer les échantillons à l'eau distillée et au méthanol et sécher.
B - Numéroter les échantillons et entreposer 48 heures pour préconditionnement.
C - Rectifier les pistes.
D - Finir les pistes au papier abrasif, les nettoyer à l'eau distillée et au méthanol et sécher.
E - Mesurer la rugosité des pistes.
F - Observer les échantillons au microscope.
G - Observer les pistes au microscope.
H - Peser les échantillons y compris le témoin.
I - Placer les échantillons sur la machine d'essai à une position azimuth de référence et mettre en marche.
J - Arrêter la machine.
K - Nettoyer les échantillons au jet d'air.

Figure 3
Organigramme de la procédure suivie lors des tests

Remerciements

Ces travaux ont été rendus possibles grâce, en partie, à une subvention du Conseil de Recherche en Sciences Naturelles et en Génie du Canada.

Références

[1] NRCC Associate Committee on Tribology, "A Strategy for Tribology in Canada", National Research Council Canada, NRCC Publication Number 26556, 1986.
[2] DOWSON, D., GODET, M. and TAYLOR, C.M., "The Wear of Non-Metallic Materials", Mechanical Engineering Publications, London, 1976.
[3] POLYMER SCIENCE AND TECHNOLOGY, Vol. 58, "Advances in Polymer Friction and Wear", Ed. Lieng-Huang Lee, Plenum Press, NY, 1974.
[4] BARTENEV, G.M. and LAVRENTEV, V.V., "Friction and Wear of Polymers", Elsevier, Amsterdam, 1981.
[5] POLYMER POLYPENCO CORPORATION, P.O. Box 422, Reading, PA 19603.
[6] PLASTICS GEARING, ABA/PGT PUBLISHING, 1395 Tolland Turnpike, Manchester, CT 06040, U.S.A.
[7] DRUMMOND McCALL CATALOGUE, 5205 Fairway, C.P. 900, Montréal, Québec H8S 4E9.

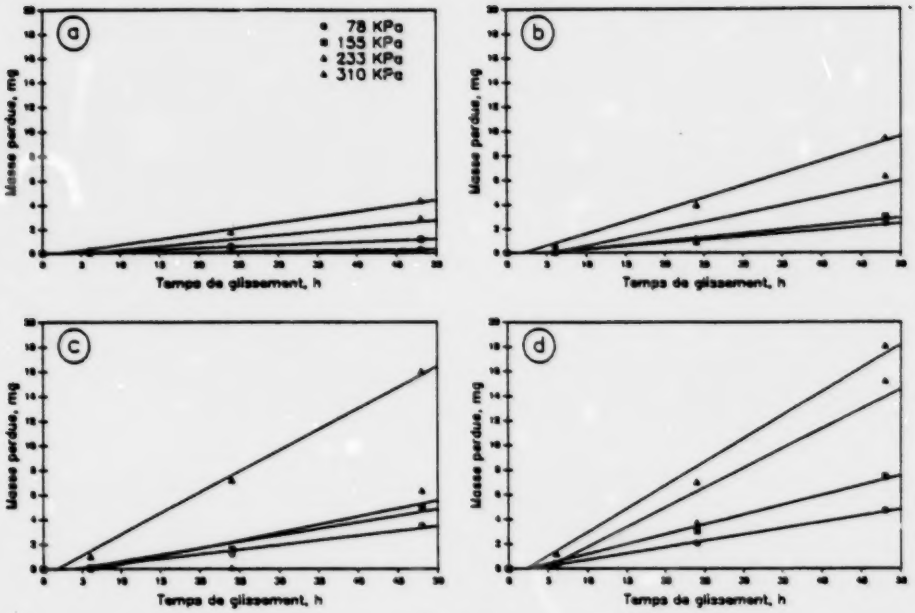

Figure 4
Perte de masse par usure des échantillons de nylon en fonction du temps
a: 0,1 m/s; b: 0,25 m/s; c: 0,35 m/s; d: 0,5 m/s

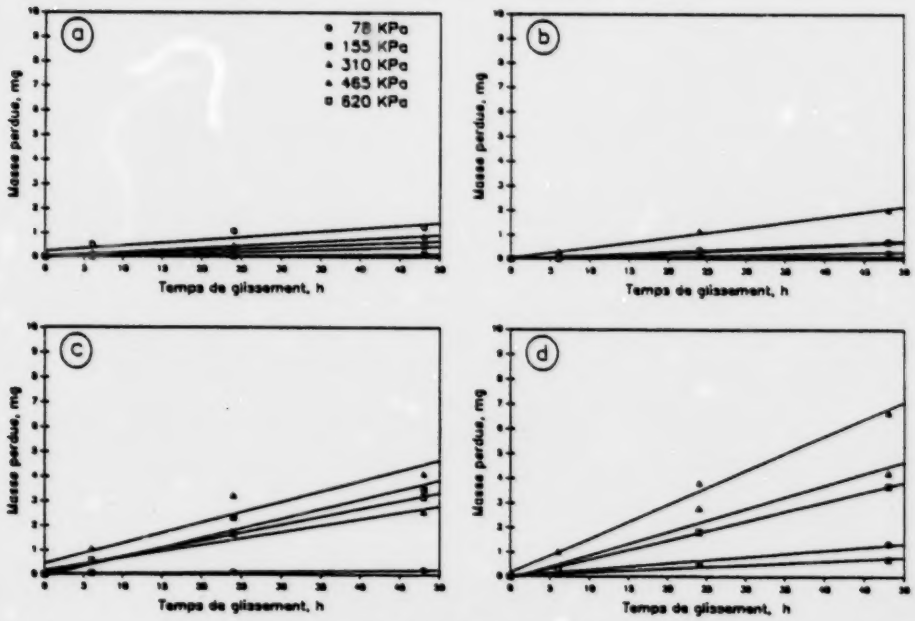

Figure 5
Perte de masse par usure des échantillons d'acétal en fonction du temps
a: 0,1 m/s; b: 0,25 m/s; c: 0,35 m/s; d: 0,5 m/s

Scientific Numeric Databases - Tools for Tribology

Gordon H. Wood
Canada Institute for Scientific and Technical Information
National Research Council
Montreal Road, Ottawa, Ontario, K1A 0S2

I. Introduction

It is well known that tribology is a multi-disciplinary field drawing on research and practice in materials and lubricants as well as component and assembly design. From the viewpoint of the practitioner, however, this rich diversity leads to problems in gathering intelligence. Not only are the results of tribology research and development published in a variety of specialized journals but the data are diverse and inconsistently described.

While not the total solution, Scientific Numeric Database Systems do provide a practical means of addressing these problems. In crystallography which, for example, impacts on a large number of fields, many researchers have been routinely using numeric databases for years and have come to regard these systems as another tool in their trade. Similar trends are developing in molecular biology where databases of protein and nucleic-acid sequences are the only practical means of handling the prodigious amount of data being produced daily. Clearly, tribological data are much more difficult to standardize than either of the two examples just cited, but significant progress is being made. It is the purpose of this paper to describe some of the databases and systems already available to the tribologist and outline some of the developments planned.

Three scientific numeric database systems with potential as tools for tribology will be described but space does not permit an exhaustive review. The intention is to give the interested reader a guide to further reading and contacts for additional information. The progression will be from the macroscopic (engineering properties) to the microscopic (fundamental properties).

II. Definitions

Databases may conveniently be partitioned into two broad categories: reference and source.[1] "Reference" includes those databases that contain bibliographic citations or references to other information sources; "source" includes those databases that contain numeric, textual-numeric, full-text or image information.

---

[1] *Directory of Online Databases*, Cuadra/Elsevier: New York, 1989; Vol. 10

Thus, a "hit" in a reference database points to the location of the desired information whereas a "hit" in a source database contains the desired information itself.

A scientific numeric database (SND) may therefore be defined as a source database, usually falling within the textual-numeric subcategory. This definition is sufficiently broad that it could include printed compendia; for purposes of this article it is understood that the SNDs are machine readable.

Good SNDs are, in fact, much more than mere compilations of numbers which one thumbs through electronically with the aid of a computer. What raises SNDs above the electronic handbook level are the value-adding features of critical evaluation and search/retrieval/analysis software. The former serves to make the data more reliable than those found in the open literature and more useful because of the rationalization of factors like material descriptors, test reporting and units of measurement; the latter makes the data truly accessible by facilitating (a) types of searches not possible or practicable in printed products and (b) varieties of analyses of those data without the time consuming and error-producing need for re-keyboarding them.

III. ACTIS - A Computerized Tribology Information System

A. Background

ACTIS has evolved from a series of seminal workshops convened in July 1985 by the ASME Research Committee on Tribology, the National Institute for Standards and Technology (formerly NBS) and the US Department of Energy.[2] The international participants summed up their deliberations by recommending the establishment of an information system containing six basic database components:

1. Numeric Data

This will be a collection of critically evaluated data on the basic properties and performance of materials, lubricants, components and systems. In each area, tribology experts will review and distil the existing data to compile a "best judgment" set of values in a standard format.

2. Design

These databases will contain design codes for selecting materials, lubricants and components along with design analysis and calculation programs. Many of these codes already exist but must

---

[2] Rumble, J. and Sibley, L. Eds., *Towards a Tribology Information System*, NBS Special Publication 737, U. S. Department of Commerce, Washington, D.C., Dec. 1987.

be evaluated and rationalized before being added. It is planned to include an expert system front end as an aid to the non-tribologist.

3. Newsletter

The communication medium for ACTIS, this component will involve a conventional hard copy newsletter as well as electronic mail services.

4. Bibliographic

A collection of reference databases, as defined above, this component will be the gateway to the literature. In principle, existing databases could satisfy the needs of most users but, in practice, there are problems with accessing the various databases not to mention differences in their coverage, their keyword schemes and their searching software.

5. Research-in-Progress

This will contain abstracts of current (not yet published) tribology research being conducted across all sectors. Additional information to be given includes the types of activities, general areas of interest, program objectives and tribology applications.

6. Product/Services Directory

As implied by the name, this component will be a compilation of commercially available tribology products and related services. Vendors will supply the data and pay a fee to have them included in the system.

B. Status

ACTIS has matured to the point that a non-profit body, with international representation on its Board of Directors, has been incorporated (ACTIS, Inc.) to take the project to self-financing status. Several subjects in the numeric databases component have been completed and are currently being field tested with release for sale scheduled for November 1989. Similarly, a number of design codes are ready for testing. The software which integrates the databases, especially so that data may be transferred between the numeric and design databases, is almost ready for field testing and should be released by the end of 1989. Material for the research-in-progress component has been gathered in a survey of some 480 individuals in the USA recently conducted by the National Science Foundation. Current plans call for the Newsletter to be

available in early 1990. Readers wanting more information should consult a recent article[3] or contact ACTIS directly.[4]

IV. The Materials Property Data Network (MPD Network)

Conceived and planned in several workshops and reports dating back to 1982, the MPD Network is a service designed to provide easy online access to databases on the engineering properties of materials. Obviously, the MPD Network is not as sharply focused on the needs of tribology as ACTIS but it is a system of which the tribologist should be aware.

The MPD Network may be thought of as a gateway linking its users to several materials properties databases which may be mounted on a variety of computers in numerous locations. The two most important values added by the MPD Network concept are a user interface to facilitate searching the different databases and a metadata system which deals with the varying nomenclature, terminology, abbreviations and other data about the data.

A not-for-profit organization, the National Materials Property Data Network, Inc., was established in 1986 to give leadership to this endeavour and bring it to a point of viability. Progress has been significant to the extent that a pilot system with three databases[5] has been available online to sponsors since August 1987. Currently, one may conveniently search by material or by property on one or all the databases. Directories point to other sources of data not yet available on the Network. The Canada Institute for Scientific and Technical Information (CISTI) is a sponsor of the MPD Network; readers interested in evaluating the prototype system are invited to contact the author.

---

[3] Jahanmir, S., Hsu, S.M., and Munro, R.G., *ACTIS: Towards a Comprehensive Tribology Database*, Computerization and Networking of Materials Databases, ASTM STP 1017, J.S. Glazman and J.R. Rumble, Jr. Eds, American Society for Testing and Materials, Philadelphia, 1989, pp. 340-348.

[4] Mr. Allan Hughes, Executive Director ACTIS, Inc., 1118 Highgate Road, Wilmington, Delaware 19808, USA.

[5] Sections of MIL-HDBK-5, some sections of the Aerospace Structural Metals Handbook and STEELTUF (a database of more than 20,000 individual toughness tests of more than 50 steels).

More details are given in a recent article by Kaufman[6] or may be obtained from the MPD Network directly[7].

V. The Canadian Scientific Numeric Database Service (CAN/SND)

CAN/SND is a service provided by CISTI, a Division of the National Research Council of Canada. Via CAN/SND, scientists and engineers have online access to databases in analysis, molecular structure and molecular biology[8]. The CAN/SND components of primary interest to tribologists are two prototype tribology-related databases and the molecular structure databases group.

In collaboration with the NRCC Associate Committee on Tribology, CAN/SND is experimenting with two widely different tribology databases. The first is a collection of unpublished, numeric wear test results of water-lubricated journal bearings; the second is a directory, largely textual, of audiovisual instructional materials for tribological practice which may be borrowed or purchased. Those interested in using these databases in prototype are invited to contact the author. It is possible, ultimately, that these and related databases will be part of ACTIS.

Insofar as the microscopic, crystallographic properties of materials are related to their macroscopic, engineering properties, it is worthwhile for the tribologist to be aware of molecular structure databases. These databases[9] are available now on the CAN/SND online system and may be accessed simply and economically via Datapac and any modem-equipped computer or computer terminal. Again, further information may be obtained from the author.

---

[6] Kaufman, J.G., *The National Materials Property Data Network, Inc. - A Cooperative Approach to Reliable Performance Data*, Computerization and Networking of Materials Databases, ASTM STP 1017, J.S. Glazman and J.R. Rumble, Jr. Eds, American Society for Testing and Materials, Philadelphia, 1989, pp. 55-62.

[7] National Materials Property Data Network, Inc., P.O. Box 02224, Columbus, OH 43202, USA.

[8] Wood, G.H., Rodgers, J.R., Gough, S.R., *Canadian Scientific Numeric Database Service*, Journal of Chemical Information and Computer Sciences, 1989, *29*, 118-123.

[9] CRYSTDAT (NIST Crystal Data Identification File); CRYSTIN (Inorganic Crystal Structure Database); CRYSTMET (NRC Metals Crystallographic Database).

MODELLING OF ROLLED JOINTS

R. Metcalfe and J.M. Pietralik

Atomic Energy of Canada Limited – Research Company

INTRODUCTION

Reliable rolled joints between zirconium alloy pressure tubes and stainless steel end fittings are crucial to the success of the CANDU* family of nuclear reactors . These joints must be leaktight, have good pullout strength, low tensile residual stresses, and be durable. Their success underpins the high capacity factors achieved to date in the Canadian stations. However, various changes to fuel channels are being proposed to improve the capital cost and lifetime of newer CANDUs, necessitating a new look at joints and new data for qualification of new designs.

Based on existing empirical data, the effects of proposed changes such as thinning the end fitting hub, using different materials or surface treatments, etc., can only be speculated. The time is ripe to develop a predictive model to account for the structural and tribological characteristics of such joints, using the capabilities of modern computing. The finite element analysis described herein represents the start of this task.

The joint assembly method of prime interest, used successfully in all recent field installations, is cold rolling whereby a tool with five rollers is rotated and expanded inside the portion of the pressure tube within the hub, thereby causing plastic deformation and high residual contact stresses at the tube-to-hub interface. The wall of the tube is thinned during this process, and some material extrudes axially out of the joint. Factors that have been recognized as important to rolling success include wall reduction, material properties, surface friction, and the geometries and relative positions of the components.

PROGRESSIVE MODELLING APPROACH

A one-dimensional model for the material well within the hub was analyzed first to explore plastic deformation and inter-related temperature effects. This was followed by simple two-dimensional modelling of the tube material outside the hub in the so-called 'transition zone' where the expanded tube flares out from its undeformed size. Two-dimensional modelling of hydraulic fitting (an interference fit, assembled by applying then releasing hydraulic pressure at the interface) of the complete ungrooved joint was then used to simulate the effects, if not the details, of the rolling process. Results from this latter model are presented here.

In practice the hub always has grooves to interlock with bulges formed on the tube during rolling to increase the pullout strength. These have been ignored in the early models since they have little influence on residual stresses elsewhere. They will be added later, as required.

Also ignored, and proposed for future analysis, is the rolling process itself. This thins, flares and work-hardens the tube within the joint by measurable amounts, permitting them to be included in a

---

* CANada Deuterium Uranium

later refinement of the present hydraulic fitting analysis. However, rolling also creates significant localized heating and introduces frictional stress distributions between tube and hub. The characteristics and importance of such additional effects will remain uncertain until rolling is analyzed in more detail.

Any inclusion of anisotropy or stress relaxation has also been deferred to later work. Values used here for tube and hub material properties at room and operating conditions (300°C, 9.65 MPa) are given in Table 1. Both materials were allowed to deform plastically according to the Prandtl-Reuss incremental flow rule wherever the Von Mises yield criterion was exceeded.

METHOD OF ANALYSIS

The joint details, based on the Darlington station, are shown in Figure 1. Analysis was by a general purpose finite element code, using a typical mesh of isoparametric, first order, quadrilateral elements (Figure 2). To calculate joint stresses/strains, initial interference was modelled by assigning negative width to a gap/friction element at the interface of the unloaded model at uniform temperature, then imposing interface coincidence. No friction or other non-linearity was allowed in this simulated fitting process; however, it is closely representative of hydraulic fitting since axial strains are insignificant in such case. Stresses were confirmed to remain elastic during initial fitting for the results presented herein. (Note that for thermal shrink-fitting, axial friction would be induced at the interface, causing a different residual stress state that would require an incremental solution.)

Once fitted, a pressure tube-to-end fitting joint in practice is subject to internal pressure, temperature change and predominantly axial load. The effects of these 'subsequent loadings' have been calculated while allowing for plasticity and friction. Plastic strain in any element was assumed to be at constant volume, and coefficients of friction of 0.2 and 0.4 were assumed at the joint interface. Linear relationships were assumed for variations of material properties with temperature (Young's moduli, Poisson's ratios, yield, thermal expansion and work hardening slope). Before fitting, all stresses were assumed zero.

The length of tube to be analyzed was chosen after confirming (by stress calculations for different lengths) that end effects were negligible. The analysis then proceeded using the mesh of Figure 2, except that results for interface pressure were also checked using a finer mesh with double the elements and found to be within 15%.

Figure 3 shows the sequence of events modelled, starting with separate tube and hub, then forcing them to fit by respectively increasing and decreasing their diameters to give a common interface. Service temperature and pressure were then applied by incrementing first to 300°C, then applying 9.65 MPa to the inside of the tube.

MODELLING RESULTS

By applying load and restraint as shown in Figure 3, and assuming no hydraulic pressure bleeding into the interface, pullout was calculated 'numerically' as shown in Figure 4. This compared well with results from the simple formula for pullout strength (= area x friction coefficient x interface pressure) and less well with a supposedly 'more accurate' formula (see Ref. 1).

Pullout strength approaches a limiting value with interference because there is a maximum value of interface pressure limited by hoop strength of the tube. Having grooves in the hub (Figure 1) would enable a higher limit to be approached, governed by axial strength of the tube.

The effect of hub thickness (Figure 5) shows its diminishing effect above ~5 mm and almost no improvement beyond ~20 mm, even when compared on the basis of the same interference. It was

noted that in fact the interface pressure and pullout strength can be made highest by choosing the tube and hub thicknesses to be 'compatible' in the sense that when they are fitted together both reach their elastic limit at the same level of interference.

In Figure 6, the one-dimensionality of interface pressure within the joint zone (i.e. within the axial extent of the hub) can be seen, evidenced by the insignificant axial variation. There is a 20-25% drop from room to operating conditions, with the temperature effect clearly overwhelming the pressure effect, which alone would cause an increase.

Figure 7 isolates the temperature effect by showing radial stress distributions at atmospheric pressure at an 'average' mid-joint position. Interface pressure (the converse of radial stress at the tube-to-hub interface) is seen in Figure 8 to reduce with hub thickness for the same interference. However, for the same allowable tube stress, a greater interference is appropriate for the thinner hub. Its interface pressure at room temperature would then be the same as for the thicker hub, and its temperature response superior (Figure 8). Interface pressure increases with operating pressure (Figure 9 compared with Figure 7), as does the corresponding hoop stress. However, there is apparently little effect due to friction in the range, 0.2 to 0.4.

CONCLUDING REMARKS

Results for finite element modelling of idealized hydraulically fitted interference joints have been presented, giving the pullout strength and the two-dimensional state of stress within such a joint and its transition zone. This allowed for yield, work-hardening, expansion and variation of material properties with temperature. Some of the calculated findings are as follows:

- Contact pressure at the joint interface (conventional design) decreases by ~14 MPa from room temperature to 300°C and increases by ~8.5 MPa due to operating pressure of ~10 MPa.

- A thin-hub joint (using the same interference and thinning) has significantly less interface pressure than a conventional hub at room temperature, but changes less as temperature increases. It could be regarded as superior to the 'thick hub' if given greater interference.

- The simplest formula (area x pressure x friction) is satisfactory (within ~10%) for pullout strength.

Despite obvious differences in this model versus the 'real thing', the results bear close resemblance to measured results for normal rolled joints. Pullout strength increases almost proportionally with friction coefficient until limited by yield strength of the tube material. Friction, however, has little effect on the way residual stresses in a hydraulically fitted joint change subsequently with pressure and temperature.

ACKNOWLEDGEMENT

This work was funded by the CANDU Owners Group. Permission to publish the results is gratefully acknowledged.

REFERENCE

1. Singh, K.P. and Soler, A.I., " Mechanical Design of Heat Exchangers and Pressure Vessel Components", (Chapter 7, "Tube-to-Tubesheet Joints"), Arcturus Publishers, Inc., Cherry Hill, N.Y., 1984.

TABLE 1. MATERIAL PROPERTIES

PARAMETER	UNIT	VALUE	
		At Room Conditions	At Operating Conditions*
Tube Young's Modulus	MPa	94 460	74 460
Hub Young's Modulus	MPa	201 300	184 100
Tube Yield Strength	MPa	510	333
Hub Yield Strength	MPa	586	497
Tube Poisson Ratio	-	0.38	0.39
Hub Poisson Ratio	-	0.283	0.29
Tube Work-Hardening Slope	MPa	1380	1100
Hub Work-Hardening Slope	MPa	345	275
Tube Thermal Expansion Coefficient	$[^{\circ}C]^{-1}$	5.2E-6	5.2E-6
Hub Thermal Expansion Coefficient	$[^{\circ}C]^{-1}$	9.43E6	10.93E-6

* 300 C, 9.65 MPa

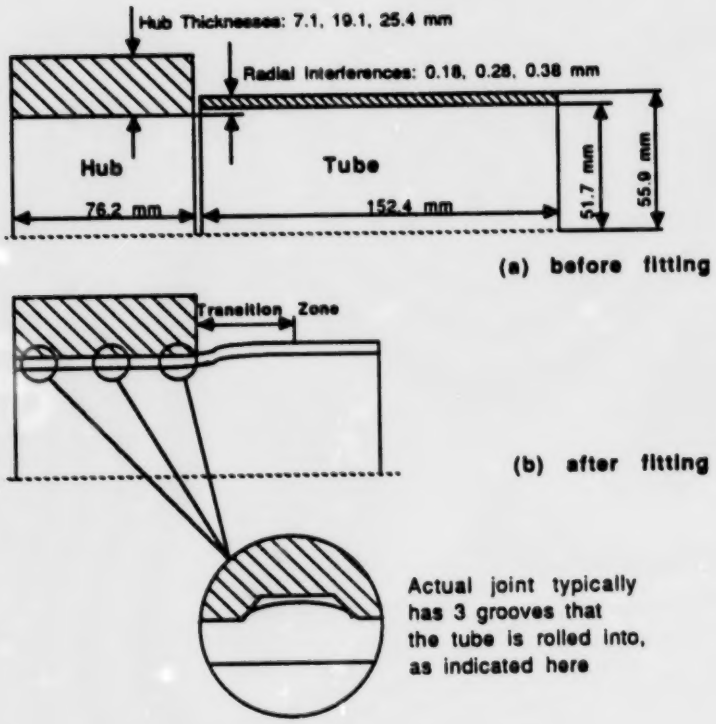

FIGURE 1: Geometry of Interference Joint Analyzed

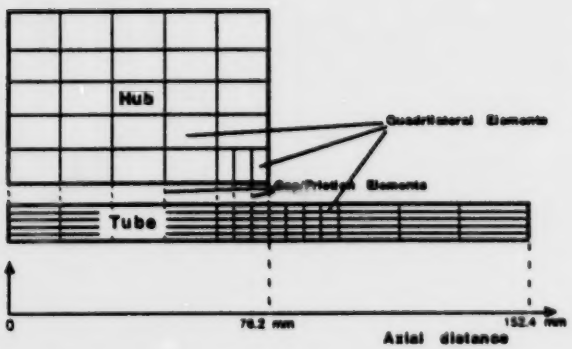

FIGURE 2: Mesh for Modelling Interference-Fitted Joint

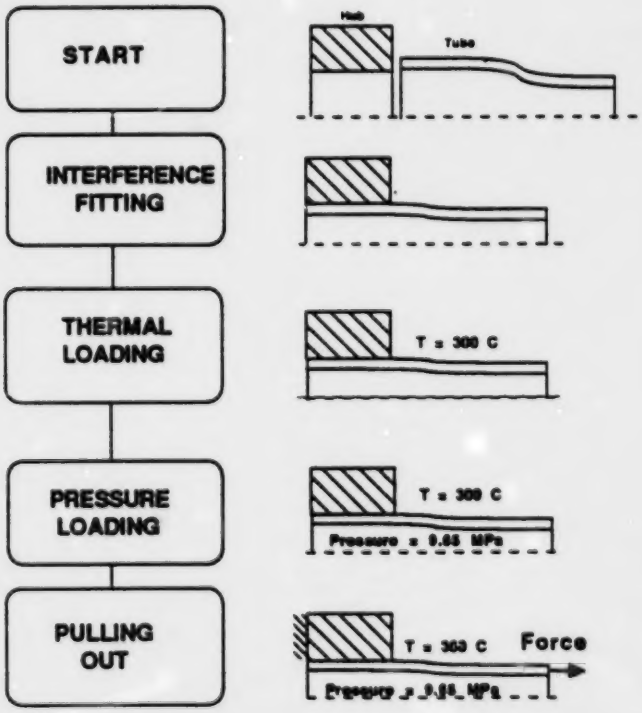

FIGURE 3: Modelled Sequence of Operations

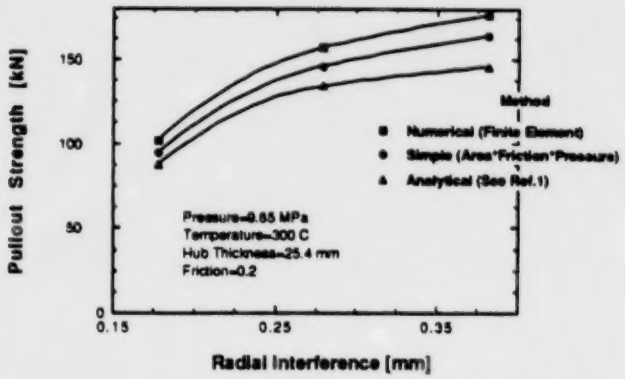

FIGURE 4: Effect of Radial Interference on Pullout Strength

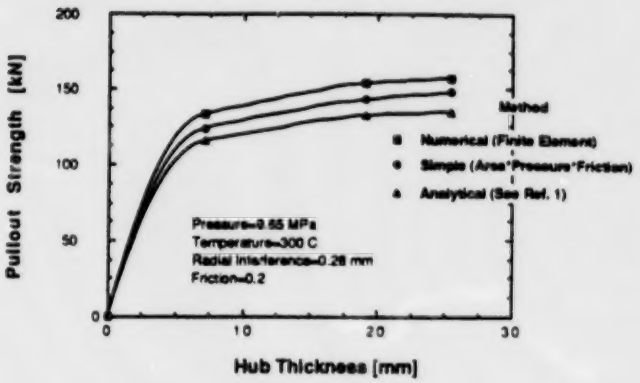

FIGURE 5: Effect of Hub Thickness on Pullout Strength

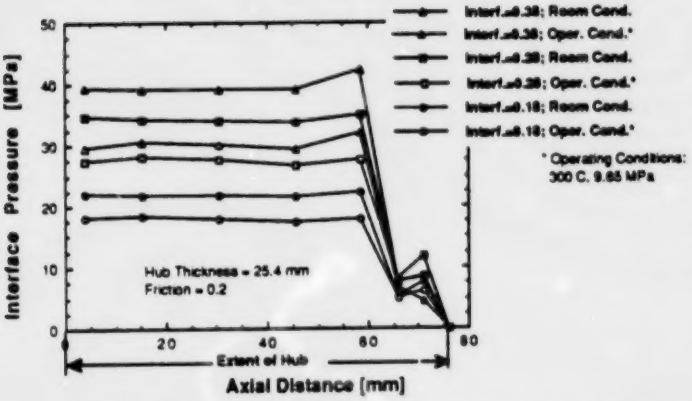

FIGURE 6: Effect of Radial Interference and Operating Conditions on Interface Pressure

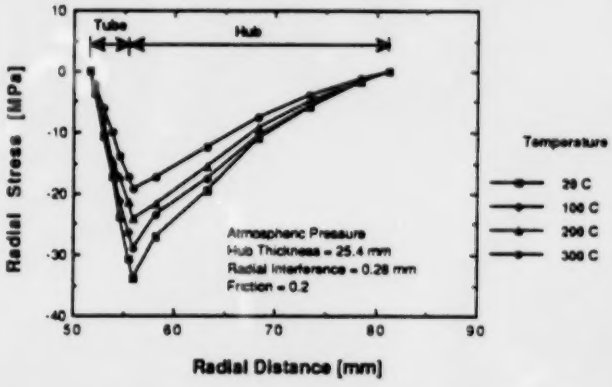

FIGURE 7: Effect of Temperature on Mid-Joint Radial Stress Distribution at Atmospheric Pressure

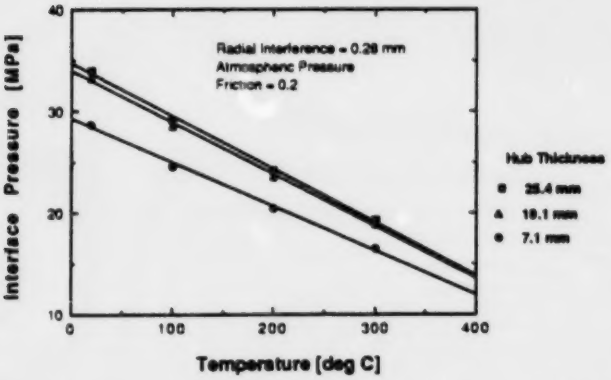

FIGURE 8: Effect of Hub Thickness and Temperature on Mid-Joint Interface Pressure

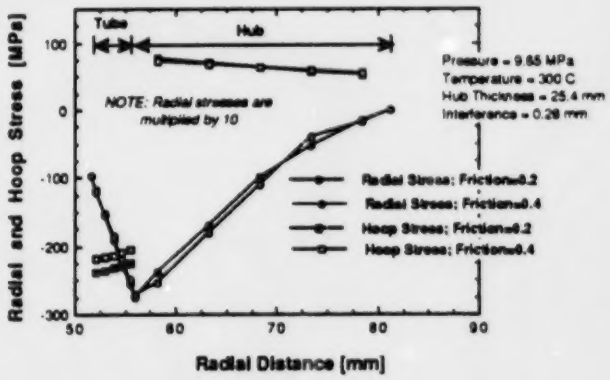

FIGURE 9: Effect of Friction on Mid-Joint Stress Distribution at Reactor Operating Conditions

Qualification Testing of Wear Materials for Mining and Extraction Applications at Syncrude's Oil Sands Plant

Rees Llevellyn

Syncrude Canada Ltd. Research

Abrasive and erosive wear attack is one of the most critical problems affecting oil sands mining, transportation and processing, at the two commercial plants producing synthetic crude oil, from the Athabasca deposits of Northern Alberta.

Syncrude Canada Ltd. is the largest operation, and in 1988 produced 54.8 million barrels of synthetic crude oil. This represented 10% of Canada's total oil requirements.

Over 20 million dollars are spent per year for the replacement of worn parts and equipment in Syncrude's open pit mining operation which handles 500,000 tonnes of overburden and oil sands per day and in the subsequent bitumen extraction stage. This cost figure does not include production losses resulting from equipment downtime due to wear attack.

The extremely abrasive conditions are caused mainly by hard particulate quartz, which is the predominant constituent of the ore body. The situation is exacerbated during winter mining by the very low operating temperatures, which consolidate the oil sand by freezing its water content.

Materials used for protection can be classified into the following three groups. These are listed in increasing order of wear resistance.

- Abrasive Resistant (A.R.) steels
- Chrome white irons
- Ceramics and carbides

They are available in a multiplicity of compositions, grades and forms, making it impractical to assess them all in the service environment.

Thus, a laboratory qualification testing program was introduced to determine wear resistance, strength, toughness, weldability and other relevant properties of the various options. Based on these performance data and economic factors, selections were made for service use or for field test evaluation.

The main assessment method is the ASTM G65-80 Dry Sand/Rubber Wheel test. This was chosen because it reflected the low stress sliding abrasion conditions, which predominate throughout Syncrude's mining operations and in the early stages of bitumen separation from solids. In addition, the abrasive medium of silica/quartz particles, is common to both the test method and to oil sands.

The validity of this approach for predicting comparative wear life, was confirmed initially in dedicated production trials. It has continued to provide reliable data during subsequent usage.

Information gathered in this program has enabled improved material selections to be made and has provided justification for more expensive options to be introduced.

Significant successes have been achieved in many areas, as typified in the following examples.

- Replacement of A.R. steel cone liners on the mine's four bucket wheel reclaimers (BWRs), with a more expensive bulk weld overlay system, has extended component life by approximately 8 times and generated direct savings of over 1.2 million dollars in labor and material costs. Of even greater impact, are the production benefits accruing from a reduction in machine downtime. These total 224 BWR operating days over an 8 year cone liner life period.

- Disc centrifuges used for separating diluted bitumen from solids and water in the extraction operation, suffer severe wear problems. The introduction of an alternative thermal spray hardfacing procedure, has reduced costs for repairing eroded bowl components by $750 K per annum.

AN INVESTIGATION OF THE STATE OF FRICTION AND OIL FILM IN OSCILLATING BEARINGS UNDER DYNAMIC LOADING

O. S. Dinç [+] M. Gediktaş[‡]

Abstract

Oscillating journal bearings under dynamic loading are studied. In a test apparatus, the state of friction of journal bearing and oil film are observed. The effects of journal bearing parameters, such as shaft rotation frequency, various bearing loads, the phase difference between load and shaft rotation frequencies, load and shaft frequency ratios, bearing clearances and the form of oil feeding grooves on friction and formation of oil film are investigated and test results are discussed. Based on the recordings of the loci of the bearing center and friction force, the contributions of the squeeze film and wedge effects on carried load are examined.

1 Introduction

The examples of oscillating bearings can be seen in some machineries, such as crosshead bearing of some diesel engines, bearing of road mechanisms and especially, connecting rod small end bearings in the internal combustion engine.

The study of Fogg and Jakeman [1] has shown the effect of various parameters on the friction by observing the friction force. Barwell, Milne and Webber [2] studied the effects of different oil grooves and appropriate bearing materials on carried load. Blount and De Guerin [3] examined the effects of various oil grooves, surface roughness and temperature on carrying load in two stroke engine rod-piston bearings. Then in the study of Cole and Hugses [4], using a transparent bearing body, whether or not a hydrodynamic oil film forms is investigated. Afterwards, Nelson and Gatcombe [5], by measuring the electrical resistance, explained that no hydrodynamic oil film is formed between the shaft and bearing. Jakobsen [6,7,8,9] published the results of his experiments on the parameters effecting the bearing performance, fricton loss, thermal balance and wearing. In addition, he discussed the relation between the shaft rotation velocity and friction force variation. Gediktas [10] and Yucenur [11] experimentally investigated the behavior of the bearing under stationary load. Yucenur theoretically analyzed the locus of the shaft center, the pressure distribution in the bearing and carried load by superposing the wedge effect and squeeze film effect. Berthier and Play [12] examined the wearing, friction force and the locus of the shaft in the contact region of a dry bearing under stationary load.

Up to now, stationary load conditions were investigated in almost every study in this field. Almost all of these studies were experimental. Since there are a few theoretical investigations of the oscillating journal bearings under dynamic loading (11,13), expereimental studies play a very important role in designing journal bearings. The test apparatus used in the study is so designed that the dynamic loading of the journal bearing can be only sinusoidal [14].

2 Test Apparatus

The test stand is so designed that the magnitude of the load can be changed and the load can also be varied from static to dynamic. The friction in the bearing, loci of the shaft center can be observed, the angular speed of the

[+]Rensselaer Polytechnic Institute
Department of Mechanical Engineering,
Troy, NY 12180
[‡]Technical University of Istanbul
Faculty of Mechanical Engineering
Gumussuyu, Istanbul, TURKEY
The authors are grateful to the FAG of Germany for technical support.

shaft, friction force and bearing load can be recorded simultaneously. Due to the hydrostatic oil film between the bearing body and the loading system, there is no metallic contact. The test stand can be used for different experimental purposes. It is designed to allow minimum errors while mounting and dismantling the bearing parts.

2.1 Structure

The body of the bearing, measuring and loading system can be seen in figure 2. Ground shaft has a 50 mm. diameter. (Center-line average roughness, R = 0.04 um.) Bronze bushes have been manufactured in precise dimensions, press-fitted into the bearing body which was ground inside and outside. Bearing body is placed between lower and upper hydrostatic bearings, each having two recesses. During the experiments, hydrostatic bearings are fed with sufficient oil so that the main bearing is free to rotate. Upper hydrostatic bearing transfers variable load to the bearing through a ball and a flat spring located on top of the bearing. Flat spring is loaded from the other end by a cam that can be changed to obtain different load amplitudes. Upper and lower hydrostatic bearings are furnished with capillary restrictors. In all experiments Mobil Vactra Oil Light with 75 cSt kinematic viscosity at 20°C is used. The oil of the hydrostatic bearings and the main bearing is supplied by the same pumping unit. Bearing shaft is driven through a four-bar mechanism to obtain the oscillating motion.

2.2 Measurement and Measuring Instruments

The test stand, measuring devices and the measuring system are shown in figures 1 and 2 respectively.

Friction force of the bearing is measured by using a ring dynamometer made of an aluminium alloy. Variable bearing load is generated by a flat spring and cam mechanism. The sinusoidal motion of the shaft is observed by the distance transducer which is attached to the end of the shaft. The straingages are placed on the ring dynamometer. Other gauges are located on the flat spring and the distance transducer is fed by seperate straingage indicators. All these three measurements are recorded into the three channel recorder simultaneously. Thus, the friction force, the load and the speed of the shaft can be observed and compared at the same time. The motion of the bearing center relative to the shaft center is traced by using two capacitive distance pick-up units perpendicular to each other and they are attached to the side of the bearing body. These pick-up units are then plugged into the oscilloscope to allow the loci of the bearing center to be seen on the screen as a closed curve.

3 Results

In all test groups, bearing pressure is between 0.1-1.5 MPa, oscillation frequency of the shaft is between 0-2000 rpc, bearing clearence ratio is between 0.0008-0.0021, oscillation angle of the shaft is 30°C. Two types of bearing bushes, which are axially and circumferentially grooved, are used. To limit the number of bushes, two shafts with different diameters are used. The frequency ratio which can be described as the ratio of the load frequency to the shaft rotation frequency, is changed as 1/2, 1 and 2 during the test. In all the test groups, stationary, unidirectional fluctuating, cyclic and alternating loads are applied sequentially to the bearing.

The test results are plotted as the variation of friction coefficients versus the varying oscillating frequency. Friction coefficient is calculated by dividing the largest friction force to the normal force in one cycle.

In figures 3a, b, c, d, e, f, results of the frictional behavior of axially and circumferentially grooved bearings under stationary, cyclic and alternating loads are plotted. For stationary load, under high loads and low speeds, friction coefficient is relatively high and it decreases by increasing speed, passes through a minimum and then increases slightly as shown in figures 3a and 3d. From figure 3a, it can be seen that at lower speeds, variation of friction force in one cycle is similar to a square wave but higher speeds it becomes sinusoidal. Since circumferential grooves feed shaft contact areas with more oil, especially under higher loads, circumferentially grooved bearings give lower frictional values.

In figures 3b and 3e, bearing load is cyclic. Friction coefficient decreases to 0.005-0.01. Friction force looses its square wave character at lower speeds and axially grooved bearing gives low frictional values. Under small loads at high speeds, because of the increasing importance of the squeeze film effect, the existence of the hydrodynamic film can be claimed. Under cyclic loading, axially grooved bearing gives lower frictional values as shown

in figures 3b and 3e, figures 7 and 8.

In figures 3c and 3f, results of the frictional behavior of the bearing under alternating load are shown. Friction coefficient increases linearly with increasing speed. Bearing load is carried by the squeeze film, and friction force becomes sinusoidal as shown in figure 3c. The magnitude of the friction force is determined by bearing clearance and sliding speed of the shaft.

The results of the friction behavior of axially grooved bearing under cyclic loading can be seen in figure 4. The ratio of the load frequency to the shaft rotation frequency is taken to be 1/2 and 2. When the ratio is 2, which means load frequency is two times the shaft frequency, the squeeze film effect is dominant in load carrying, as shown in figure 4b. On the other hand when the ratio is 1/2, the wedge effect is more important, as shown in figure 4a. Figure 9 shows the loci of the bearing center when the ratios are 1/2 and 2.

Loci of the bearing center is seen in figure 5 when the load is alternating. It can be seen that the bearing center is concentric with shaft center and the amplitude of loci decreases with increasing load frequency. In figure 6, it can be seen that at the same frequency, while load changes from alternating to unidirectional fluctuating load, the shaft tends to contact the bearing. In figure 7 and 8, under cyclic loading, the locus of the bearing center can be seen for axially grooved and circumferentially grooved bushing respectively.

It is known that under alternating loading, bearing center rotates with low amplitude around the shaft center as shown in figure 5. When the bearing is lightly loaded, alternating loading condition resembles 'Petroff model'. Friction values are calculated by using Petroff model [14] and these values are compared with the test results shown in figure 10. Only a 5 % to 15 % difference is encountered between the experimental and theoretical results. Therefore, it can be proposed that under alternating loading, the Petroff model can be easily used to predict the frictional behavior.

4 Conclusions

The results of this study on the behavior of oscillating journal bearings under different type of loads can be summarized as follows;

1. Under stationary loads; the load carrying fluid film may not be formed, the boundary friction exists in the bearing, the friction coefficient is greater than 0.02 and also increases with the increasing shaft frequency and the coexistence of axial grooves with the circumferential ones are advantageous in bearing desing.

2. When the load is cyclic, similar results are observed but friction coefficient drops to 0.005-0.01, the load is carried by the squeeze film while the shaft is much closer to the bearing. The parameters such as bearing clearance, type of oil groove, frequency ratio and the phase difference between the shaft and the load frequencies, effect on the friction. It can be said that the axially grooved bearing gives alower friction coefficient than the circumferential grooved bearing does.

3. If the load is alternating, it is carried by the squeeze film and the bearing friction is viscous type. Under different load frequencies, bearing clearance and groove type, the load was carried by the squeeze film.

4. As a next step, a new dimensionless number like "Sommerfeld number" can be defined to characterise the bearing behavior.

NOMENCLATURE

μ	Coefficient of the friction
n_m	Oscillation frequency of the shaft (cpm)
n_y	Frequency of the load
w	Angular speed of the shaft ($= w_o Sin\omega t$)
F_s	Friction force
F	Load of the bearing
F_{max}	Maximum load of the bearing
F_{st}	Stationary load of the bearing
p	Average pressure of the bearing
p_{max}	Maximum pressure of the bearing ($= F_{max}/b.d$)
p_g	Inlet oil pressure
d	Diameter of the bearing
b	Width of the bearing
ϵ	Eccentricity ratio (=e/c)
ψ	Dimensionless bearing clearance ratio (=2c/d)
c	Radial clearance

References

[1] Fogg, A. ,Jakeman, C. , "The Friction of an Oscillating Bearing", Engineering,Vol. 146,1938,pp.170.

[2] Barwell, F. T. ,Milne, A. A. ,Webber, J. S. , "Some Experiment on Oscillating Bearings",Trans. Inst. Engrs. Shipbuilders Scot. ,Vol. 98,1955

[3] Blount, E. A. ,De Guerin, D. , "The Importance of Surface Finish,Loaded Area Conformity and Operating Temperature in Small End Plain Bearings for High Duty Two Stroke Engines"Inst. Mech. Engrs. ,London,paper no. 80,1957.

[4] Cole, J. A. ,Hughes, C. J. , "Visual Study of Film Extent in Hydrodynamic Loaded Complete Journal Bearings",Inst. Mech. Engrs. ,London,paper no. 87,1957

[5] Nelson, G. G. ,Gatcombe, K. ,"Oscillating Bearing Study",ASME Ann. Meeting,New York,paper 58-A-156,Nov-Dec. ,1958.

[6] Jakobsen, K. ,Christensen, H. ,"Performance of Oscillating Bearings",Proc. Inst. Mech. Engrs. ,Vol. 183 Pt. 3P,pp. 66-73,1968-69.

[7] Jakobsen, K. ,"Oscillatory Journal Bearings",Tribology Handbook,Chapter A12,1972.

[8] Jakobsen, K. ,"Oscillating Bearing; A Theoretical end Experimental Investigation with Special Reference to Crosshead Bearings in Large Marine Diesel Engines",SINTEF Publication,Oct. 1965.

[9] Jacobsen, K. ,"Thermal Instabilty in Oscillating Bearings, Lubrication and Wear, Fundamentals and Application",Proc. Inst. Mech. Engrs. ,Vol. 182 Pt. 3A, pp. 137,1967-68.

[10] Gediktas, M. ,"Uber die Reibung und Schmierung der Schwenkbeweglichen Radial-Gleitlager", Publication of Mech. Eng. Dept of I. T. U. no. 45, Istanbul, 1972.

[11] Yucenur, S. ,"Salinim Hareketli Radyal Kaymali Yatakta Surtunme ve Film Durumu", Ph. D. Thesis, Istanbul Technical University, Istanbul 1979.

[12] Berthier, Y. ,Play, D. ,"Wear Mechanism in Oscillating Bearings", Wear Mater. , 1981, 30th March-April, 1981 ASME Paper, pp. 358-366.

[13] Gupta, B. K. , Phelan, R. M. , "The Load Capacity of a Short Journal Bearings with Oscillating Effective Speed", Trans. of the ASME, June 1964, pp. 348-354

[14] Dinc, S. ,"Degisken Yuklu Salinim Hareketi Yapan Kaymali Yatak, Surtunme ve Film Durumu", Ph. D. Thesis, Istanbul Technical University, Istanbul, 1986.

[15] Hays, F. D. ,"Squeeze Films; A Finite Journal Bearing With a Fluctuating Load", ASME Journal of Basic Engineering, Dec. 1961, pp. 579.

[16] Tichy, J. A. , Smith, R. N. ,"The Thermal Behavior of Oscillating Squeeze Films" ASME Journal of Lubrication Technology, Vol. 105, 1983, pp. 13-21.

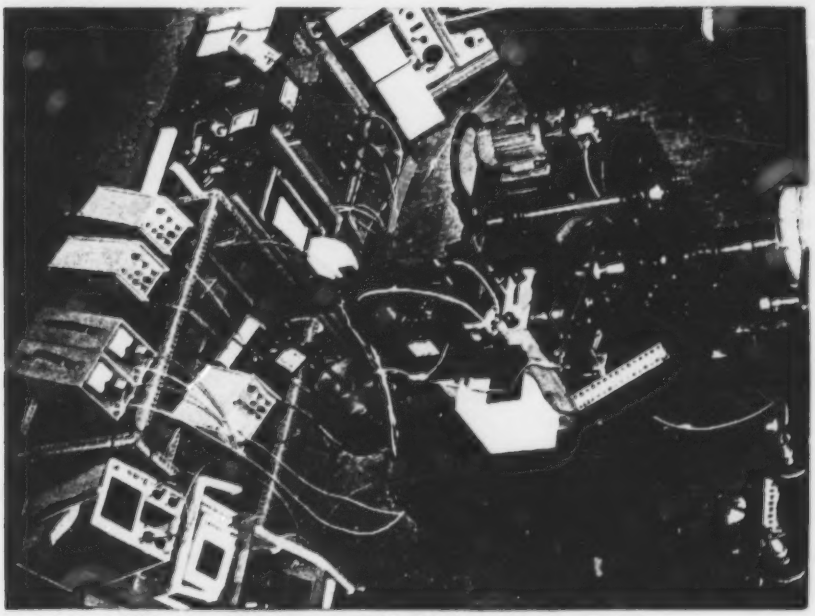

Fig. 1. The test stand and measuring system.

1	Bearing Shaft
2	Bearing bush
3	Bearing body
4	Lower Hydrostatic bearing
5	Upper Hydrostatic bearing
6	Flat - spring
7	Capacitive pick-up (Displacement transducer)
8	Ball
9	Ring dynamometer
10	Pretension spring
11	Frame
12	Hanging rod
13	Oil inlet

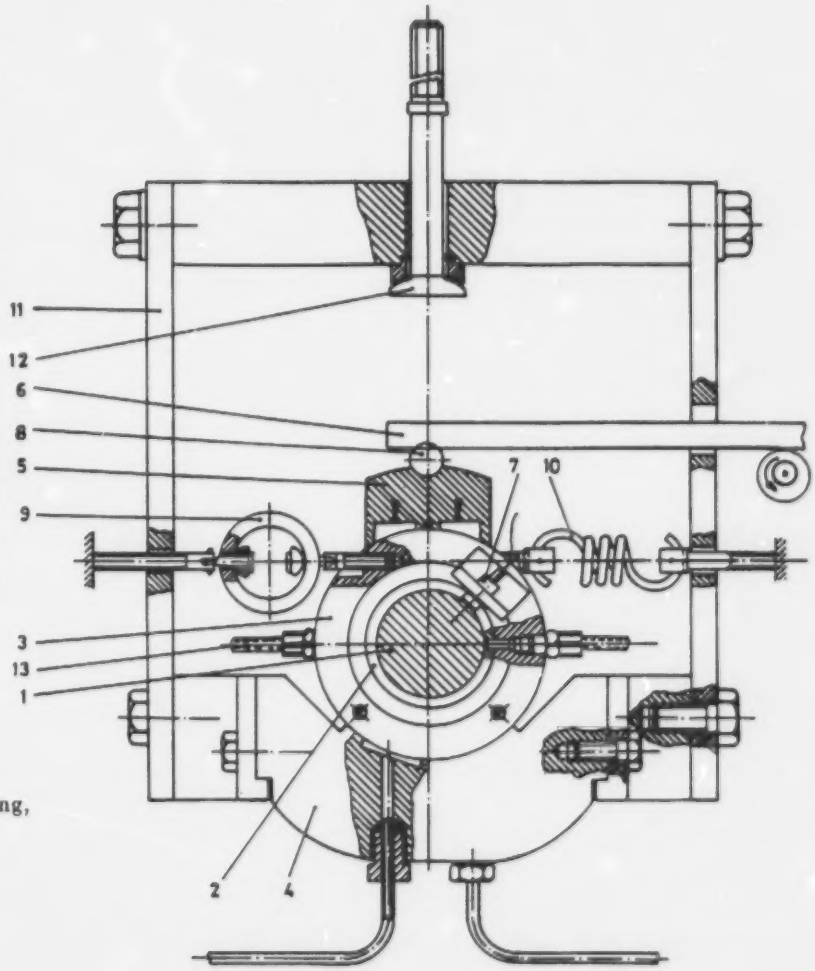

Fig. 2. The body of the bearing, measuring and loading system.

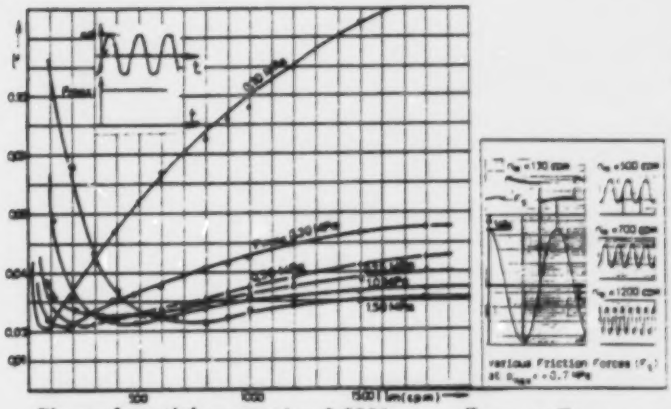

Circumferential groove, $\psi = 0.0021$, a. $F_{max} = F_{stationary}$;

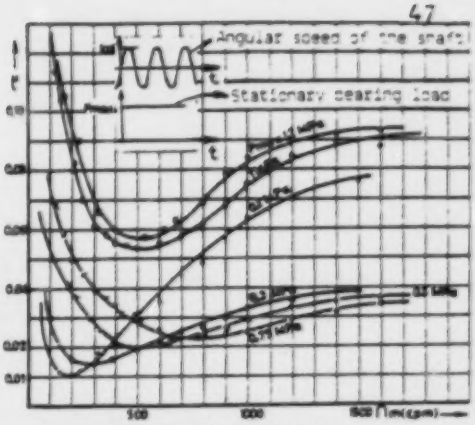

Axially grooves, $\psi = 0.0019$, d. $F_{max} = F_{stationary}$;

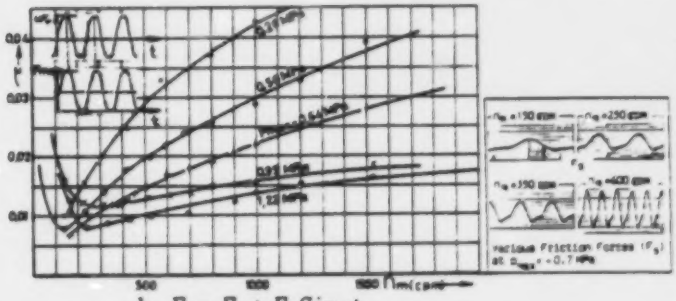

b. $F = F_0 + F_0 Sin\omega t$,

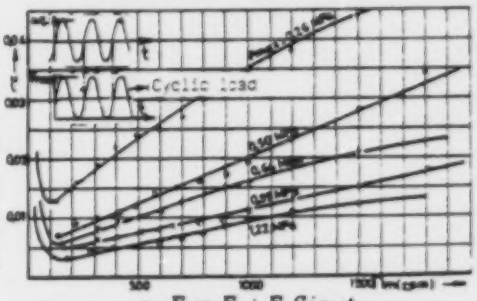

e. $F = F_0 + F_0 Sin\omega t$,

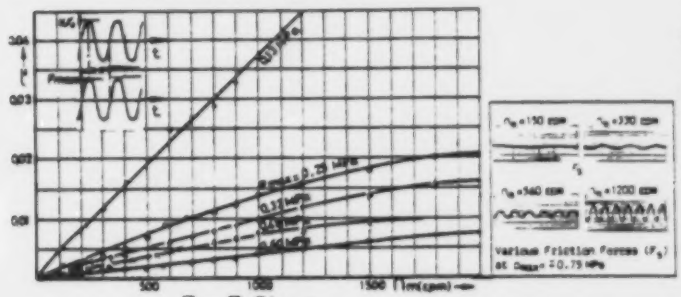

c. $F = F_0 Sin\omega t$

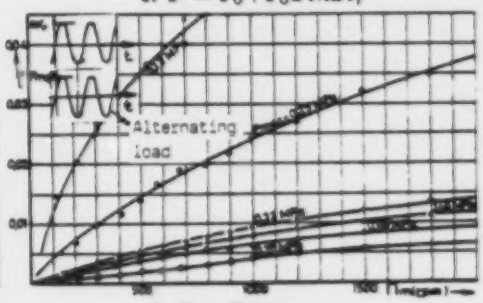

f. $F = F_0 Sin\omega t$

Fig. 3. The curves of the friction coefficient-shaft rotation frequency. $\frac{n_x}{n_m} = 1$, $b/d = 1$, $P_g = 0.5$ bar,

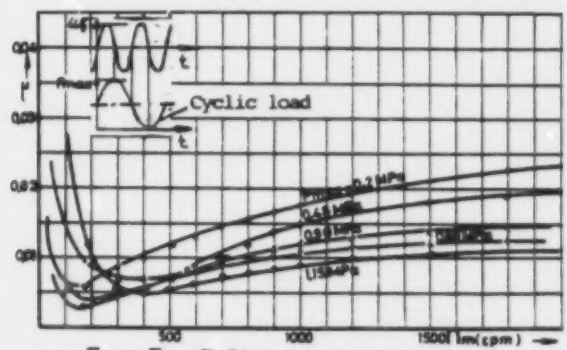

a. $F = F_0 + F_0 Sin\omega t$, $n_y/n_m = 1/2$,

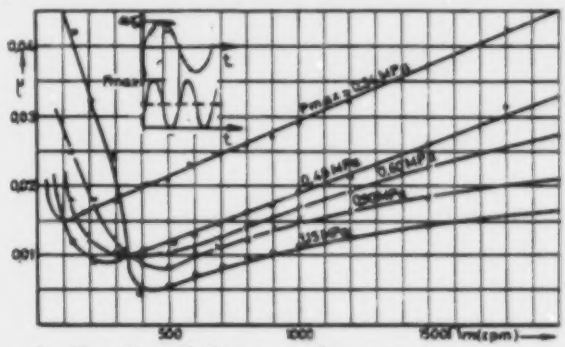

b. $F = F_0 + F_0 Sin\omega t$ $n_y/n_m = 2$,

Fig. 4. The curves of the friction coefficient-shaft rotation frequency. Axially grooves, $\psi = 0.0019$, $b/d = 1$, $P_g = 0.5$ bar,

a. n_m = 100 rpc, b. n_m = 750 rpc,

Fig. 5. The loci of the bearing center Axially grooves, ψ = 0.0

a. p_{max} = +0.25 MPa, b. p_{max} = +0.37 MPa

Fig. 6. The loci of the bearing center Axially grooves, ψ = 0.0

Fig. 7. The loci of the bearing center, Axially grooves, ψ = 0.0019, n_y/n_m = 1 , p_{max} = +0.96 MPa.,
a. n_m = 500 rpc, b. n_m = 1000 rpc

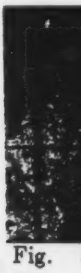

Fig.
Circum
a. n_m =

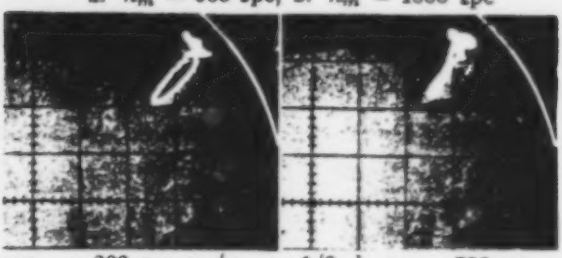

a. n_m = 200 rpc, n_y/n_m = 1/2, b. n_m = 700 rpc,

Fig. 9. The loci of the bearing center, Axially grooves, ψ = 0.0

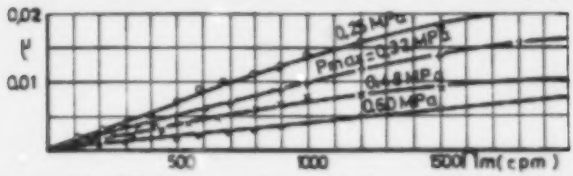

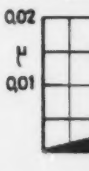

Fig. 10. The curves of the friction coefficient under alternatin

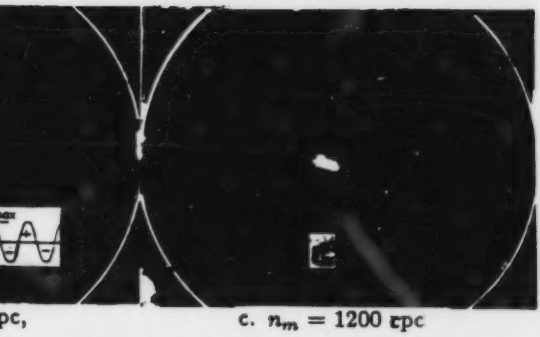

pc, c. $n_m = 1200$ rpc

$= 0.0019$, $n_y/n_m = 1$, $p_{max} = 0.25$ MPa.

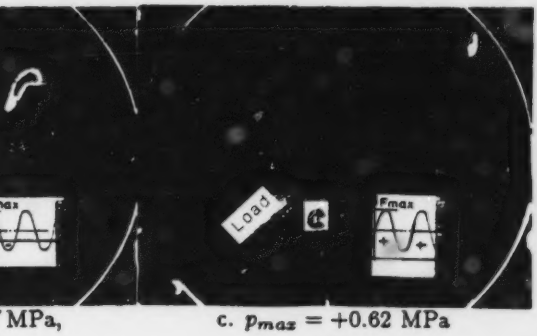

MPa, c. $p_{max} = +0.62$ MPa

$= 0.0019$, $n_y/n_m = 1$, $n_m = 750$ rpc .

ig. 8. The loci of the bearing center,
ircumferential groove; $= 0.0021$, $p_{max} = +1.50$ MPa,
$n_m = 300$ rpc, b. $n_m = 700$ rpc

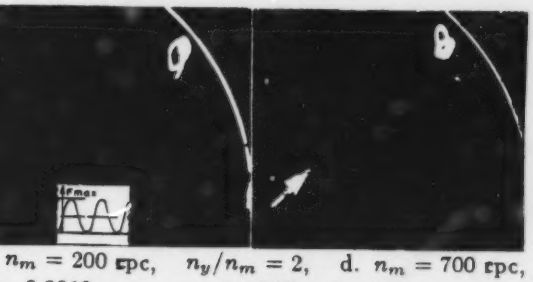

$n_m = 200$ rpc, $n_y/n_m = 2$, d. $n_m = 700$ rpc,
$= 0.0019$, $p_{max} = +0.6$ MPa., Cyclic load

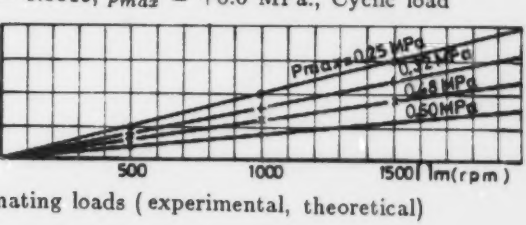

nating loads (experimental, theoretical)

LUBRICATION

DEVELOPMENT OF A METHOD FOR THE PREDICTION OF VISCOSITY OF LIQUID LUBRICANTS

Birbal Singh, V.R. Puttagunta

School of Engineering
Lakehead University

INTRODUCTION

Engineers and scientists involved in various aspects of the design, construction and operation of tribological elements in heavily loaded machine contacts often need to estimate the viscosity of lubricants at temperatures and pressures relevant to the specific situations. Research in the areas of lubricant film thickness and traction phenomenon in elastohydrodynamic (EHD) lubrication regimes has created a need for lubricant viscosity data at pressure above 50,000 psi and temperatures above 100 F (Brooks and Hopkins, 1975). Systematic viscosity measurements at such high pressures and temperatures are very time consuming and expensive. Thus it is common practice to rely upon empirical equations to represent the viscosity-pressure-temperature behaviour of different lubricants. However, most of the available equations have been developed either for specific lubricant samples and hence have limited applicability, or are based on some general theory resulting in poor predictability.

The purpose of this paper is to provide a brief review of the theoretical and empirical models for lubricant viscosity, and to present a new correlation to predict lubricant over a wide range of temperatures and pressures encountered in tribological problems. The most important advantage of the proposed method lies in the fact that to predict the viscosity of any lubricant, it requires only one viscosity measurement at a convenient temperature and atmospheric pressure, thus making it very useful and economical for numerical simulation of complex tribological problems.

THEORETICAL MODELS FOR LIQUID VISCOSITY

Although the dependence of the viscosity of liquids on temperature and pressure has been studied by many investigators, a complete theory to describe the liquid viscosity is still not fully developed. Theories based on statistical mechanics require solution of very complex equations and yet are only capable of predicting viscosity of simple and pure fluids like argon. Since lubricants are mixtures of high molecular weight polycyclic compounds, the models based on statistical mechanics are impractical to be used. Similarly, the corresponding states principle, when applied to the viscosity of liquids, yields equations that are

complicated and contain parameters dificult to evaluate accurately.

Eyring (1936) analyzed the motion of liquid molecules and developed an equation of viscosity based on activation energies of flow. Batschinski (1913) put forward a theory that the dependence of the viscosity of a liquid on temperature is due to a change in volume. Hildebrand (1971) proposed a modification of Batschinski's theory by relating liquid viscosity to ratio of intermolecular volume (or free volume). The theories based on activation energy, and free volume have been developed to a stage where the viscosities of pure liquids with simple molecules can be predicted with reasonable accuracy, but they are not suitable for predicting the viscosity of complex mixtures such as liquid lubricants.

EMPRICAL CORRELATIONS FOR LUBRICANT VISCOSITY

Over the years a large number of viscosity-temperature and viscosity-temperature-pressure correlations have been formulated by investigators for usage in tribological studies. Althogh, most of these correlations are based on data-fitting by regression techniques, and have little or no theoretical basis, they do provide important and useful tools to the practicing engineer. The most commonly used correlations are those developed by Andrade (1930), Walther (1933), Roelands et al (1963), Fresco et al (1969), So and Klaus (1980), Yasutomi et al (1984), and Wu et al (1989).

The common limitation of the above mentioned correlations is the requirement of determining two or more adjustable parameters. To determine the adjustable parameters, viscosity measurements are required at various temperatures and pressures, and such measurements are very time consuming and expensive, especially at higher temperatures and pressures.

DEVELOPMENT AND DISCUSSION OF A NEW CORRELATION

In view of the foregoing discussion, it was decided to develop a generalized empirical model for the correlation and prediction of the viscosity of liquid lubricants. In order to keep the correlation work simple and applicability of the model broad based, it was decided to isolate a viscosity characterization parameter first. Available viscosity data in the literature for liquid lubricants were collected and attempts were made to relate viscosity to molecular weight, density, and thermal properties, none of which proved successful. Finally, it was decided to use the oil viscosity at a suitable temperature and pressure to characterize the particular lubricant. It was found that the viscosity of any lubricant could be predicted with good accuracy by knowing the viscosity of the same lubricant at 100 F (37.78 C) and 1

atmospheric pressure, which can be readily measured by any commercial laboratory.

The following new empirical correlation has proved successful over a wide range of temperatures and pressures, for describing the viscosity of several liquid lubricants selected from the ASME Pressure-Viscosity Report (Bradbury et al, 1953):

$$\ln\mu = 2.30259 \left(\frac{b}{\left(1 + \frac{T - 37.78}{310.93}\right)^{s}} + C \right) + B_0 * P * \exp (d * T) \qquad (1)$$

where b is the characterization parameter determined by a single viscosity measurement at 100 F (37.78 C), and B_0, s, and d are parameters which depend on b and T. C is a constant, P is gauge pressue in psig, T is temperature in ^{0}C, and μ is the viscosity in Pa.s. In equation (1) there is only one independent parameter, all parameters can be determined by a single viscosity measurement.

The parameter b, may be conceived as indicative of the viscosity of the lubricant at 100 F (37.78 C). Among other parameters, s may be conceived as a measure of the variation of the viscosity with temperature, and B_0, and d as measure of the variation of viscosity with temperature and pressure. The constant C may analytically be put equal to the symbolic viscosity at infinite temperature. The constant 310.93 can be interpreted such that the viscosity of all lubricants becomes infinite at absolute zero temperature. Of course, even temperatures well above 0 K, the present correlation will neither be applicable nor be needed.

The correlation was applied to several lubricants selected from the ASME Pressure-Viscosity Report. With temperatures ranging from 32 F to 425 F (0 C to 218.3 C) and pressures ranging from 0 to 150,000 psig, the correlation predicted the viscosity with an average absolute deviation of 11% for eight lubricating oils with a total of 254 data points.

CONCLUSIONS

A generalized viscosity correlation capable of predicting viscosities of liquid lubricants over a wide range of temperatures and pressures has been developed. The correlation has a unique feature that to predict viscosity of any lubricant it only requires a single viscosity measurement at a convenient temperature and atmospheric pressure. A detailed report outlining the method and procedures to calculate various parameters (which can not be included here due to

space limitations) and results in tabular and plot form are available from the authors.

REFERENCES

Andrade, E.N. (1930) The Viscosity of Liquids. **Nature**, 125, 309-310.

Batschinski, A.J. (1913) Viscosity Law for Liquids. **Physik. Z.**, 84, 643.

Bradbury, D., Mark, M. and Kleinschmidt, R.V. (1953) Pressure-Viscosity Report. **ASME**, New York.

Brooks, F.C. and Hopkins, V. (1975) Viscosity and Density Characteristics of Five Lubricant Base Stocks at Elevated Pressures and Temperatures. **ASLE Transactions**, 20, 25-35.

Eyring, H. (1936) Viscosity, Plasticity and Diffusion. **J. Chem. Phys.**, 4, 283-291.

Fresco, G.P., Klaus, E.E. and Tewksbury, E.J. (1969) Measurement and Prediction of Viscosity-Pressure Characteristics of Liquids. **Journal of Lubrication Technology**, 91, 451-458.

Hildebrand, J.H. (1971) Motions of Molecules in Liquids: Viscosity and Diffusivity. **Science**, 174, 490-493.

Roelands, C.J.A., Vlugter, J.C. and Waterman, H.I. (1963) The Viscosity-Temperature-Pressure Relationship of Lubricating Oils and its Correlation with Chemical Constitution. **Journal of Basic Engineering**, 601-608.

So, B.Y.C. and Klaus, E.E. (1980) Viscosity-Pressure Correlation of Liquids. **ASLE Transactions**, 23, 409-421.

Walther, C. (1933) **Proc. World Pet. Congess**, 2, 419.

Wu, C.S., Klaus, E.E. and Duda, J.L. (1989) Development of a Method for the Prediction of Pressure-Viscosity Coefficients of Lubricating Oils Based on Free-Volume Theory. **Journal of Tribology**, 111, 121-128.

Yasutomi, S., Bair, S. and Winer, W.O. (1984) An Application of a Free-Volume Model to Lubricant Rheology I - Dependence of Viscosity on Temperature and Pressure. **Journal of Tribology**, 106, 291-303.

ACKNOWLEDGEMENTS

Financial support for this research was provided by NSERC.

EXPERIMENTAL DETERMINATION OF THE STEADY STATE AND DYNAMIC PERFORMANCE CHARACTERISTICS OF A JOURNAL BEARING

By

K. Brockwell[1], W. Dmochowski[2] and D. Kleinbub[1]

INTRODUCTION

In a hydrodynamic journal bearing, where the two surfaces are separated by a thin film of lubricant, relative motion generates sufficient pressure to transmit a force and prevent the surfaces coming into direct contact. This hydrodynamic pressure is generated mainly through viscous shear stresses. For these stresses to lead to a positive pressure in a steadily loaded bearing, a convergent wedge shaped film is necessary.

For a given operating condition, the bearing designer will try to achieve a film thickness which is sufficiently large to prevent contact between the stationary and moving elements of the bearing. The relationship between the film thickness and the applied load can be predicted from the basic equations of fluid mechanics, assuming that the film thickness is small in comparison with the shaft radius and that fluid inertia effects are negligible (1). Also of concern to the bearing designer will be bearing temperature. As a result of the shearing of the oil film, there will be an increase in bearing and shaft temperatures as well as an increase in lubricant temperature. The limiting acceptable bearing temperature depends upon the bearing lining material.

The journal bearing supporting a rotating shaft is also part of a complex dynamic system whose design is crucial in governing the dynamic behavior of the entire machine. Bearing damping controls the vibration amplitude as well as the machine sensitivity to unbalance, and is usually important if it is necessary to run the machine through the first shaft critical. A high bearing stiffness may be needed if it is found that the running speed is not far below the shaft critical. Destabilising effects such as cross coupling may also determine whether the rotor will be dynamically stable.

Recently, the use of smaller diameter shafts operating at higher rotational speeds has led to a large increase in the power to weight ratio of rotating machinery. The tilting pad journal bearing has been used to accommodate these more demanding duties, even though experimental data remains very scarce. In response to this growth in popularity, a recent study of the five shoe bearing has been undertaken. This paper presents results from a 76.2 mm diameter bearing with L/d ratio's of 0.46 and 0.75, and zero preload. The bearing was loaded "between pads".

EXPERIMENTAL APPARATUS

The test rig has been described elsewhere (2). Briefly, it comprises of a rotating shaft supported on angular contact ball bearings. The test bearing is mounted in a special housing which is located midway between the support bearings. Tensioned wires attached to the housing are used to apply steady state loads, and dynamic loads

are applied from two electromagnetic shakers (Figure 1). Eddy current probes are used to measure the displacement of the bearing with respect to the shaft, and accelerometers monitor bearing/housing acceleration. Bearing and oil temperatures, shaft speed and loads (steady and dynamic) are also measured. All data is collected by a high speed data acquisition system.

STEADY STATE PERFORMANCE

Designers analyzing the steady state performance of hydrodynamic journal bearings are mainly concerned about minimum oil film thickness and maximum bearing temperature. The limiting conditions of load and speed for a bearing of specific size, geometry and grade of lubricant can be represented by the operating envelope shown in Figure 2. This shows that load capacity is limited by an allowable oil film thickness, as well as by the bearing lining material (3). In the case of the tilting pad bearing, there may be a further limit imposed by pivot stress.

The minimum film thickness in a journal bearing is calculated from the following equation:

$$h_{min} = c(1-\varepsilon) \qquad (1)$$

where C is the radial clearance and ε is the shaft eccentricity ratio. When the shaft and bearing are concentic $\varepsilon = 0$, and when $\varepsilon = 1$ there is full contact between the two surfaces. In the tilting pad journal bearing, eccentricity ratio's greater than one are possible because loaded pads tilt to allow the shaft to move outside the clearance space. In this study, shaft eccentricity was measured by proximity probes which were located some distance from the test bearing. Therefore, it was important to take account of shaft deflection to obtain the true displacement of the bearing with respect to the shaft. This was done by applying a correction to the measured displacements. Figure 3 shows the true bearing displacements (as a function of) plotted against bearing load for 30 Hz (1800 rev/min) and 150 Hz (9000 rev/min) shaft speeds. Although not shown in this figure, it was found that the shaft loci were almost a straight line in the direction of the applied load. This indicated that the cross coupled dynamic coefficients were small in comparison with the direct coefficients. This was later confirmed by the dynamic study.

Figure 4 shows the variation of maximum bearing temperature with bearing load for a shaft speed of 150 Hz (9000 rev/min). It is of interest to note that the maximum temperature fell well short of the limiting acceptable temperature of 120°C for babbitt lined bearings.

DYNAMIC PERFORMANCE

In Figures (5) - (6), the direct stiffness and damping coefficients are shown plotted against bearing load, for a shaft speed of 30 Hz (1800 rev.min). These "bearing" coefficients, which characterize the flexibility and damping characteristics of the bearing oil film only, have been calculated from the measured coefficients. These measured coefficients were considered as equivalent coefficients since they include the effect of shaft flexibility. The influence of shaft

flexibility, and the equations used to calculate the pure "bearing" coefficients from the "equivalent" coefficients, is discussed elsewhere (4).

Dynamic testing of the bearing has confirmed that the cross coupled coefficients are negligible. For the bearing configuration and operating conditions pertaining to this study, it was found that only a single excitation force was needed to obtain a vertical straight line orbit, when the bearing was shaken in the "y" direction. A similar behavior was observed when the bearing was shaken in the "x" direction (90° to the load vector).

CONCLUSIONS

The dynamic and steady state operating characteristics of a five shoe, tilting pad journal bearing have been measured on a new experimental facility. In this paper, the dynamic coefficients, shaft eccentricity ratio and maximum bearing temperature of a 76.2 mm diameter bearing are presented for a range of loads and speeds.

Experimental results such as these may be used to verify computer models that calculate bearing performance. Rig testing also enables new bearing designs to be studied under realistic operating conditions.

REFERENCES

1. Reynolds, O., "On the theory of lubrication and its application to Mr. Beauchamp Tower's experiments", Phil. Trans. Roy. Soc., Series A, 177, 1886, p. 157-234.

2. Brockwell, K. and Dmochowski, W., "Experimental determination of the journal bearing oil film coefficients by the method of selective vibration orbits", Proceedings of the 12th Biennial ASME Conf. on Mechanical Vibration and Noise, Montreal, Sept. 1989.

3. Martin, F., "Minimum allowable oil film thickness in steadily loaded journal bearings", Proc. Instn. Mech. Engrs., Vol. 178, Pt 3N, 1963-64, p. 161-167.

4. Brockwell, K., Dmochowski, W. and Kleinbub, D., "Measurement and calculation of the dynamic operating characteristics of the five shoe, tilting pad journal bearing.," Presented at the STLE/ASME Tribology Conference, Fort Lauderdale, Oct. 1989.

[1]Tribology and Mechanics Laboratory
National Research Council
3650 Wesbrook Mall
Vancouver, B.C.
V6S 2L2 (604) 666-6189

[2]Institute of Fluid Flow Machinery
Polish Academy of Sciences
ul. Gen. Fiszera 14
80-952 Gdansk
Poland 41-12-71

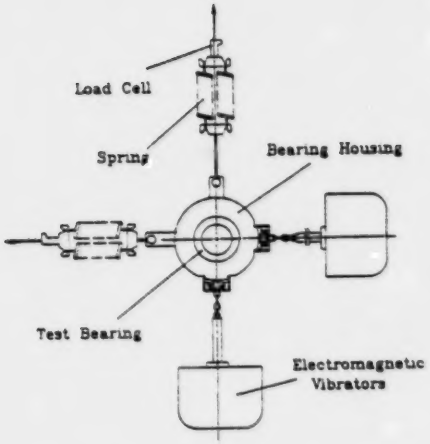

Fig. 1 Schematic of, the bearing loading system.

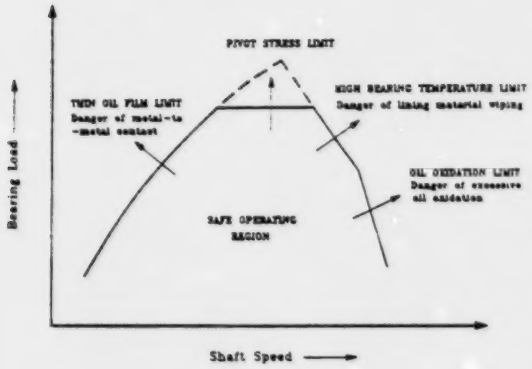

Fig. 2 Region of safe operation for tilting pad journal bearings.

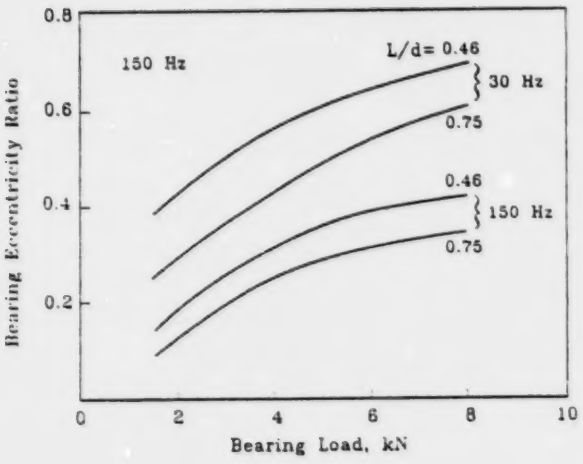

Fig. 3 Bearing eccentricity vs. load.

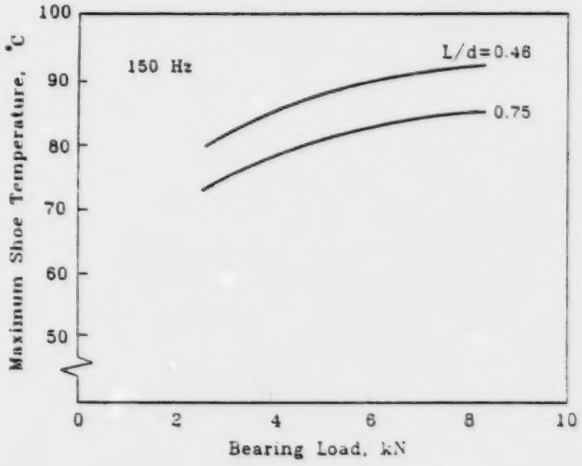

Fig. 4 Maximum pad temperature vs. load.

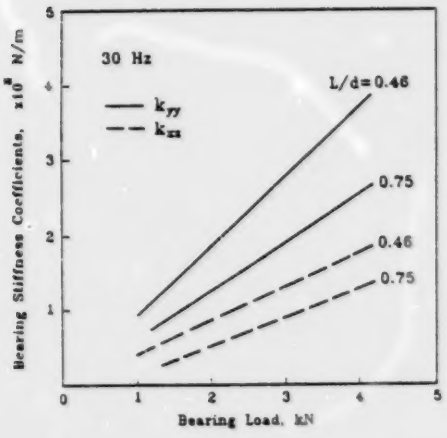

Fig. 5 Stiffness coefficients vs. load (K_{yy} stiffness in the direction of load; K_{xx} stiffness perpendicular to the load).

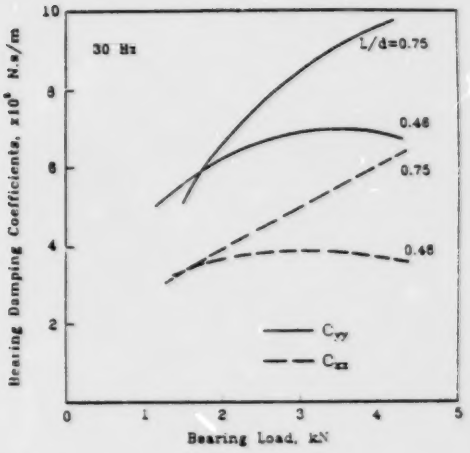

Fig. 6 Damping coefficients vs. load (C_{yy} damping in the direction of load; C_{xx} damping perpendicular to the load).

ELASTOHYDRODYNAMIC LUBRICATION AND MONITORING

by
Albert Koehler, Ph.D, TRIBOTEC INT. LTD.
Coquitlam, B.C. V3C 3T6

INTRODUCTION

The elastohydrodynamic lubrication is a special form of lubrication with very thin oil films and high loads. In the following it is not intended to analyze the many theoretical and experimental investigations that have been carried out in the past, but to highlight some important aspects of EHL-contacts and methods. The prefix "elasto" has been added to the commonly known hydrodynamic lubrication, because the elastic deformation of the surfaces in contact can be considerable and has to be considered in all calculations and experiments when applying transducers. Contact pressures can rise to 2.6 GPa (300.000 psi) while lubricant film thicknesses are in the range of 0.2 to 5 micrometers.

LUBRICANT SELECTION

To maintain a proper lubrication condition, the selection of the right lubricant, respectively viscosity of the lubricant is most important. As a help there are today some good calculation methods and diagrams available to determine the appropriate viscosity for known load-speed conditions, which mainly is of interest for gears and rolling element bearings. It is almost essential to have an EP-additive (extreme pressure) in the lubricant. Material welding and surface seizure can be avoided when in a case of metal to metal contact the EP additives react with the metal surface and form a smooth active layer. Large scale surface damage can be prevented and wear reduced.

As EP additives are active chemicals the compatibility with all involved materials has to be checked. The common EP-additives, like sulfur and chlorine are only effective when the temperature rises due to increased friction. Like other additives, they can be "used up", which means the special EHL protection is not provided any more. Regular oil checks including an additive analysis are a method to control the lubricant condition.

LATEST EXPERIMENTS

While it was always a problem to measure the pressure and temperature distribution in EHL contacts, a new transducer application technique enables a realistic data acquisition. The main problem was the size of available transducers and the application without influencing the contact geometry and/or the elasticity, which in return would effect the accuracy of the measurements and lead to unrealistic data. The measurements within vaporizing plants developed mini transducers

confirmed formerly calculated pressure distributions in Hertzian and EHL contacts. The further application of these transducers in different bearing types and tribo contacts was a tremendous help for the design of new bearings. The slides shown in the presentation demonstrate the process.

FAILURE OF EHL CONTACTS

The normal failure is a material fatigue failure but most of the failures in the field are due to overload, vibration and/or wrong lubricant, as well as contaminated lubricant. Very often costly down time is related to such a failure, which in many instances can be predicted by using special techniques to monitor the health condition of the tribo contact.

MONITORING EHL IN MACHINERY

Today's monitoring techniques allow a complete health condition monitoring of EHL contacts. The monitoring can be performed by several "tools", such as temperature, oil analysis, and vibration. A special vibration analysis technique enables the detection of developing cracks or pittings on any of the bearing elements or on gear teeth at a very early stage. Depending on the first changes in a vibration spectrum it, for instance, is possible to determine whether or not enough lubricant is in the contact and how long it takes the bearing to fail, or at what part of a bearing the damage develops. Although certain calculations methods exist to predict the lubrication condition and life time of bearing and gears, the field conditions often cannot exactly enough specified to satisfy the needs in industry. Thus the sophisticated predictive maintenance programs on the market today are a tremendous help in production and maintenance. It is the only efficient technique to evaluate and predict the health condition of equipment and save operating costs. The final and most beneficial approach is the EHL-predictive maintenance-failure analysis approach, also known as "root" maintenance, where any failure and damage is to be analyzed and its cause investigated to avoid recurrence. The presentations slides demonstrate the basics of the EHL-contact and the measurement techniques, as well as the predictive maintenance approach.

TRIBOLOGY OF LARGE SPHERICAL ROLLER BEARINGS USED IN PAPER MACHINES

Stephen D. Fysh, Edward M. Oravec[1] and John B. Medley

Dept. of Mechanical Engineering
University of Waterloo

[1]Oakville Research Centre
Shell Canada Ltd.

Introduction

A paper machine is an integrated manufacturing facility that processes wood pulp into paper. The dryer roll in a paper paper machine has super-heated steam pumped through the centre of the support shafts and into the core of the roll in order to evapourate the residual water in the paper. The influences of the heat and water reduce the life of the supporting spherical roller bearings (Sullivan and Lyman, 1960). It is likely that the heat transfer from the central region of the support shafts causes a reduction in the lubricant viscosity. The lower viscosity results in the absence of an elastohydrodynamic film which is required to protect the bearing surfaces from damage.

The long term objectives of the present study were to investigate the role of heat transfer and water contamination on the performance of the spherical roller bearings. The conditions found in the field were simulated by a laboratory apparatus. An exact simulation, however, was not desirable because even the reduced lifetime of dryer roller bearings was often in excess of 5 years. Thus, to achieve results in a reasonable time period, the capability to accelerate the influence of both heat transfer and water contamination was part of the design criterion.

The short term objectives of the present study were to complete the design and fabrication of the apparatus and to initiate the commissioning procedure. The first step in the commissioning procedure involved a demonstration that excessive heat transfer could produce surface damage by reducing the protection provided by elastohydrodynamic lubrication.

Apparatus

The apparatus (Fig. 1) was designed and built over a period of about two years (Fysh, 1989).[1] The tests were performed on 230 type spherical roller bearings (23024 ASK MB-C3) which were supplied by FAG Bearings Ltd. and had nominal inner diameters of 0.11 m. These bearings were smaller than the 230 type bearings used in paper machines which had nominal inner diameters of about 0.25 m. The rated loads and speeds of the test bearings were established by consulting the manufacturer's design manual. However, the apparatus was designed to apply a loads of about 7% of the rated loads. These load levels corresponded to the same proportions of rated loads which existed in the paper machine bearings. The speeds of the test bearings were also well below their rated speeds. They were set so that the shaft surface speeds of apparatus and paper machine were about the same. The apparatus could test either two or four bearings simultaneously.

The heat transfer from the central region of the shaft to the bearings was simulated by placing 500 W heating cartridges in the hollow ends of the shafts of the apparatus. A temperature probe was placed in each bearing casing to provide feedback for control of the bearing operating temperature. Further

[1]The authors would like to acknowledge the assistance of Oakville Research Centre during the design and construction period

temperature probes were placed in the inlet and outlet lines of the lubricant supply system for each bearing.

The lubricant supply system consisted of a 90 l sump, a pump, a heater and a cooler. The system supplied all of the test bearings and could accomodate oil-water emulsions.

The apparatus was designed to run 24 hours a day. To avoid damage to the apparatus in the event of a catastrophic bearing failure, shock pulse monitors made by SPM Industries were placed on each bearing and were set to stop the drive motor if a sufficiently high shock load occurred at a frequency of 32 kHz.

Analysis of the Test Bearings

The apparatus was run continuously over much of a 6 month period. A total of 10 bearings were tested for 18 days and 4 of these 10 bearings were tested for a further 18 days. Various combinations of lubricants and lubricant temperatures gave low, medium or high viscosity (Table 1). Loads and speeds remained essentially constant for all of the tests.

The analysis consisted of determining the contact conditions such as entrainment velocity, load, geometry, surface roughness, lubricant properties and the material properties of the surfaces. Detailed explanations of the required calculations and measurements were provided by Fysh(1989).

The geometrical representation of a nominal line contact was adopted and the theoretical formaula developed by Ping Pan and Hamrock(1989) was applied to calculate the central film thickness. Other theoretical formulae were found in the literature but Fysh(1989) argued that the chosen formula maintained the best and most consistent agreement with the data in the literature. Also, Fysh found that temperature rises caused by the shearing of the lubricant in the contact had a neglibible effect on the film thickness.

Following Johnson et al(1972), the lambda ratio was used to characterize the extent of film protection for the surfaces as follows:

$$\lambda = \frac{h_c}{\sqrt{\sigma_1^2 + \sigma_2^2}}$$

where h_c = central film thickness and σ_1, σ_2 = RMS (root mean square) surface roughness. For each of the 10 bearings tested, a low, medium or high lambda ratio was calculated (Table 2).

Results and Discussion

The surface roughness of the rollers and the races were measured before testing to establish the initial lambda ratio. The surface traces featured some very deep valleys and a few high peaks (Fig. 2). Further surface roughness measurements were taken after 18 days and for some bearings after 36 days of testing. For all the bearings, the RMS roughness decreased with time and a running-in process was assumed to have occurred. However, the traces of the bearings with low lambda ratios did not show the deep valleys (Fig. 3) while those with the high lambda ratios retained the deep valleys. These findings suggested that progressive wear occurred in the bearings subjected to low lambda ratios.

Conclusions

The short term objectives of the present study were achieved in that the apparatus was designed and fabricated. Furthermore, the first step in the commissioning procedure had demonstrated that indeed excessive heat transfer could promote wear of the surfaces by reducing the lambda ratio.

References

Fysh, S.D. (1989) An experimental study of the tribology of large spherical roller bearings used in paper machines. *MASc Thesis*, Dept. of Mechanical Engineering, University of Waterloo.

Johnson, K.L., Greenwood, J.A. and Poon, S.Y. (1972) A simple theory of asperity contact in elastohydrodynamic lubrication. *Wear, 19*, 91-108.

Ping Pan and Hamrock, B.J. (1989) Simple formulas for performance parameters used in elastohydrodynamically lubricated line contacts. *J. of Tribology, 111*, 246-251.

Sullivan, F.J. and Lyman, J.R. (1960) Drier roller bearing lubrication. *Tappi, 43*, 6, 513-518.

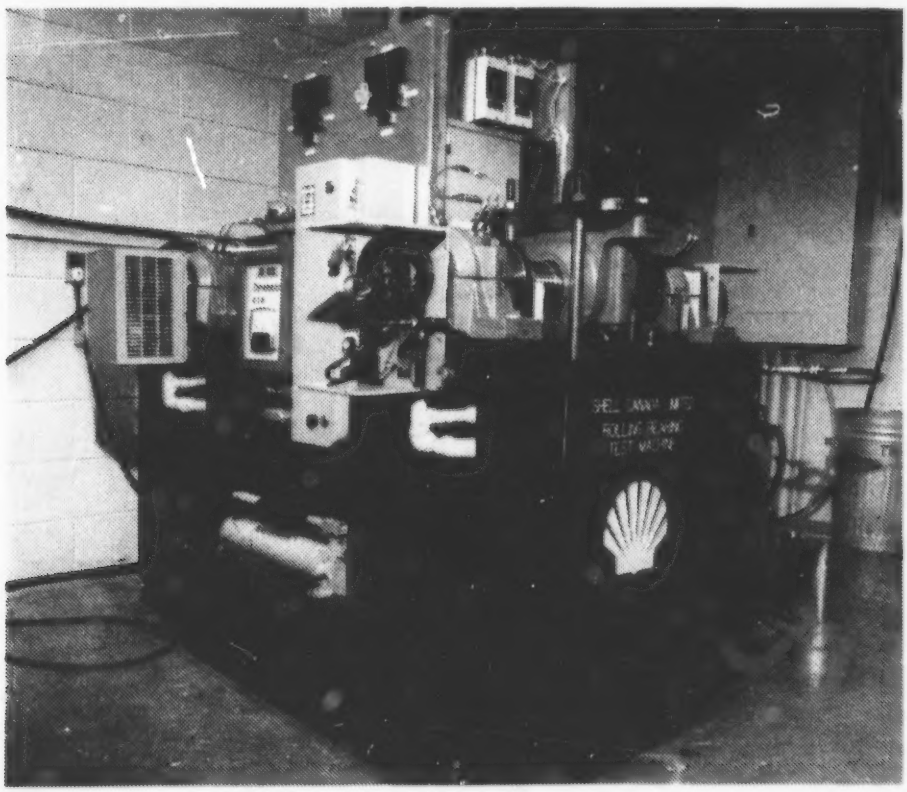

Fig. 1: The experimental apparatus.

Table 1: Some of the test conditions.

Brg No.	Test Time (Days)	Load (kN)	Speed (RPM)	Oil Type	Inlet Viscosity (mPa.s)
1	18	27.0	409	MVI65	3.62
1	18	27.2	407	MVI65	3.11
2	18	27.0	409	MVI65	3.27
2	18	27.2	407	MVI65	2.95
3	18	27.2	413	MVI65	3.27
4	18	27.2	413	MVI65	2.95
5	18	26.4	407	MVI65	11.1
6	18	26.4	407	MVI65	10.8
7	18	26.5	390	HVI250	41.0
7	18*	26.0	400	HVI250	35.9
8	18	26.5	390	HVI250	35.9
8	18*	26.0	400	HVI250	35.9
9	18*	26.0	406	HVI250	41.0
10	18*	26.0	406	HVI250	35.9

* In progress - estimated test conditions shown.

Table 2: The imposed lambda ratios.

Brg	λ
1	0.26
1	0.23
2	0.24
2	0.22
3	0.24
4	0.22
5	0.63
6	0.62
7	1.4
7	1.3
8	1.3
8	1.3
9	1.5
10	1.3

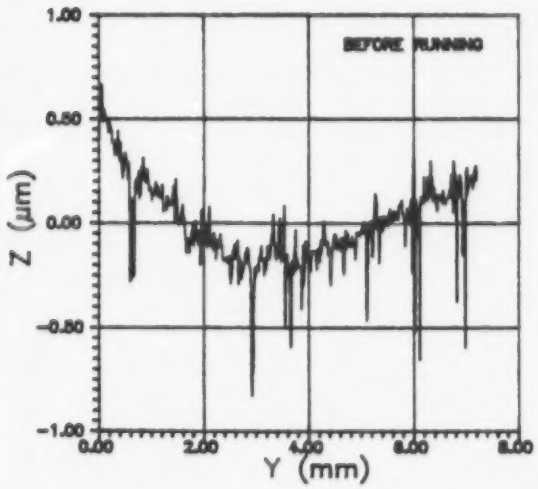

Fig. 2: A surface roughness trace of an outer race before testing.

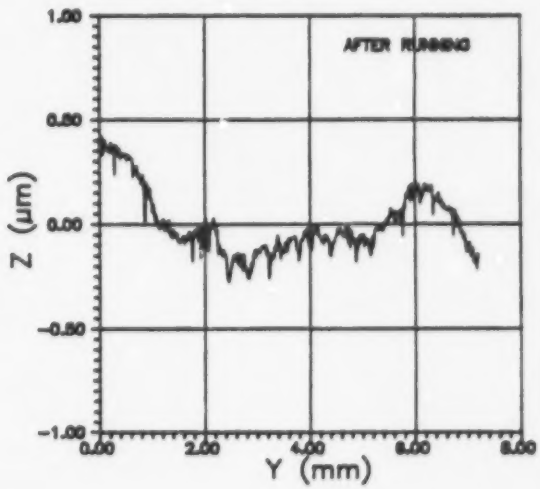

Fig. 3: The surface roughness trace of the outer race of bearing number 2 after 36 days of testing.

METALLOGRAPHIC EXAMINATION OF FAILED JET ENGINE COMPRESSOR BLADES

Pak L. Ko, J. Kalousek and M. Robertson

National Research Council of Canada

1.0 INTRODUCTION

Compressor blade failures in jet engines could lead to engine fires with severe consequence.

This paper presents the results of metallographic examination of a number of service exposed blades provided by the research group in Orenda Division of Hawker Siddeley Canada Inc, and discusses a number of the probable failure mechanisms.

2.0 RESULTS OF METALLOGRAPHIC EXAMINATIONS

The compressor blades are forged from Ti-6Al-4V alloy and their pressure faces on the blade roots are plasma sprayed with an anti-fretting Cu-Ni-In coating about 0.1 mm thick.

The examination revealed both mild and severe wear damage on the coating. The mild wear scars (Figure 1) are possibly formed during installation, handling and/or start-up which result in sliding wear with evidence of material transfer. Under high load and vibratory (fretting wear and fretting fatigue) conditions, plastic flow occurs on the coating surface resulting in rippled surfaces with crack formation, and eventually delamination and flaking, Figure 2.

In areas where severe loading conditions exist, relative movement between the blade root and the disc would be severely restricted and stress concentration factors would be very high. In these areas, such as that along the ridges, cracks which may have been the result of fretting fatigue, propagate and penetrate the whole depth of the coating, Figure 3. However, based on the sectioned micrographs these cracks do not extend to the titanium base material, nor is there evidence of severe wear depth on the coating surface where the crack opened.

Under certain engine operating conditions combined with the deteriorated condition of the coating, very severe and localized loading due to centrifugal force (normal) and the blade force (tangential) on the pressure surface could occur which would lead to crack formation on the base material.

Figure 4 shows an overall view of the dovetail pressure surfaces of a blade. The concave side of the pressure face appears to be very smooth. It has all the failure modes shown in other blade specimens examined, e.g., plastic flow, surface cracks, delamination and flaking. These are evidences that the surface has been subjected to heavy loading in both normal and tangential directions. Contrary to this, the convex side of the pressure face is quite rough and has the same appearance as that of the unworn coating. The crack which appears to have originated from the severely delaminated area on the upper right hand corner has extended to the end face of the blade root. The cross-section along this severely damaged area reveals several cracks on the titanium base material. Figure 5 also shows that the coating on the concave

side has been worn and deformed to a thickness of less than one half of the original thickness.

The cracks were found in an area where the coating was broken and partially detached from the titanium base. Similar coating damage with cracks visible on the end face were also found in two other service exposed blades. Figure 6 shows one of these cracked blades. These cracks also appear to have initiated from an area near the upper right hand corner on the concave pressure face. Also common to the three damaged blades is the appearance of severe plastic flow on the right hand side edge of the pressure face and a second wear mark, albeit less visible, on the left hand side of the concave pressure face.

3.0 PROBABLE FAILURE MECHANISMS

3.1 Fretting Fatigue on the coating

Fretting fatigue can occur when contacting components are subjected to cyclic stress conditions and the associated cyclic strains result in relative movement at the interfaces. Metal coating is one of several surface modification techniques that could be employed as palliatives in fretting fatigue and fretting wear situations. Waterhouse et al. (1962) found that in general coating effectiveness increased with coating thickness (from 19 μm to 125 μm). They also found that the softer coatings were extruded easily from the interface.

3.2 Crack Initiation

The initiation of fatigue cracks under fretting condition depends on the stress state in the surface layer. The induced stress is restricted to a very thin surface layer; the high reversed stress decreases rapidly with the increase of depth from the surface (Nishioka & Hirakawa, 1969). Thus shallow fatigue cracks originate at the contact surface due to this high reversed stress and develop into the specimen. However, they soon come into the region of lower stress and crack growth will be retarded if fretting fatigue is the only mechanism present. In the presence of other contact stresses, such as stresses due to uneven loading or bending, surface cracks caused by fretting fatigue will propagate with ordinary fatigue as the dominating mechanism.

3.3 Delamination

Under the conditions of severe plastic flow, unidirectional shearing of the metal surface nucleates subsurface voids giving rise to a crack just below the surface. It propagates, at first parallel to the surface, and, when it is large enough, breaks out to give a flake-like wear particle.

3.4 Asymmetrical Loading Hypothesis

The loading vector on the blade root may be resolved into normal and tangential components (Figure 7a). The loading at the blade root corner can be modelled either as a quarter-space supporting a non-Hertzian contact load or as a cantilever with a point load. A two-dimensional model of a stress field at the quarter-space was studied by Bower, Johnson and Kalousek (1986). Non-Hertzian contact loading would initiate the crack at any imperfection within the titanium located along the arc of collapse shown in Figure 7b. At this arc the sum of the shear stresses [$\tau_{max} = (\sigma_1-\sigma_3)/2$] at all points reaches a

maximum and the crack growth in this model is by Mode II (shear); whereas in the simple cantilever model both crack initiation and propagation are by Mode I (tensile). It is very likely that a mixed mode of initiation, asisted by the imperfections at the titatium Cu-Ni-In coating interface, and a mixed mode of crack growth are involved in the present case.

4.0 DISCUSSION

The appearance of the coating on the cracked blades and the location of the cracks all point to the probable cause being uneven loading causing extremely high stress concentration factor. There is a remarkable similarity between the shape of crack at the root of the blade and the shape of the arc of collapse due to normal loading of a quarterspace (with or without friction) discussed earlier. Since the faces of the blade root are loaded by normal and tangential forces, there is also an arc along which the sum of shear stresses reaches a maximum. It is reasonable to assume that the crack will also develop along this arc.

The uneven loading problem may be compounded by the non-conformity of the blade pressure surfaces (a rectilinear plane) to the slotted area of the third stage disc (a curved plane), and the reduced coating thickness on the concave side of the cracked blades.

5.0 CONCLUSIONS

1. The primary mechanism is uneven loading causing exceedingly high stress on one corner of the blade. This combined with a cyclic tangential stress results in crack initiation and rapid propagation on the titanium metal part.

2. A secondary mechanism is cyclic stress due to fretting fatigue on the coating which together with fretting wear causes delamination and flaking of the coating.

3. The depletion of this coating hinders its effectiveness and further enhance the primary mechanism of crack propagation.

ACKNOWLEDGMENT

The authors would like to thank Orenda Division of Hawker Siddeley Canada Inc for permitting the information in this paper to be presented.

REFERENCES

BOWER, A.F., K.L. JOHNSON, and J. KALOUSEK. 1986 ; "A Ratchetting Limit for Plastic Deformation of a Quarter-space under Rolling Contact Loads," Contact Mechanics and Wear of Rail/Wheel Systems II, University of Waterloo Press, 117-131.

NISHIOKA, Kunio and Kenji HIRAKAWA. 1969 ; "Fundamental Investigations of Fretting Fatigue : Part 3, Some Phenomena and Mechanisms of Surface Cracks," Bulletin of JSME, 12(51); 397-407.

WATERHOUSE, R.B., P.A. BROOK and M.C. LEE. 1962 ; "The Effect of Electrodeposited Metals on the Fatigue Behaviour of Mild Steel Under Conditions of Fretting Corrosion" Wear, 5(3); 235-244.

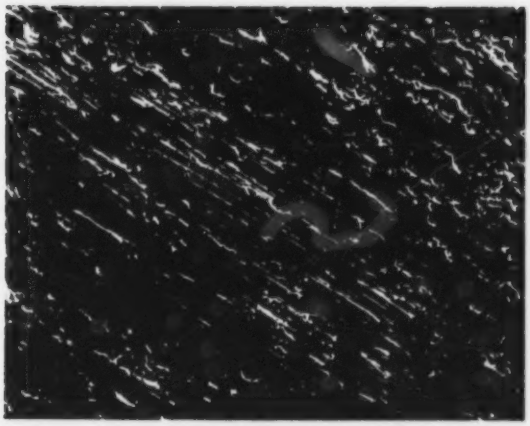

Fig. 1. Mild sliding wear mark.

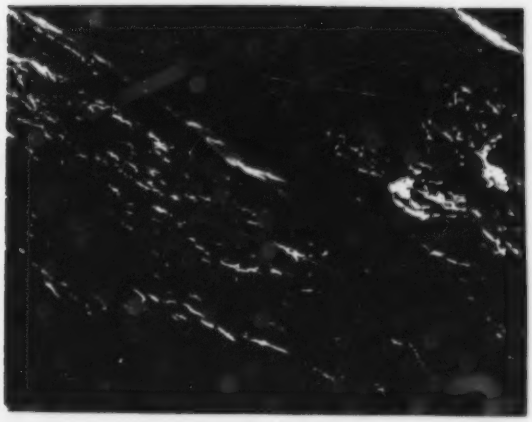

Fig. 2. Surface and subsurface cracks leading to delamination and flaking.

Fig. 3. Sectioned view of a crack on the coating.

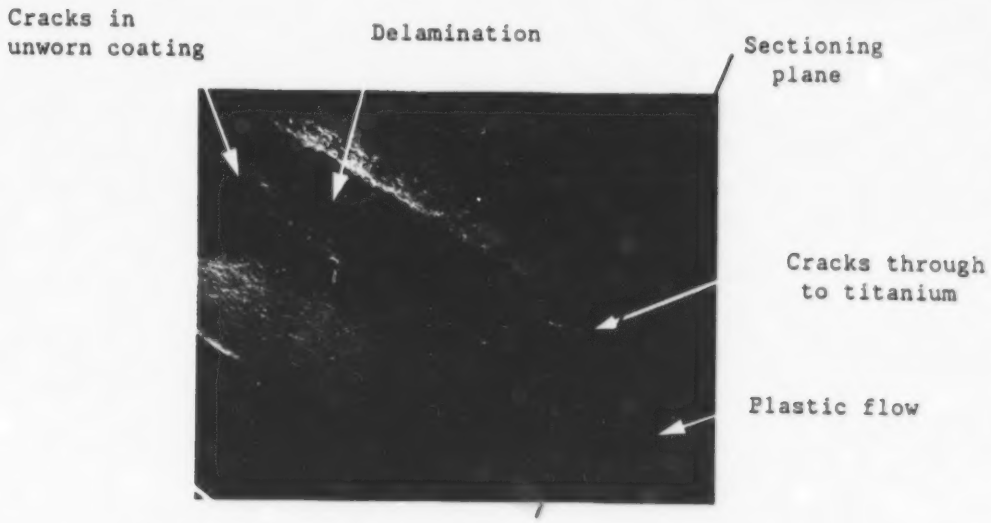

Fig. 4. Overall view of the dovetail pressure surfaces of a damaged blade showing one side is severely deformed while the other side appears to be intact.

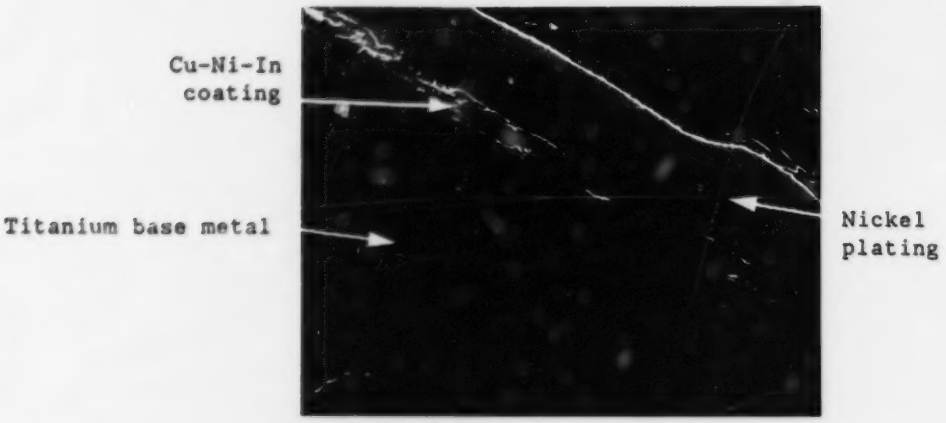

Fig. 5. Sectioned view of the damaged blade showing cracks on the titanium metal and the thickness of the coating has been worn or extruded to about half of its original thickness.

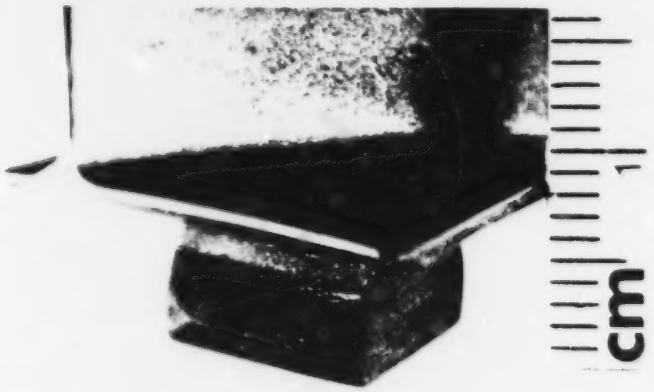

Fig. 6. Front view of a blade root showing an extensive crack and other worn areas.

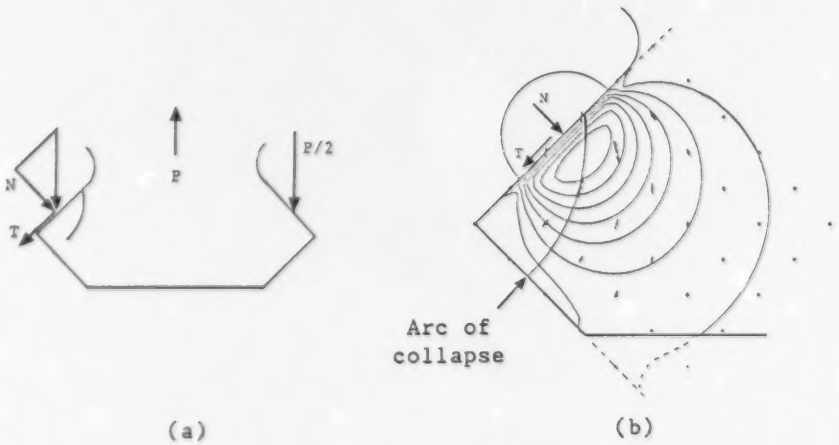

Fig. 7. Similarity between (a) crack in the root of the blade and (b) arc of collapse in a quarter-space under Hertzian load.

WEAR I

Wear Studies Using Acoustic Emission Techniques

by R.J. Boness, S.L. McBride and M. Sobczyk
Royal Military College of Canada, Kingston, Ontario

Introduction

In spite of the considerable effort made over many years, a complete understanding of the wear mechanisms occurring between dry and lubricated contacts in relative motion still eludes us.

More than thirty years ago, following the classic work of Bowden and Tabor[1], Archard[2] derived an important wear model for unlubricated surfaces in the simplified form of:

$$\text{Wear rate } V/L = K.W/H$$

Expressed in this way wear rate, defined as volume of material removed (**V**) per unit sliding distance (**L**), is proportional to the normal load (**W**) and inversely proportional to the hardness of the softer material (**H**). The dimensionless parameter **K** of this equation is called the wear coefficient.

Although many observations do not follow the behaviour predicted by this model, it is now generally accepted as a suitable framework within which the quantitative aspects of this tribological subject can be discussed. The problem lies in the specific interpretation of **K**.

Experimental measurements of unlubricated wear (see Archard[3]) show that wear rates, and consequently the wear coefficient **K**, vary over a considerable range: almost 10^5. This range is increased even further when lubrication and other wear reduction techniques are present.

It is known that **K** depends on the nature of the materials used, on the geometry and topography of the contacting surfaces, and on interfacial friction. The problem is further complicated by the presence of a lubricant film between the surfaces, whether it be a thick hydrodynamic film keeping the surfaces completely apart, an elastohydrodynamic film (1 μm thick), or even boundary lubricant effects which provide protective films by chemically reacting with the surfaces in contact.

At this stage is important to realise that two engineering surfaces which are loaded together touch only over a very small part of their apparent area of contact. That is, the load is supported by a limited number of asperities on opposing surfaces, contacting each other.

The most common interpretation of the meaning of the wear coefficient **K** is that it represents the proportion of all asperity contacts which result in the production of a wear particle. The problem is to be able to relate the wear coefficient **K** to specified operating conditions.

This paper shows that asperity contact can be detected by acoustic emission measurements, and that such measurements can provide a vital understanding of the complex wear processes in both dry and lubricated situations.

Experimental Apparatus and Procedure

Historically, wear measurements have been conducted on specialized test rigs which enable simple test pieces to be loaded and rubbed against each other, either dry or lubricated, and with a combination of rolling and sliding motions.

These particular tests were carried out on a ball and cylinder test rig[4] under conditions of pure sliding: a stationary ball being loaded against a rotating cyllinder. Details of the test matrials are given in Table 1.

	Diameter mm	Material	Hardness Rc	Surface Roughness μm Ra
Ball	12.7	52100 steel	64	0.2
Cylinder	49.0	8720 steel	61	0.56
Lubricant:	SAE30 oil, dynamic viscosity 0.44 Pas @ 20°C.			

Table 1. Test Materials and Conditions

In many situations, standardized test procedures require the measurement of a wear scar in order to calculate the amount of material removed during a pre-set test time[5]. As discussed earlier, such tests do not distinguish between different types of wear processes.

In this work, acoustic emission events were detected by a transducer mounted directly on the ball housing. The resulting voltage signal from the transducer was amplified, envelope followed and digitized[6]. Peak amplitudes, rise rates, decay rates and pulse lengths as a function of time were recorded in a microprocessor and subsequently stored on floppy disk.

Test Results and Discussion

Acoustic emission measurements were obtained for a cylinder speed of 225 rev/min and an applied load of 10 N, for both lubricated and unlubricated cases. A direct relationship between the RMS acoustic emission signal and the volume of material removed from the ball has been obtained. Also, of particular significance are the differences between the amplitudes (Figure 1) and rise rates (Figure 2) of the acoustic emission events for the lubricated and dry tests. During the lubricated contact, peak amplitudes are seen to be in a band substantially lower and narrower than the amplitudes during the dry contact (Figures 1).

The rise rates are also very different. For the lubricated contact, over 14000 events had rise rates greater than 250 μsec/6dB (Figure 2a), compared to the short 5-10 μsec/6dB rise rates for the dry contact events (Figure 2b). These numbers suggest a mechanism of plastic deformation for lubricated contact, and micro-fracture for dry contact.

Scanning electron microscope (SEM) photomicrographs of the ball surface when lubricated show a polished scar with little wear. A similar examination of the cylinder shows that significant plastic flow of the original surface irregularities (Figure 3a) has occurred, and the final wear track (Figure 3b) is relatively smooth. For the dry contact SEM micrographs showed a distinct wear scar. The cylinder (Figure 3c) shows a wear track with evidence of material transference and wear debris.

Based on elastohydrodynamic theory[7], the film thickness between the ball and the cylinder for the lubricated case was estimated to be 0.25 μm. With an original combination surface roughness of 0.76 μm Ra, substantial asperity contact was expected to occur. We therefore conclude from this work that actual removal of material is characterized by high amplitude, short rise rate acoustic emission signals, and that running-in wear and plastic flow results in lower amplitude signals with much longer rise rates.

Conclusions

It has been demonstrated that measurements of acoustic emission events can be a valuable tool in the study of wear mechanisms of dry and lubricated loaded surfaces in relative motion. The direct relationship between the RMS acoustic emission signal and the volume of material removed from the ball enables the wear coefficient **K** to be continuously estimated during the test, without stopping the rig in order to make wear measurements.

Acknowledgements

The authors wish to express their appreciation to M.D. Pollard and M.R. Viner for developing the software used in the analysis.

References

1. Bowden, F.P. and Tabor, D. "The Friction and Lubrication"; Clarendon Press, Oxford, 1954.
2. Archard, J.F., "Contact and Rubbing of Flat Surfaces"; J. App. Phys. 24, pp. 981-988, 1953.
3. Archard, J.F., "Wear Theory and Mechanisms"; Wear Control Handbook ASME, pp. 35-80, 1980.
4. Furey, M.J., "Metallic Contact and Friction Between Sliding Surfaces"; ASLE Trans. 4, pp. 1-11, 1961.
5. ASTM, "Ball-on-Cylinder Lubricity Evaluator Measurement of Lubricity of Liquid Hydrocarbon Fuels Test Method"; ASTM D02.J.10, 1988.
6. McBride, S.L., Pollard, M.D., MacPhail, J.D., Bowman, P.S. and Peters, D.T., "Acoustic Emission Detection of Crack Presence and Crack Advance During Flight"; World meeting on Acoustic Emission, Charlotte, N.C., March 1989.
7. Hamrock, B.J. and Dowson, D., "Ball Bearing Lubrication"; Wiley Press, 1981.

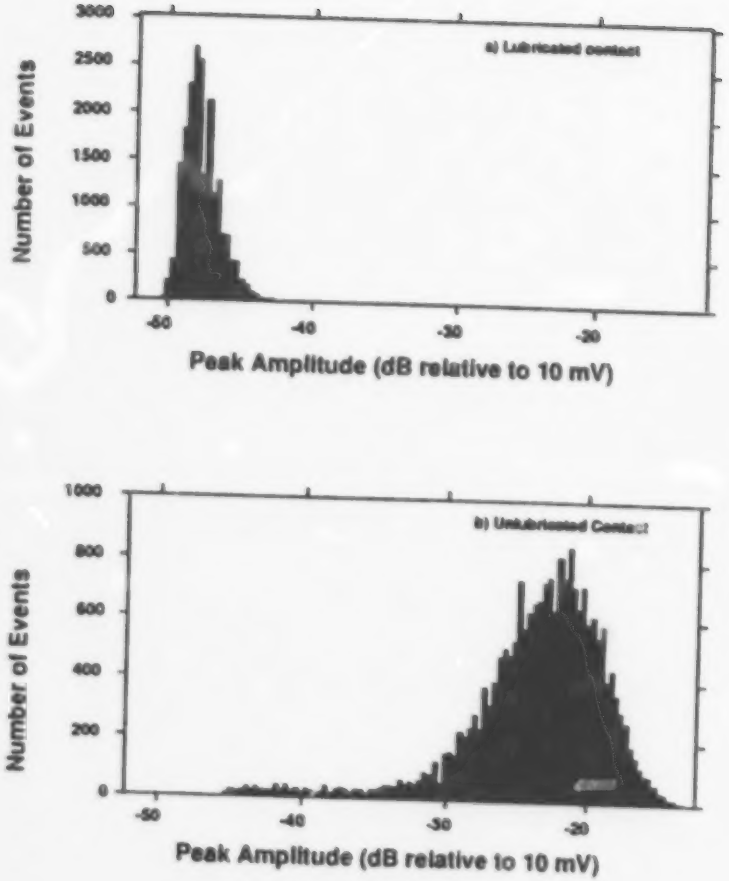
a) Lubricated contact
Number of Events
Peak Amplitude (dB relative to 10 mV)
b) Unlubricated Contact
Number of Events
Peak Amplitude (dB relative to 10 mV)

Figure 1. Histograms of peak amplitude for acoustic emission event a) from test with lubricated contact
b) from test with unlubricated contact

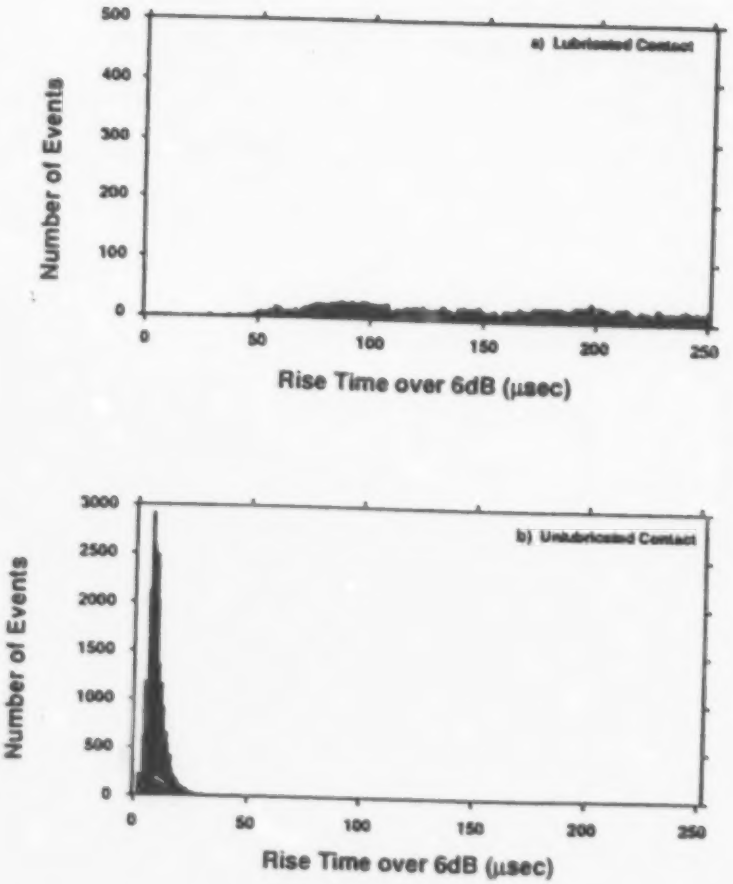

Figure 2. Histograms of rise time for acoustic emission events
a) from test with lubricated contact
b) from test with unlubricated contact

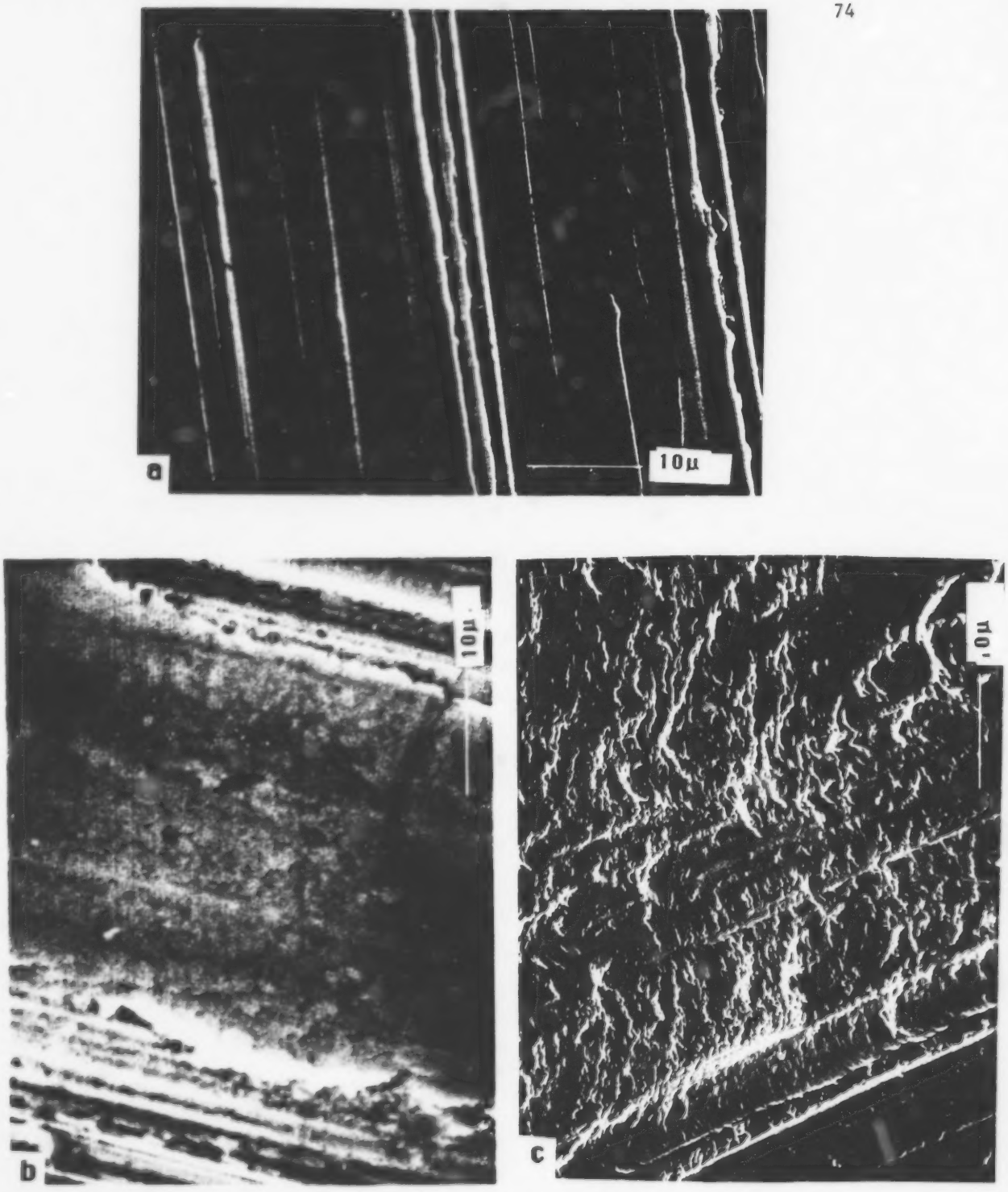

Figure 3. Photomicrographs of test cylinder:
a) original surface
b) wear scar after test with lubricated contact
c) wear scar after test with dry contact

DEVELOPMENT OF A PROTOTYPE ABRASIVE WEAR TESTER FOR TILLAGE TOOL MATERIAL

He-Jin Yu and S.D.Bhole
Faculty of Engineering, University of Regina
Regina, Saskatchewan, Canada

Introduction:

Most of the tillage tools in common usage, such as sweeps, shovels and chisels, are made from a couple of high carbon or low alloy steels which give adequate performance in average soil conditions. However, in some areas, the rocky soil is very harsh on tools such as sweeps and banding knives and they wear out at unacceptably high rates. The main mode of failure is wear of the tools which occurs under conditions of low stress abrasion. The Canadian economy loses around 3.9 billion dollars due to wear annually. Of this total, the estimated losses due solely to abrasion are around 2.5 billion dollars per year (Huard et al, 1987). Hence, the need for research into abrasive wear has become more desirable. In general, the current materials used for tillage tools are the plain high carbon steels, such as AISI 1070, 1080, 1090. These materials can be effectively heat treated and hardened. They are available to the minimum hardness required, 53 HRC, which gives acceptable wear resistance.

The abrasive wear resistance depends not only on the intrinsic conditions the material, but also on the service conditions. The important material factor are the chemical composition, production history, mechanical propertics and the microstructure. Important soil characteristics are the particle shape, size, strength, density, and rock and gravel contents (Moore, 1975 and Foley, 1984). Based on the above, agricultural areas of Saskatchewan were classified into two groups— high wear areas and low wear areas(Bhole, 1988).

The ASTM dry sand/rubber wheel test is the most commonly used test for abrasive wear. However it is not entirely satisfactory for assessing the abrasive wear characteristics experienced by tillage tools. Since the test utilizes a standardized dry sand mixture as the abrasive medium. There is no simple relationship between the abrasive wear resistance and any of the common mechanical properties.

For these reasons, a prototype wear testing machine is needed to simulate soil tillage conditions.

Objective:

1. To design and develop a prototype machine for abrasive wear testing under simulated soil tillage conditions. The apparatus should allow the control of soil characteristics, moisture and speed.

2. Abrasive testing of the tillage tool materials. Other than the commonly used high carbon steels, there is wide range of other materials available that may be good substitutes. In this project, four carbon and low-alloy steels and two alloying white cast irons were selected for study. They are all commercial abrasive materials, viz. AISI 1070, AISI 4130, AISI 5160, AR 00, Ni-hard cast iron, and High-Cr cast iron. There are a number of soil properties that have been identified as influencing wear in tillage tools. They are the hardness of soil particles; soil particle angularity; soil strength, density and water content; and rock and gravel content of the soil. The sand, clay, silt and gravel content and the moisture content of soil will be monitored and controlled during the tests.

Design of Tester:

A preliminary design of the tester is shown in Figure 1. The test assembly comprises four major subassemblies:

1. Frame — fabricated from 2.5in x 2.5in hollow structural steel sections. The frame is the main support structure for the drum and the transmission and power systems.

2. Drum — fabricated from 36in diameter steel pipe. The drum holds the soil in which the tillage specimen is rotated.

3. Arm sub-assembly — comprises arms, rollers, specimen holders and support pipe. This is the rotating component of the test system and it moves the tillage specimen through the soil in the drum and also compacts the soil ahead of the specimen.

4. Power transmission system — The arm assembly shaft is rotated by a hydraulic motor which is powered by a hydraulic pump. The pump is run by a 10 HP electric motor. This system is mounted on the base of the frame.

Conclusion:

A prototype abrasive wear tester has been designed and built to carry out tests on tillage tool materials under simulated soil conditions. The test allows testing using soils with different characteristics under controlled conditions. The aim of the work is to establish suitable tool materials for different agricultural soils in Saskatchewan.

References

Bhole,S.D. (1988), Materials Data-base for Tillage Tools, Faculty of Engineering Report, Project No.S-86-02-0026, University of Regina, p.32

Foley,A.G. et al (1984), The Use of Alumina Ceramic to Reduce wear of Soil-engaging Components, J.Agric. Engng, Res., 30 p.7

Huard,G. et al (1987), Tribological Factual Data Base for the Mining Industry. CIM Bulletin, 80, (906), P.48

Moore,M.A. (1975), Abrasive Wear by Soil, Tribology InternAtional, June, p.105

Moore.M.A. (1975), The Abrasive Wear Resistance of Surface Coatings, J.Agric. Engng, Res.. 20. p.167

Acknowledgements:

Financial support was provided by a grant from "Canada/Saskatchewan ERDA Agreements".

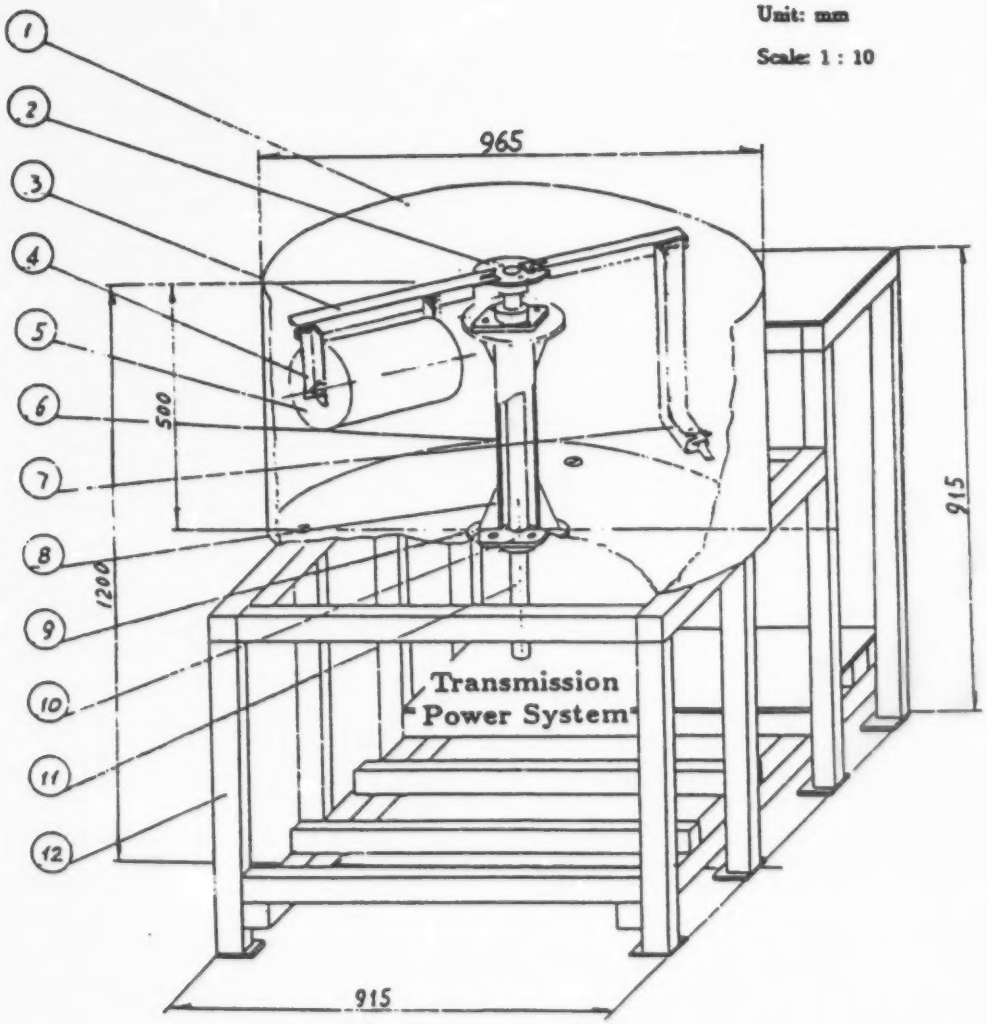

1. Drum
2. Flange mounting
3. Arms (2 pieces)
4. Roller holders (4 pieces)
5. Rollers (2 pieces)
6. Support pipe
7. Specimen holders (2 pieces)
8. Ribs (8 pieces)
9. Plates (2 pieces)
10. Bearings (2 pieces)
11. Main vertical shaft
12. Frame

Figure 1. Abrasive Wear Tester

THE FRICTION AND WEAR OF POLYMERIC AND CERAMIC BASED MATERIALS IN A HIGH VACUUM TRIBOSYSTEM

H.M.Hawthorne
Tribology & Mechanics Laboratory
National Research Council of Canada

Introduction

The asbestos/phenolic brake material operating successfully on the Shuttle Remote Manipulator System (Canadarm) eventually develops anomalously low friction after more extensive sliding in accelerated tests in vacuum. Alternative friction pad materials are therefore being sought for use on permanently orbiting Space Station manipulators.

Experimental Method

Annular disc pairs of selected polymer and ceramic materials were tested by sliding in a high vacuum tribometer (Fig. 1) simulating the continuously conforming contact geometry, and other conditions (e.g. load, speed, temperature, rig stiffness) of the brake mechanism. Friction torque was monitored during sliding and wear was determined by weight loss measurements.

Results

The friction results for the two types of materials are shown in Figure 2. All of the polymeric based materials exhibit a decreasing friction trend from high initial, to lower, more or less steady values with accumulated sliding distance. This is similar to previously reported behaviour of the asbestos/phenolic brake material [1]. The silicon carbide whisker reinforced silicon nitride quickly developed similar low friction sliding and the titanium diboride reinforced silicon carbide exhibited variable friction behaviour. In contrast, the two other ceramics, the silicon carbide whisker reinforced alumina and the modified reinforced silicon nitride, show continued high friction behaviour during extensive sliding. These trends are related to the structure and properties of the wear debris layers generated, and trapped, at the sliding interface of these tribosystems [2]. Comparison of the friction results with corresponding wear results, Table 1, indicates that, except for the unreinforced polyimide material, low wear is associated with low friction. The moderate wear rates of the high friction materials are comparable to those of some industrial brake compositions in air [3].

Conclusions

Despite a lower wear resistance than the current Canadarm brake materials, the two ceramic composites (Al_2O_3/SiC and Si_3N_4/SiC/X) may still be suitable candidates for long term use in space mechanisms because of their high friction stability in the vacuum environment. Preliminary results from some ceramic and cermet coatings also suggests their potential suitability for application in this unusual tribosystem.

Acknowledgement

The assistance of S.Yick in performing the experiments, and the support from Spar Aerospace, is acknowledged, with gratitude.

References

1. H.M.Hawthorne "Wear debris induced friction anomalies of organic brake materials in-vacuo." Proc. Wear of Materials Conf., ASME, Houston, 1987, 381-387.

2. H.M.Hawthorne "Tribological aspects of ceramic composites in conforming contacts." Proc. Internl. Symposium on Advances in Processing & Applications of Ceramic & Metal Matrix Composites, CIM, Halifax, Aug. 1989.

3. A.E.Anderson "Wear of brake materials" In Wear Control Handbook, (Eds. M.B.Peterson & W.O.Winer), ASME, 1980.

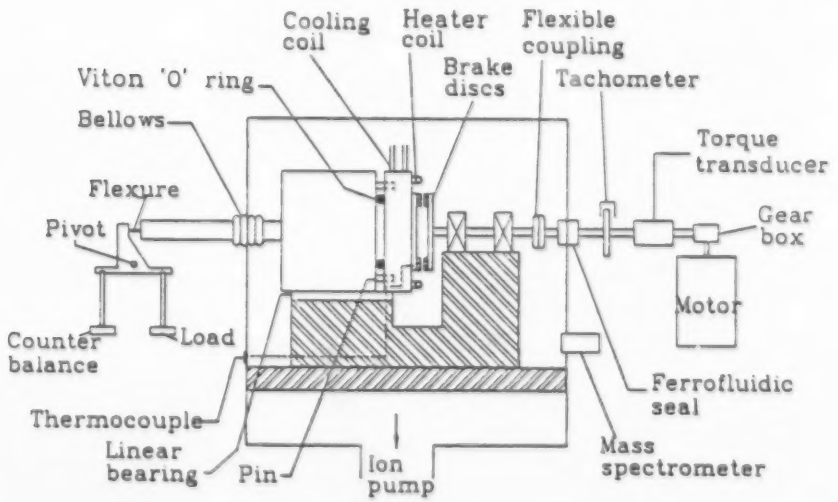

Fig.1 Schematic of the high vacuum tribometer

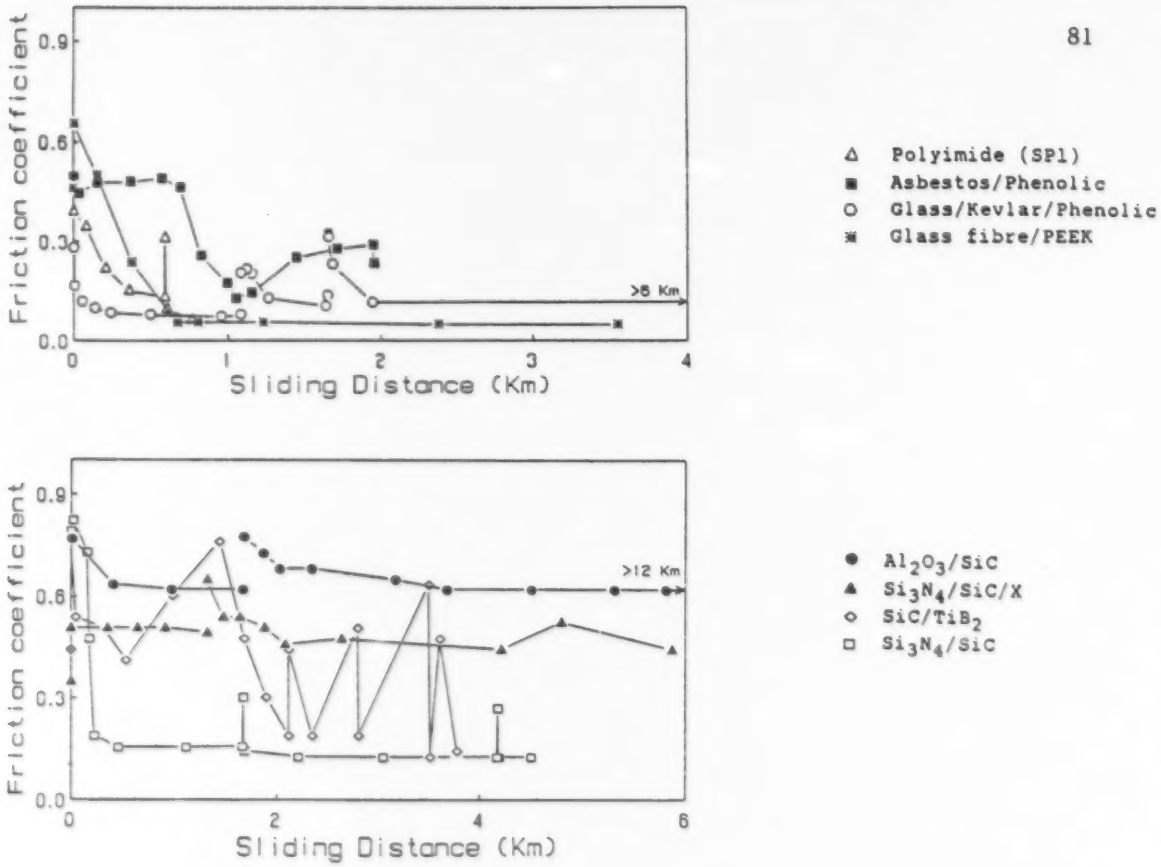

Fig.2 Sliding friction results

Table 1
Wear results of polymeric and ceramic materials

Material	Specific Wear Rate ($X\ 10^{-5}$ $mm^3/N\ m$)
Polyimide (SP 1)	29
Asbestos/phenolic	1.6 (High μ)
Glass fibre/Kevlar/phenolic	1.1 (Mixed μ)
Glass fibre/ PEEK	0.69
Si_3N_4/SiC	15 (High μ)
Al_2O_3/SiC	11.8
$Si_3N_4/SiC/X$	6.5
SiC/TiB_2	4.5
Si_3N_4/SiC	0.5 (Low μ)

A Reciprocating Wear Test for Evaluating Boundary Lubrication

J.S. Sheasby[1], T.A. Caughlin[1], A.G. Blahey[2] and K.E. Laycock[2].

[1] Department of Materials Engineering, Faculty of Engineering Science, UWO, London, On. N6A 5B9.

[2] Tribology Applications Group, Esso Petroleum Canada, Sarnia, On N7T 7M1.

INTRODUCTION

Zinc dialkyldithiophosphates (ZDDP) are the principle antiwear/antioxidant additives in crankcase oils (1). It has been shown that the antiwear action of ZDDPs results from the formation of relatively thick films on the rubbing surfaces (2). Although these films have been the subject of extensive research it is not clear how to rate ZDDP containing oils for practical uses.

This research explored the use of a reciprocating wear test rig for this purpose. The rig was a modified version of that described by Mills and Cameron (3) and by Furey (4).

Experimental Technique

A schematic of the basic features of the wear rig is shown in Figure 1. The roller was moved at 25 Hz with a 7 mm stroke perpendicular to its length. The grinding marks on the roller were oriented parallel to the grinding marks on the coupon. The friction force and resistance (roller-coupon) were monitored by chart recorder and oscilloscope.

Rollers	-6 mm diameter, 13 mm long, circumferentially ground, Ra 0.22 μm, hardened steel Rc 33-41, grade probably W1 tool steel.
Coupon	-ground steel plates Ra 0.25 μm, grade A2, hardened to Rc 61.5.
Oil	-20 ml per test, oils: a) Mineral base stock, kinematic viscosity at 100°C 4.98 cSt. b) Base + 2 wt % ZDDP.
Force	-roller to coupon was usually 50N.
Time	-standard 30 mins.
Atmosphere	-usually air

RESULTS

Figure 2 shows typical records of friction and resistance from a roller-coupon-oil combination that gave a good antiwear film (base + ZDDP, 100°C). The friction force fell in the first minutes and stayed essentially constant to the end of the run. The resistance trace left zero ohms after 1-2 mins, built with minor fluctuations to full resistance, and showed only minor deviations thereafter. By interrupting runs it was established that the high resistance was associated with the formation of a film on the wear scar and the cessation of wear. The film was difficult to detect until washed, whereupon it developed yellow, blue and brown colours. Before the development of the resistance the scar appeared smooth, bright and metallic.

Figure 3 shows stylized records of a run in base stock.
The friction record had the same pattern as the formulated oil. Resistance records were less reproducible than for the formulated oil as explained below. Figure 3 shows loss of full metal contact after about 6 mins, increasing irregularly to about 10% no contact by the end of the run. Other runs had essentially continuous metal contact throughout. Wear scars were larger than the scars formed with the ZDDP and had scratches, regions of bare metal and patches of red/brown material. The latter were rich in Fe and O and were assumed to be compacted oxide, i.e. glaze, as they did not form when the runs were done under N_2 cover. The resistance of the contact would depend upon the balance of glaze to metal. As these regions were relatively large compared to the area of the whole wear scar, fluctuations in the balance would have a large effect on the resistance.

The initial friction peak was associated with a smoothing of the rubbing surfaces and not with the formation of the surface film (or resistance rise). The association of the high initial friction with smoothing was demonstrated by:
1) the absence of a friction peak when restarting wear of a run-in roller on an old track.
2) the presence of a friction peak when restarting wear of a run-in roller on a new track.
3) the reduction of the friction peak when wearing against metallurgically polished coupons of chromium or steel.

Growth of the wear scar in oils containing ZDDPs could not be detected once a uniform antiwear film had formed. Whereas wear scars in the base stock or a white oil continued to grow despite the presence of glaze films. The time to film formation in the ZDDP oils was reduced by polishing one or both of the surfaces, indicating that mechanical stability of the surfaces was necessary for antiwear film formation. This was demonstrated by interrupting a run with and without coupon changes, Figure 4. Values of the scar size between microscope measurements were interpolated from the resistance readings (no resistance = wear, resistance = no wear).

It was interesting that polishing both surfaces, whilst giving a short time to film formation, also caused localised scoring. Apparently a certain roughness is necessary to allow debris to escape from the contact zone.

Two rollers worn at 1 Hz had larger wear scars, 0.16 and 0.18 mm, than the normal 25 Hz scar of 0.09 mm. The effect of load was small: scar 0.07 mm @ 12.5 N, 0.09mm @ 50 N, 0.11mm @ 150 N.

Rollers were worn against metallurgically polished steel and chromium coupons. The smoother coupons developed films on the rollers more quickly than rough surfaces, and were themselves more heavily coated with antiwear film. The chemistry and behaviour of all the ZDDP antiwear films could not be distinguished.

Rollers worn against Cr coupons, in addition to forming antiwear films, also developed local prows or accretions of oxide rich debris that scratched the coupon. Recognition of this mode of damage is important for the correct rating of oils. The prows cause deep scratching which must be unacceptable, but by carrying the load cause the wear scar to be unusually small.

Two rollers were worn in base stock with ZDDP on coupons with the texture oriented perpendicular to the direction of sliding. Contrary to expectations both wear scars were smaller than usual. The wear scars had an unusual dark debris aligned along the length of the roller and the coupon was scratched. Apparently this orientation of the texture aided prow formation.

An exploratory investigation was made into the effect of roller hardness on the performance of several antiwear agents. Oil containing ZDDP showed a sharp improvement in wear resistance between roller hardnesses of 25 and 33 Rc, which was associated with a change in the surface films from oxide to the normal ZDDP type antiwear film.

The following experiments were performed to evaluate the strengths/stabilities/wear resistances of antiwear films.

1) measurements of wear rate after the antiwear films had formed.
   -no wear could be detected.

2) resistance of a preformed film to being worn away.
   - films were formed on rollers by wearing in base with ZDDP for 15 mins and then the oil changed to base stock. Most films survived 15 hrs when the tests were discontinued. The two that failed did so immediately after the oil change, probably due to a misalignment as these were runs in which the roller was removed from the machine at the time of the change.

These experiments established that the anti-wear films were wear resistant, however they were judged to be too irreproducible to be of value for rating film strength.

DISCUSSION

This work confirmed that ZDDP additives in oil give antiwear action by forming a film on the rubbing surfaces. The antiwear films are thick enough to be seen by optical microscopy and appeared similar to oxide glaze films from which they can be distinguished only with difficulty. Antiwear films tend to be primarily blue and yellow, whereas oxide glazes have more brown and red. However no significance could be attached to colour in either type of film.

The steady state wear rate in the presence of antiwear films was too low to measure. The wear rig therefore predominantly rates the ability of the antiwear films to get established.

The ability of an antiwear film to get established (as determined by the final scar size after a 30 min test) is probably as good a measure as any of the films quality. It can be used to define the limits of operation of an additive for temperature, pressure, material, velocity, etc. However as the time for film formation is sensitive to sample roughness and hardness, it is essential to have these parameters under control if oil formulations are to be so rated.

REFERENCES

1. J.J. Habeeb and W.H. Stover, "The Role of Hydroperoxides in Engine Oil and the Effect of Zinc Dialkylthiophosphates", ASLE Trans., 30 (1987) 419-426.

2. J.M. Georges, J.M. Martin, T. Mathia, Ph. Kapsa, G. Meille and H.Montes, "Mechanism of Boundary Lubrication With Zinc Dithiophosphate", Wear, 53 (1979) 9-34.

3. T.N. Mills and A. Cameron, "Basic studies in boundary E.P. and piston ring lubrication using a special apparatus", ASLE Trans., 25 (1982) 117-124.

4. M.J. Furey, "Metallic Contact and Friction between Sliding Surfaces," ASLE Trans., 4 (1961)1.

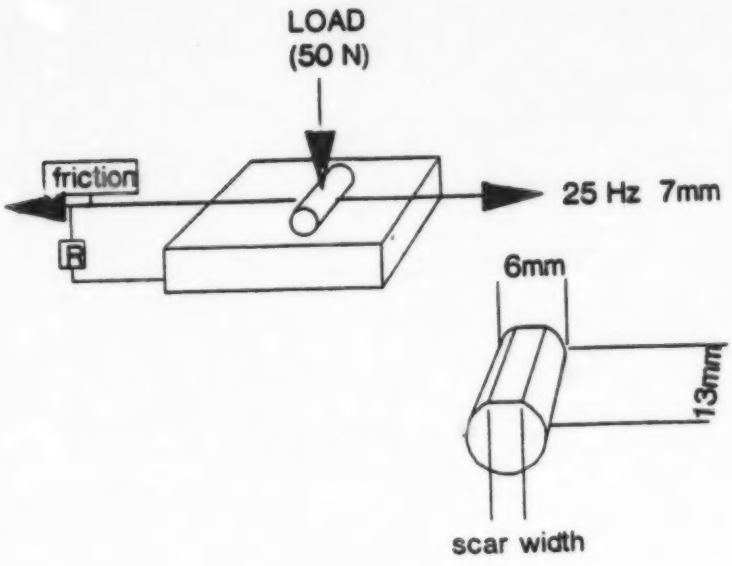

Figure 1: Schematic of the Cameron Plint High Frequency Wear Tester.

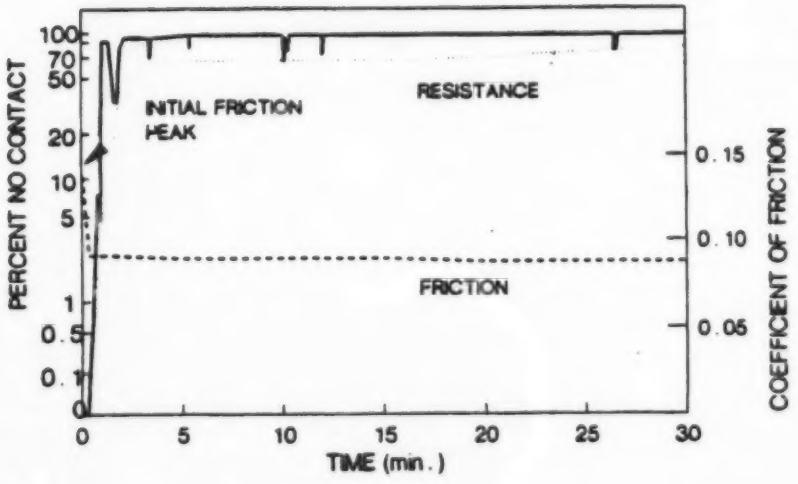

Figure 2: Annotated friction and resistance recordings from the CP when wearing in base with secondary ZDDP. An antiwear film was established by 2 - 3 minutes.

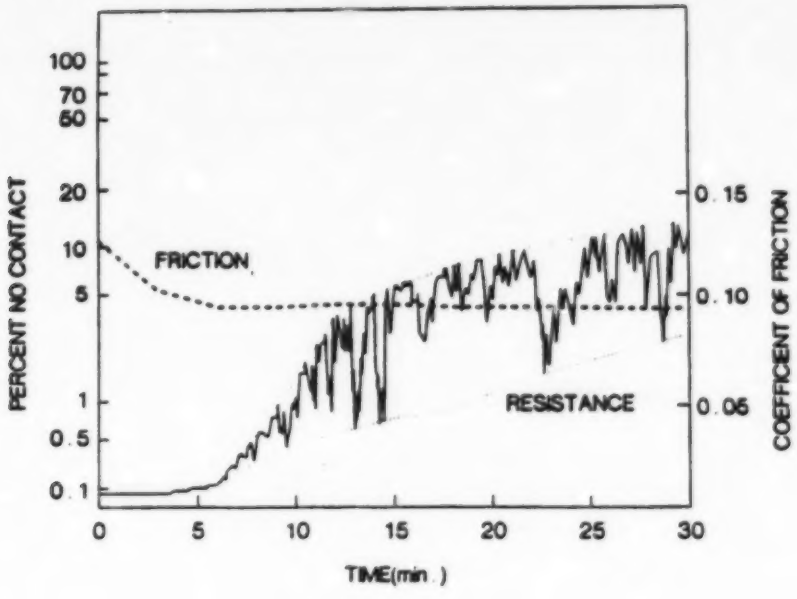

Figure 3: Annotated friction and resistance recordings from the CP when wearing in base stock.

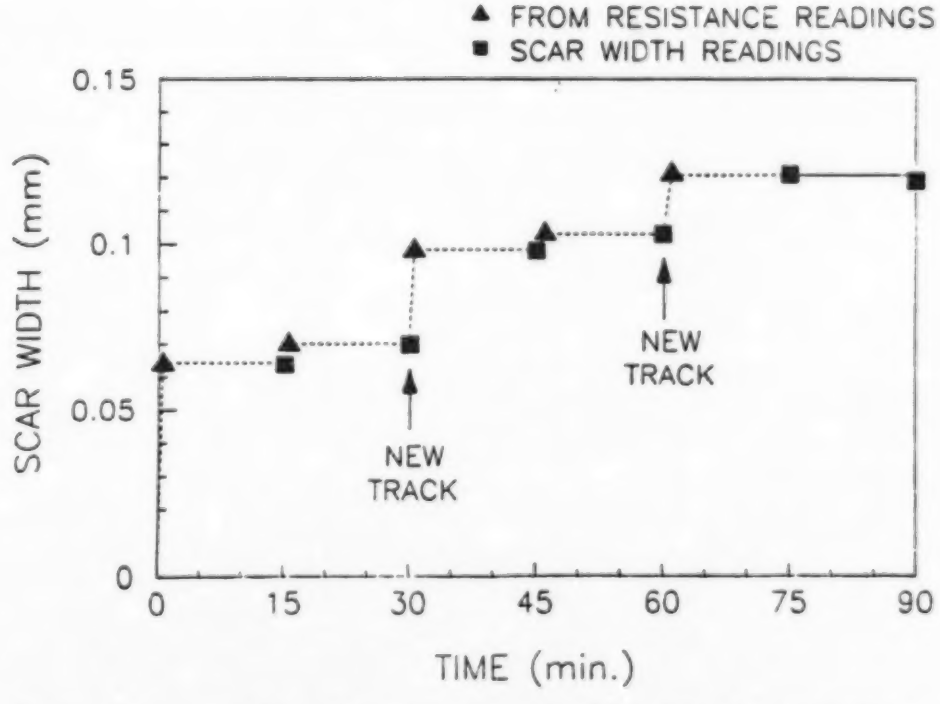

Figure 4: The effect of changing to new countersurfaces on scar size when wearing in base with secondary ZDDP. The roller had to be removed from the CP for measurement, resulting in slight misalignment and so wear on replacing. Replacing onto a new track caused considerably more wear.

WEAR II

Effect of the abrasive nature on the impact and impact-abrasion wear rate of a martensitic cast iron.

Michel Fiset
Université Laval
Ste-Foy, Québec

Gilles Huard and Jacques Masounave
Industrial Materials Research Institute
National Research Council Canada
Boucherville, Québec

INTRODUCTION

General tendencies of the effect of the abrasive size and shape are already established for abrasion of materials: a coarser abrasive paper leads to higher wear rates, and so do more angular abrasive particles. Combined influence of these parameters may however alter the wear behaviour of a material which will depart from these established rules [1]. Tests were carried out to investigate the extent of these effects when a material is submitted to impact and impact-abrasion wear. They showed that the impact wear rate is very dependent on the size and shape of the abrasive. It was also found that the deterioration of the abrasive particles during the impact has a major influence on the abrasion component they produce after the impact.

TEST METHOD

Impact and impact-abrasion tests were carried out on a martensitic high-chromium cast iron (3.05%C, 17.00%Cr, 0.50%Mn, 0.50%Si - 31,9 vol% carbide - 62 HRC) with an abrasion pin-test apparatus using standard abrasive belts available on the market. More information is given elsewhere about this test [2]. The test consists of a series of 540 impact-abrasion cycles on the flat end of a pin made out of the material to be investigated. Each cycle includes an impact drop of 550 MPa on unworn abrasive paper, the pin acting as the hammer. In the case of the impact-abrasion tests, each drop was followed by a complete rotation of the specimen (at 60 rpm) on the impacting abrasive paper under a constant static load of approximately 100 N. The specimens were cleaned and weighed with a precision of 0.1 mg prior and after each measurement done after 90, 180, 270, 360 and 540 cycles. The mass loss was used as wear value. Five different abrasive papers were used: SiC (180 and 425 µm), Al_2O_3 (180 and 425 µm) and garnet (180 µm).

RESULTS

Figure 1 shows typical results obtained with SiC papers. A short running-in period is observed with the finer papers, but it was found that it could be ignored when comparing the mass loss after 540-cycle tests. Similar observations applied with Al_2O_3 and garnet papers.

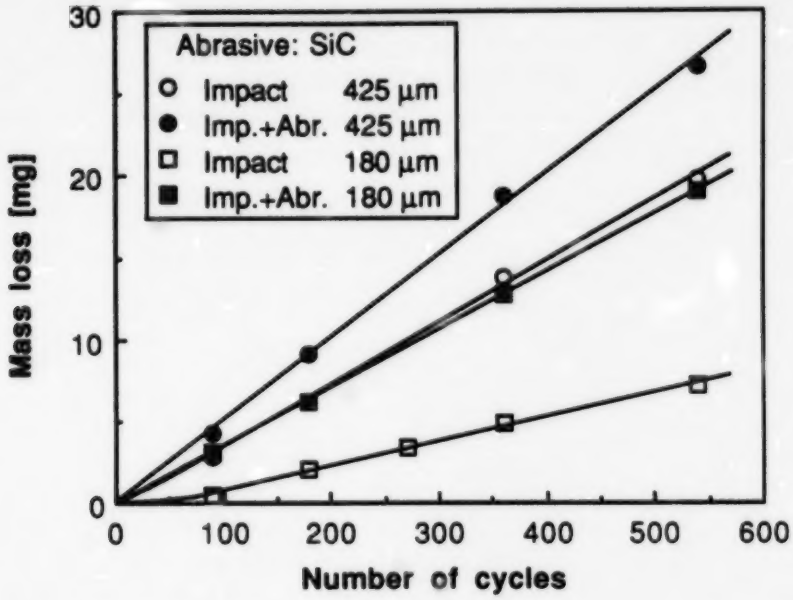

Figure 1. Wear loss of the martensitic chromium cast iron

Figure 2 gathers the results obtained with the five abrasive papers. For each one, the first column represents the specimen mass loss after 540 impact-abrasion cycles and will be refered to as the total wear loss. The second column is the mass loss after 540 impact cycles without abrasion. Finally, the third column gives the abrasion component of the impact-abrasion tests, estimated by the difference between the first and the second column.

Several observations can be done in Figure 2. As expected, the total loss against SiC is higher than against Al_2O_3, for both abrasive sizes, but the garnet produces a higher total loss than Al_2O_3. If impact wear only is considered, the relatively soft garnet is found to be more efficient than the other papers of the same grade. It is even more abrasive than the coarser Al_2O_3. Finally, when each paper grade is considered separately, the usual relation between the abrasion wear and the abrasive hardness is respected, a higher wear loss going with a harder abrasive, although for each abrasive type, the finer grade leads to higher values than the coarser.

DISCUSSION

Three main characteristics of abrasive particles have to be considered with regards to their efficiency of material removal: their nature, size and shape. When using abrasive papers for impact tests, the resistance to crushing and the number of particles per unit area are also parameters of importance. Figure 3 shows the aspect of the three types of unworn finer papers. Garnet grains are seen to be more angular than the other two and their number per unit area appears higher. This could be an explanation to the surprisingly higher impact wear loss it produces on the martensitic cast iron. When considering the abrasion component only, the wear against garnet is greatly reduced. This is the usual observation made with a softer abrasive and agrees well with previous data obtained from pure sliding abrasion wear tests carried out on the same materials [3-5].

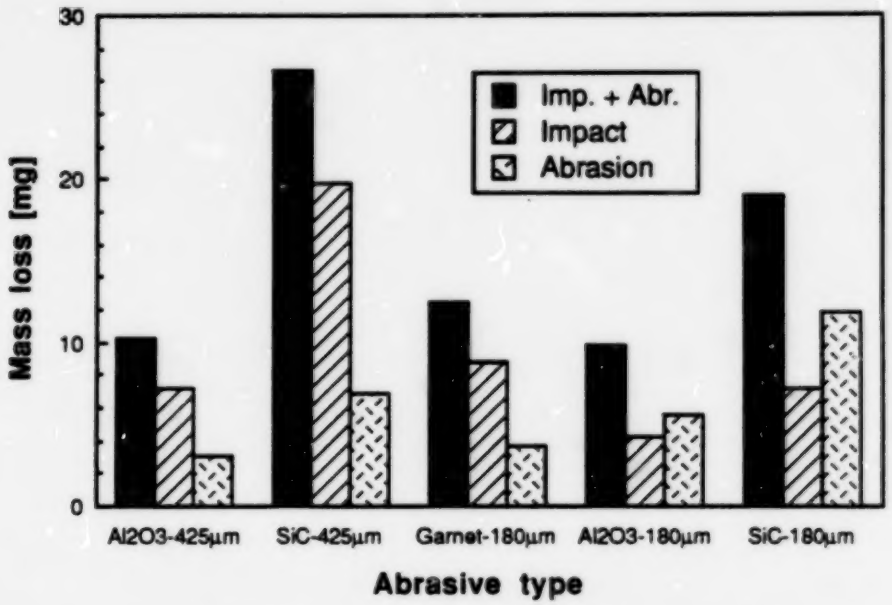

Figure 2. Mass loss of the cast iron as related to the abrasive type.

The effect of abrasive grain size may be investigated by comparing different grades of the same abrasive. In sliding abrasion,a coarser abrasive particle may indent deeper into the material surface and cause higher damage by microcracking. Coarser particles are however more susceptible to be broken at the impact, a phenomenon also enhanced by the higher impact load supported by each particle. This would result in a higher number of free fine particles promoting less efficient three-body abrasion mechanisms. The higher impact wear and the smaller abrasion component with coarser papers both support these asumptions, which can therefore be retained as possible explanations.

CONCLUSIONS

Impact and impact-abrasion wear rates are very dependent on the characteristics of the abrasive papers on which the tests are conducted, particularly on the shape of the abrasive particles. The wear behaviour can differ from what is usually observed with simple abrasion tests. Garnet can produce higher impact wear losses than less angular SiC and Al_2O_3 for tests carried out on abrasive papers of the same grit size. The expected higher impact wear loss was found with coarser SiC or Al_2O_3 compared to a finer grade of the same paper. However, the abrasion component measured in impact-abrasion tests was lower, a phenomenon attributed to a higher deterioration of the coarser abrasive during the impact with the cast iron specimen.

ACKNOWLEDGEMENTS

The authors wish to thank M. Léon Leclercq form Magotteaux Canada for having supplied the cast iron balls and Sylvain Turenne form IMRI for his comments on the papers.

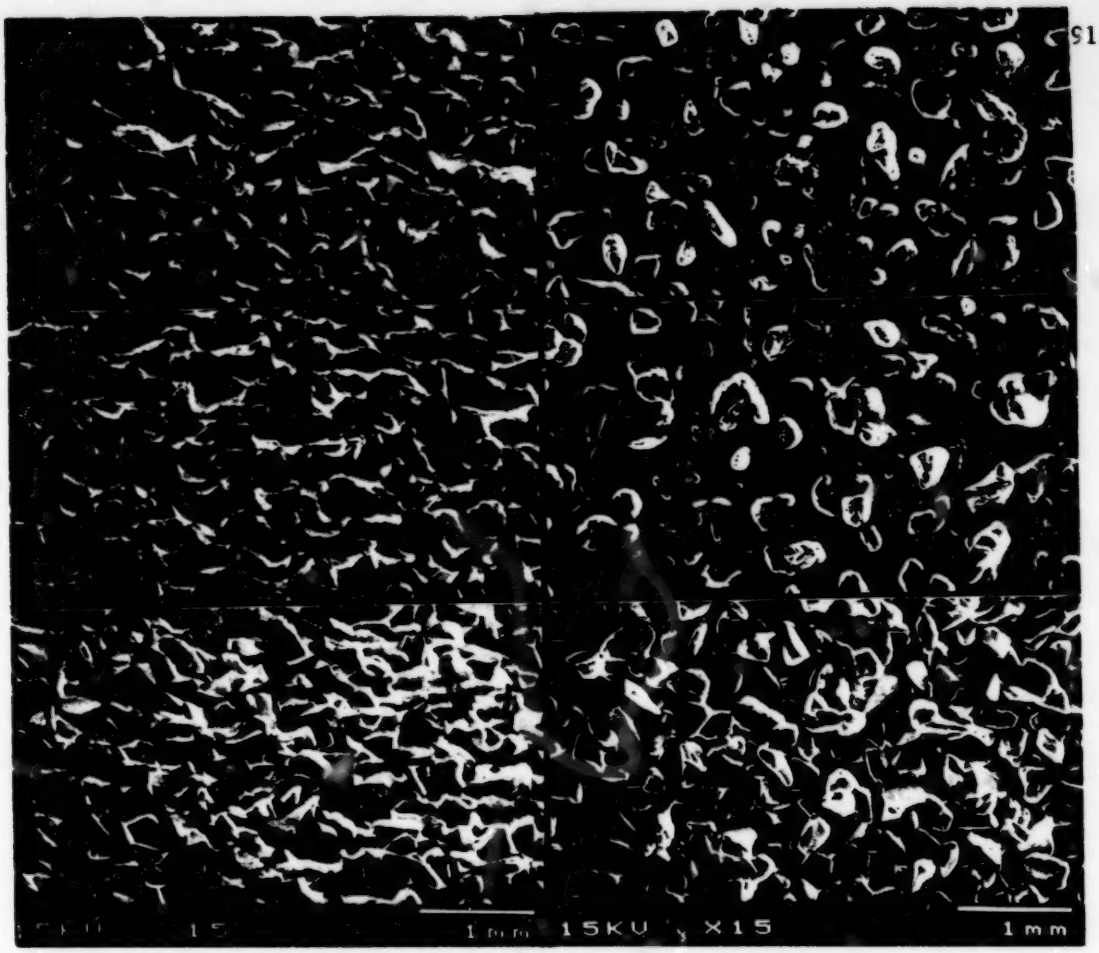

Figure 3. Aspect of the unworn abrasive papers
(180 µm particle size; viewed at 60° (left) and 90° (right))

REFERENCES

1. G. Huard , M. Fiset, J. Masounave, Y. Côté and D. Noël, The Effects of Size and Shape of Abrasive Particles on the Measurement of Wear Rate Using a Dry Sand Rubber Wheel Test, Proc. of the Int. Conf. on Wear of Materials 1987, Houston, USA, 689-699.

2. M. Fiset, G. Huard and J. Masounave, Correlation Between a Laboratory Impact-Abrasion Test and an *in-situ* Marked-Ball Test, published elsewhere in these Proceedings and submitted to Tribology International.

3. F. Lavallée, S. Turenne and J. Masounave, Etude de l'usure sévère des fontes blanches au chrome, Research Report IGM87RT-204-641-G, CNRC 28423, National Research Council Canada, August 1987, 55p.

4. S. Turenne, F. Lavallée and J. Masounave, Matrix Microstructure Effect on the Abrasion Wear Resistance of High-Chromium White Cast Iron, to be published in Journal of Materials Science.

5. S. Turenne, F. Lavallée and J. Masounave, The Effect of Matrix Microstructure on the Abrasion Resistance of High-Cr Cast Irons, Proc. of the Conf. on Wear Resistance of Metals and Alloys held in conjunction with the 1988 World Materials Congress, Chicago. Ill., USA, September 1988, 105-113.

The Influence of Corrosion on the Low-Stress Abrasion Resistance of Refiner Plate Stainless Steels and Cast Irons

C.B. Thompson
Pulp and Paper Research Institute of Canada
570 St. John's Boulevard
Pointe Claire, H9R 3J9, Quebec

Introduction

As part of a development program aimed at increasing the wear resistance of high-consistency chip refiner plates, abrasion testing has been performed for eight cast irons and cast stainless steels. The aim of the testing was to evaluate the resistance of refiner plate alloys to bar rounding, which occurs by a low-stress abrasion mechanism (1). Testing was performed in both dry and wet conditions, to see if the metallurgical factors influencing abrasion resistance could be applied under corrosive conditions.

Experimental

Abrasion resistance was determined using i) a Dry Sand Rubber Wheel test and ii) a slurry abrasion test.

All specimens were cut from used refiner plates; chemical compositions, hardnesses and primary carbide volume fractions are given in Table 1. In both abrasion tests, specimens were 17 mm diameter cylinders, with testing being done on the end faces. These faces were wet-ground to a 240 grit finish and degreased before testing. Abrasion losses were measured gravimetrically to $\pm$ 0.01 mg and then converted to a volumetric basis using a density of 7.8 $g.cm^{-3}$.

Dry Sand Rubber Wheel Testing

With one exception, the test rig was run according to the requirements set-out in ASTM Standard Practice G65-81, Procedure A, which is recommended for ranking materials of medium to extreme abrasion resistance (2). The exception was with regard to the specimen size and geometry. Due to their hard, brittle nature, it was not possible to prepare the rectangular specimens specified in the standard. Instead, 17 mm diameter cylindrical specimens were mounted in AISI 1020 carbon steel holders, which had the overall dimensions referred-to in the standard. Each test specimen was held in its steel holder by means of set-screws.

Slurry Abrasion Testing

This rig is based on an original design by Madsen (3); the operation has been described in detail elsewhere (4). The principle of the test is to induce abrasive wear by moving a sand-liquid slurry past specimens by an impeller. This particular design of rig was chosen because the abrading action simulates that which occurs during refiner plate bar rounding. In operation, 16 cylindrical specimens were held in individual tapered plastic blocks, clamped between two

Table I. Chemical Analyses, Hardnesses and Carbide Volume Fractions of the Test Alloys.

Alloy Type	Identification Alloy Number	Element (% by weight)								Carbide Volume Fraction	Bulk Hardness (R_C)
		C	Cr	Ni	Si	Mo	Mn	P	S		
White Cast Irons	1	3.33	2.35	4.01	1.19	0.31	0.61	0.03	0.141	40	56.9
	2	2.73	23.16	0.35	0.54	2.01	0.71	0.016	0.024	29	53.4
	3	2.53	23.35	0.50	0.55	0.14	0.52	0.027	0.046	20	48.9
	4	2.95	27.69	1.13	0.60	0.12	0.54	0.032	0.028	28	55.2
Cast Stainless Steels	5	0.35	16.66	2.10	1.24	0.37	0.66	0.027	0.030	0.01	50.2
	6	0.84	18.0	1.35	0.85	0.51	0.59	0.025	0.015	3	53.8
	7	1.00	18.15	1.47	0.68	0.65	0.50	0.011	0.015	3	53.7
	8	1.63	16.26	1.49	1.07	0.87	0.59	0.013	0.017	11	55.4

stainless steel plates to form a water-tight chamber. The test solution was mixed with silica sand (of the type used in the Dry Sand Rubber Wheel test) and then pumped into the test chamber. The sand was used on a once-through basis, with the filtered solution being recirculated on a continuous basis. The slurry used in these tests had a sand concentration of 1.5% by weight; at this value, the abrasion was similar to that observed on actual refiner plates. Test solutions used were; pH 4.5 synthetic newsprint whitewater (20 ppm Cl^-, 100 ppm SO_4^{2-}) and pH 7.5 sodium borate-buffered distilled water. These solutions were chosen to represent corrosive and non-corrosive conditions respectively.

Results

Average volume losses obtained from the rubber wheel test for the eight test alloys are shown in Table II.

Table II

Average Rubber Wheel Abrasion Losses for the Eight Irons and Steels

Alloy Type	Alloy Description	Average Volume Loss (mm^3)
	2.7C, 23Cr, 2Mo	21.0
Cast	2.9C, 27Cr	21.7
White Irons	2.5C, 23Cr	23.9
	3.3C, 2Cr, 4Ni	26.8
	1.6C, 16Cr, 1.5Ni	41.7
	1C, 18Cr, 1.5Ni	92.4
Cast	0.8C, 18Cr, 1.5Ni	120.3
Stainless Steels	0.4C, 17Cr, 2Ni	184.2

It can be seen that the cast irons and the cast stainless steels form two distinct groups, with the cast irons having the greater abrasion resistance. Also, despite representing a wider range of compositions, there is a smaller overall range of volume losses for the cast irons (about 7 mm^3) compared to the cast stainless steels (about 142 mm^3), indicating that the irons are more uniform in their response to abrasion.

Carbon content plays an important role in the abrasion resistance of ferrous materials (5). Correlating the rubber wheel data with carbon content showed that abrasion resistance increased with carbon content up to about 2.7 - 3 wt%. Above this value, abrasion resistance started to decrease again. A similar trend was found for carbide volume fraction, with maximum abrasion resistance occurring at about 30% volume fraction.

The results obtained with the slurry rig are summarized in Table III. Initial testing was done in the pH 7.5 borate-buffered distilled water. As this

solution is essentially non-corrosive, alloy ranking should be determined by abrasion resistance alone. As a group, the cast irons again had greater wear resistance than the stainless steels, due mainly to their higher carbon content. Alloy ranking was similar to that obtained in the rubber wheel test, except that no abrasion resistance maximum was observed in terms of carbon content or carbide volume fraction. Consequently, the 3.3C, 2Cr, 4Ni alloy changed from being the worst of the cast irons in the rubber wheel test to the best in the slurry test. Other workers have also observed that an abrasion resistance maximum varies with the type of test (6). The variation may be related to the type of abrasion occurring in each test, e.g. two-body versus three-body, and the relative proportion of cutting and ploughing versus rolling (7)(8).

Table III

Average Slurry Abrasion Losses for the Eight Irons and Steels

Alloy Description	Average Volume Loss (mm^3) Buffered distilled water pH 7.5	Synthetic whitewater pH 4.5
3.3C, 2Cr, 4Ni	0.5	4.2
2.9C, 27Cr	0.5	1.6
2.7C, 23Cr, 2Mo	0.6	2.2
2.5C, 23Cr	...*	1.7
1.6C, 16Cr, 1.5Ni	0.9	2.0
1C, 18Cr, 1.5Ni	0.9	1.4
0.8C, 18Cr, 1.5Ni	1.3	3.0
0.4C, 17Cr, 2Ni	2.2	3.3

* Alloy not available at time of test.

Alloy ranking changed significantly when testing was done in the corrosive pH 4.5 whitewater (Table III). In contrast to the data for buffered distilled water, comparable wear behaviour was obtained from different types of alloy, because of the influence of corrosion. In particular, the 1C, 18Cr stainless steel performed well, with a volume loss similar to that of the 2.9C, 27Cr and 2.5C, 23Cr white irons. Other significant changes in ranking compared to the non-corrosive test included the 3.3C, 2Cr, 4Ni cast iron and the 0.8C, 18Cr stainless steel. The 3.3C cast iron had the lowest abrasion resistance at pH 4.5, due to its poor corrosion resistance. Note that the performance of this alloy had already started to deteriorate when tested in a pH 7 buffered whitewater, showing the sensitivity of the alloy to attack.

Supplementary corrosion testing in pH 4.5 synthetic whitewater was performed to determine corrosion rates in the absence of any abrasion. Results are given for four alloys in Table IV, and confirm that the 1C, 18Cr steel that gave good performance in the pH 4.5 slurry test had the lowest corrosion rate; more than twice as low as the 2.9C, 27Cr white iron, and about fourteen times lower than the 3.3C, 2Cr cast iron.

Table IV

Corrosion Rates in pH 4.5 Synthetic Whitewater

Alloy Description	Corrosion Rate (μm/year)
1C, 18Cr, 1.5Ni	38.1
2.9C, 27Cr	83.8
0.8C, 18Cr, 1.5Ni	152.4
3.3C, 2Cr, 4Ni	546.1

The performance of the 0.8C, 18Cr, 1.5Ni steel is interesting. Microscopic examination of this specimen after pH 4.5 slurry abrasion showed that the primary carbides had been removed. Consequently, this alloy had greater wear than would be expected from either its composition or its primary carbide volume fraction. Additional experiments, using re-austenitized samples, showed that a chromium depletion, or sensitization, mechanism was responsible for the premature carbide loss. No carbide removal took place when the alloy was either water quenched (i.e. no precipitation of secondary carbides) or tempered at 200°C (too low a temperature for appreciable chromium diffusion to existing primary carbides or for precipitation of chromium-rich secondary carbides (9)). Similar effects of sensitization have been discussed for 13% chromium steels (10) and for a 10% chromium cast iron (11).

Conclusions

1. Alloy carbon content had a strong influence on abrasive wear as determined by the rubber wheel tester. Abrasion resistance increased with carbon content up to about 2.7-3 wt%. Above this level, abrasion resistance started to decrease.

2. For the slurry rig, alloy carbon content could only be used as a guide to abrasive wear for non-corrosive conditions. No abrasion resistance maximum was observed in this test.

3. In pH 4.5 synthetic newsprint whitewater, alloy performance was dependent upon both corrosion and abrasion resistance. Because of the influence of corrosion, alloy carbon content or primary carbide volume fraction cannot be used as a reliable guide to refiner plate bar rounding abrasion.

4. Premature removal of primary carbides in one of the stainless steels tested was due to sensitization.

References

1. Thompson, C.B. and Garner, A. Pulp and Paper Canada 88, 8 p.T294 (1987).

2. Standard Practice G65-81, Annual Book of ASTM Standards, Section 3, Volume 03.02, American Society for Testing and Materials, Philadelphia.

3. Madsen, B.W., Proc. 1985 Int. Conf. on Wear of Materials, p.345, ASME, New York (1985).

4. Thompson, C.B. and Garner, A., Tappi Journal, 70, 6, p.95 (1988).

5. Borik, F., Chapter in Wear Control Handbook, M.B. Peterson and W.O. Winer, Eds., p.327, ASME, New York (1980).

6. Zum-Gahr, K.-H. and Eldis, G.T., Wear, 64 p.175 (1980).

7. Misra, A. and Finnie, I., Wear, 68, p. 33 (1981).

8. Rabinowicz, E., Dunn, L.A. and Russell, P.G., Wear, 4 p.345 (1961).

9. Heat Treating, in Metals Handbook, Vol. 4, p.73, American Society for Metals (1981).

10. Truman, J.E., Brit. Corr. J., 11, 2. p.92 (1976).

11. Madsen, B.W., Mat. Perf. 26, 1. p.21 (1987).

Development of CANMETCOAT Digger Teeth for Oil Sands Bucket Wheel Reclaimer Service

Keith Davies: Metals Technology Laboratories, Canmet, Ottava

Glenn Doonanco: Syncrude Canada Ltd., Fort McMurray

Rees Llevellyn: Syncrude Canada Ltd., Research, Edmonton

The CANMETCOAT procedure for the production of castings with in-situ hardfacing, has been developed primarily with the minerals extraction industry in mind. The basic concept is that instead of first making a casting and then hardfacing high-wear areas by a welding procedure, powder of abrasion-resistant material is held in place on the surface of the mould cavity by vacuum. When the base metal is poured, it is drawn into the powder and the surface layer so formed becomes an integral part of the casting.

In early trials, green powder compacts were set into the mould cavity walls. They rarely bonded properly to the casting. The parent metal did not penetrate the powder; thus no metallurgical bond was formed and blow holes were often produced at the casting / compact interface. The concept of using vacuum behind the compact was then introduced, to enhance penetration and prevent blow hole formation. Later, it was realized that with the use of vacuum suction, a compact was no longer needed and a loose powder layer could be held in place by the pressure differential set up across it.

Of the numerous severe wear attack applications in Syncrude's oil sands operations, digger teeth for bucket wheel reclaimers (BWRs) were selected as appropriate components for service evaluation of the CANMETCOAT procedure.

A "vacuum core" method was used in digger tooth production. This consisted of a welded metal box with a vacuum manifold at the back. The manifold was separated from the rest of the box by perforated metal sheet, which was covered by a small layer of bonded sand. Vacuum was applied to the manifold, and the rest of the box was filled with loose sand which "set" under the influence of the vacuum. The sand was scraped off to a depth of about 3 mm from the box surface and the space re-filled with a fine grade of abrasion-resistant powder. The vacuum core was then placed into a hole in the mould, located so that the abrasion-resistant powder layer formed part of the mould cavity surface, and the casting was poured with the vacuum still applied. Molten metal was sucked through the abrasion-resistant powder to produce a layer of wear-resistant material over selected areas of the part's surface.

The first batch of 12 trial teeth was made from AISI 4340 steel, heat treated to a hardness of 480 HB. Six were coated using tungsten carbide powder and the remainder with chromium carbide.

Prototype teeth exhibited superior performance in a BWR service trial, when compared with standard commercial parts. These were composed of a proprietary 0.27% carbon alloy steel casting at 495 HB hardness and protected by a 20% chromium 5.2% carbon ferrous-based hardfacing layer. This has been applied by a labour intensive weld-deposition method. The more expensive tungsten carbide type did not exhibit any service life advantage over the chromium carbide variant. Thus subsequent work was focused on the latter system.

Some process, material and design modifications were carried out and further tooth trials confirmed an approximately 2:1 life superiority over standard teeth.

This improvement has been ascribed mainly to the production of a surface layer with a very high chromium carbide content and a limited dilution zone. This condition is produced on solidification, after the molten base steel initially dissolves the chromium carbide powder layer on the mould wall. Such a structure has demonstrated much higher A.S.T.M. G65-80 wear test values compared to conventional hardfacing deposits.

Latterly, development work has been extended to involve a commercial foundry, where CANMETCOAT teeth were cast using a commercial steel alloy and standard production facilities. Field trials with these components reconfirmed the earlier encouraging results.

Based on evidence obtained to-date with BWR digger teeth, it is concluded that the process has strong potential for other oil sands wear applications.

TRIBOTESTING OF MATERIALS FOR AEROENGINE FLEXIBLE ELEMENT SEALS

H.M.Hawthorne

Tribology & Mechanics Laboratory
National Research Council of Canada

Introduction

The viability of the concept of using a narrow ring of tightly packed flexible elements, or brush, as a gas path seal in aircraft engines depends critically upon finding sliding component materials with sufficient wear resistance under high sliding speed and temperature conditions to provide useful seal lifetimes. Laboratory simulation testing [1] to explore the wear characteristics of selected material combinations is described.

Experimental

A brush-on-disc tribometer was developed, as shown schematically in Figure 1, to slide a countersurface against a small brush specimen under normal loads of 0.2-5 N at speeds to 100 m/s and temperatures to 500°C. Heat resistant steel or superalloy counterface discs were used to resist the combined centrifugal forces and thermal stress gradients from the peripherally heated, large diameter discs rotating at up to 7500 rpm. Countersurfaces were either the bare metal or ceramic, or cermet, coatings. Densely packed brush specimens with planar end surfaces were fabricated by various techniques from polymeric and ceramic fibres, and fine metal wires. Tribotesting consisted of long periods of sliding at constant conditions with continuous monitoring of friction and periodic stops to measure brush and countersurface wear by weight loss and surface profilometry, respectively. Light normal loads only were applied to the brushes, sufficient to provide good sweeping contact without excessive deflection of their flexible elements.

Results and Discussion

Use of polymer fibre specimens served only to develop brush construction and test apparatus and methods. Experiments soon showed that fibres melted and wore rapidly, even at 250°C test temperature, because of the high sliding speeds and consequent high asperity (flash) temperatures at the interface. Some ceramic fibres also melted and formed a glaze layer at the sliding interface, as shown in Figure 2a. Ceramic fibres and metal wires were both tested against metal and ceramic surfaces. A well run-in surface of wear resistant flexible elements, in this case superalloy wires, is shown in Figure 2b.

Brush specimen wear results from the best combination of seal components found so far, are summarized in Figure 3. Such long running-in effects are obtained when sliding on ceramic coated

countersurfaces, mainly due to the slow build up of adherent wear debris in the surface texture valleys.

Although varying with specific combinations, the relative ranking of the wear resistance of flexible element and countersurface materials tested to date is essentially as listed in Table 1. A number of possible ways to reduce seal component wear rates, such as the use of solid lubricants [2], have also been investigated in these laboratory tribotests.

The vertical orientation of the flexible elements and wide test brushes were much stiffer (at ≈ 20 N/mm for the superalloy wire specimens) than actual seals with a narrow band of slanted elements. For practical interferences, seal elements would be subject to lighter loads than the 2-5 N values used here on the superalloy brushes. On the other hand, sliding severity would be increased by the greater operational speeds (≥ 3 times maximum test values) required for aircraft engine seals. Although the best materials identified so far may give acceptable seal life the potential of ion and energy beam surface modification techniques [3] should be fertile ground for seeking further improvements in the wear resistance of seal components.

Conclusions

The laboratory tests to date have shown that, from a tribological viewpoint, superalloy wires sliding on ceramic countersurfaces is the most promising combination of materials for potential use in flexible element seals for aircraft engines.

Acknowledgements

The contributions of M.F.Robertson and S.K.Yick in performing experiments and T.Vanderhoek in rig design are acknowledged, as is the partial support of Pratt & Whitney Canada, and the interaction with J. Greer, of P & WC.

References

1. H.M.Hawthorne &, in part, M.F.Robertson & S.K.Yick. "Compliant Seal Wear Testing" Phases I-IV, NRC/DME Technical Reports CTR-WE-41 (1984), CTR-WE-45 (1985), CTR-TM-003 (1987) and CTR-TM-004 (1988).

2. H.E.Sliney. "Solid lubricant materials for high temperatures -- A review". Tribology International **15** (1982) 303-314.

3. W.H.Roberts. "Surface Engineering" International Tribology Conf., 1987, Melbourne, Aust.Inst. Engineers. Paper Preprints pp 438-451.

Table 1
Wear ranking of materials in tribotests

Flexible element materials	Countersurface materials
Nomex fibres	410 S/Steel
Kevlar "	Greek ascaloy
Nextel "	A 286
Carbon "	Chromium oxide
Boron "	Chromium carbide
Nicalon "	
304 Steel wires	
Nichrome "	
Haynes 25 "	
Inconel x750 "	

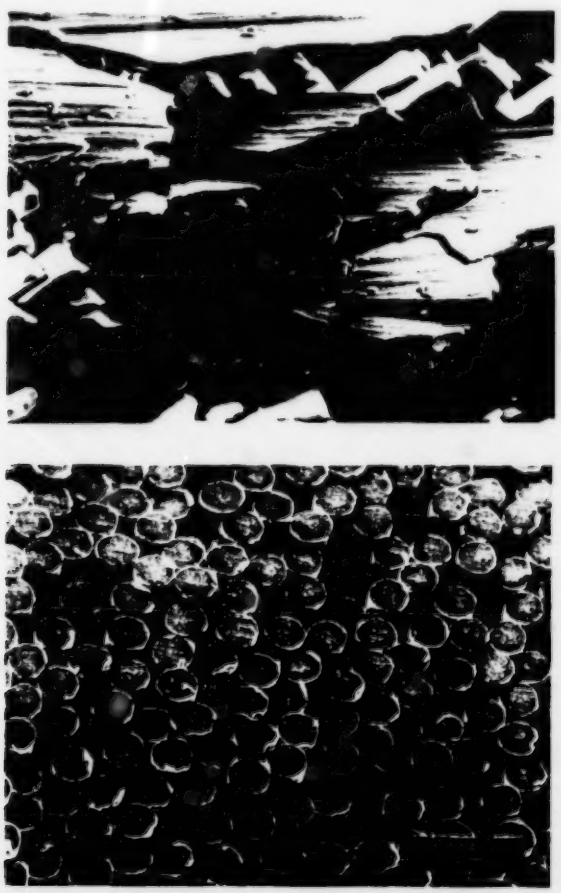

(a)

(b)

Fig. 2. Worn brush seal surfaces of candidate materials.
(a) Unsuitable ceramic fibres which melted and wore rapidly.
(b) Wear resistant superalloy wires.

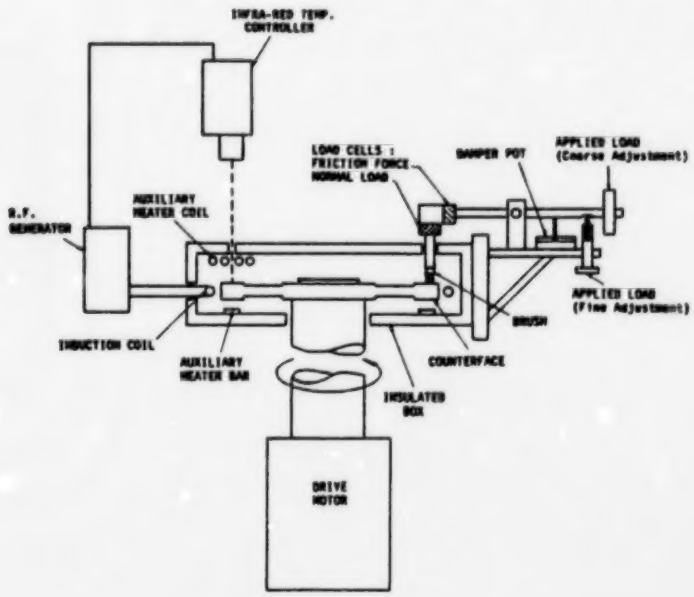

Fig. 1. Schematic of wear test rig.

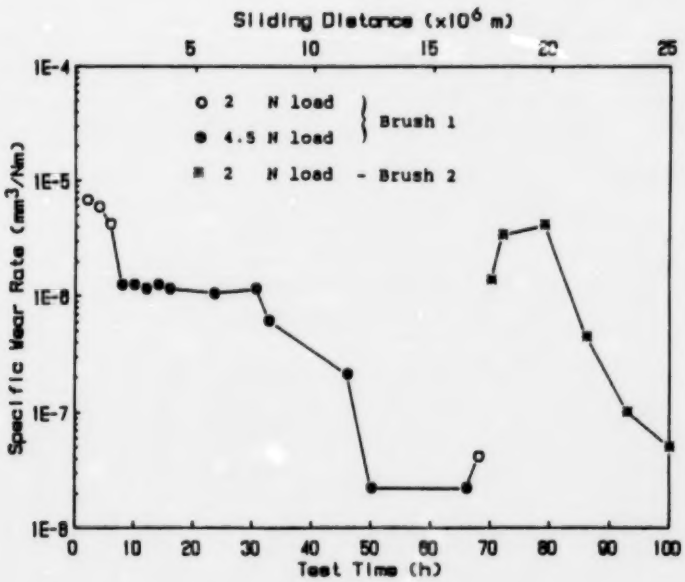

Fig. 3. Wear trend for best combination of flexible elements and countersurface.

AUTHOR INDEX

	Page
Alpas, A.T.	5
Amarouch, M.	25
Benabdalla, S.M.H.	8
Bhole, S.D.	75
Blahey, A.G.	82
Boness, R.J.	69
Bravo, Isobel	7
Brockwell, K.	53
Cameron, John	7
Caughlin, T.A.	82
Chalifoux, J.P.	8
Davies, Keith	98
Dinc, O.S.	42
Dmochowski, W.	53
Doonanco, Glenn	98
Embury, J.D.	5
Fiset, Michel	16,88
Fysh, Stephen D.	60
Gediktas, M.	42
Hawthorne, H.M.	79,100
Huard, Gilles	16,88
Kalousek, J.	64
Kleinbub, D.	53
Ko, Pak L.	64
Koehler, Albert	58
Kushwaha, R.L.	20
Laycock, K.E.	82
Llewellyn, Rees	40,98
Mackay, William	7
Masounave, Jacques	16,88
McBride, S.L.	69
Medley, John B.	60
Metcalfe, R.	34
Oravec, Edward M.	60
Pietralik, J.M.	34
Puttagunta, V.R.	49
Robertson, M.	64
Roy, C.	20
Schey, John A.	1
Sheasby, J.S.	82
Singh, Birbal	49
Smith, R.W.	7
Sobczyk, M.	69
Thompson, C.B.	92
Wood, Gordon	29
Yelle, H.	25
Yu, He-Jin	75